NTNU – Trondheim
Norwegian University of
Science and Technology

Materials Development of Steel-and Basalt Fiber-Reinforced Concretes

Usama Abbas

Abstract

Concrete is a structural composite material with excellent properties when subjected to compression. But the poor ability to resist tensile stresses forces the concrete to be used with reinforcement. Commonly, large continuous steel bars have been applied as reinforcement since mid-1800's to carry the tensile loads. Placing the steel bars takes many man-hours, which contributes to a significant part of the total concrete costs. By eliminating the reinforcement part of the construction work, the costs can be reduced considerably.

Fibers have been incorporated into building materials since ancient times to improve the properties. Today, fibers are incorporated in concretes to improve certain properties of this material. They are added to enhance the ductility of the concretes. Additionally, the tensile and the flexural strengths of the material are enhanced. The crack widths and their propagation are decreased by the insertion of fibers.

Research over the years have shown that fiber reinforcement has sufficient strength and ductility to be used as a complete replacement to conventional steel bars in some types of structures; foundations, walls, slabs. Fibers are also used in beams in combination with conventional reinforcement which increase the capacity and the stiffness of the concrete.

The technology that is available today has made is possible to consider fiber reinforcement without the use of conventional steel bars in load carrying structures. For this to be a reality, the fibers must be distributed and oriented as expected, which is difficult. If fibers can be used without the need of steel reinforcement bars, the reinforcement part of the construction work will be eliminated. Hence, the construction costs will be significantly reduced.

In recent years, a project within COIN has set the aim to develop a high tensile strength all-round concrete which exhibits a residual flexural tensile strength in the range of 10-15 MPa and that can be applied in load carrying structures. This MSc-thesis is a part of this work and it has consisted of testing fiber-reinforced self-compacting concretes with different types and contents of fibers, namely steel fibers and basalt fibers. The different concrete mixes were tested and the corresponding fresh and hardened concrete properties were evaluated and compared.

Based upon the results achieved in these experiments, the conclusion was taken of whether or not the different concrete mixes could be used for the purpose the COIN project was aiming for.

Acknowledgements

This MSc-thesis was written for the Department of Structural Engineering at the Norwegian University of Science and Technology (NTNU) in Trondheim, Norway. The project was in collaboration between NTNU, SINTEF and the Concrete Innovation Centre (COIN).

The target group was students and supervisors at NTNU and other universities in Norway and other countries.

I would like to thank everybody that helped me in this thesis, especially my supervisor Terje Kanstad who gave me the opportunity to work with this project in the summer of 2013. Also, I would like to thank everybody who participated with me in the experiments; Miguel Roca Boix (a master student), Gunrid Kjellmark (research engineer at SINTEF) and Malene Sommerstad (summerintership at SINTEF).

Also, the PhD candidate Elena Vidal Sarmiento helped me with this thesis by providing information on different parts of my work and I appreciate it.

I would also like to thank Knut Lervik at SINTEF and other employs at the NTNU laboratories.

31 October 2013, Trondheim, Norway

Usama Abbas

Table of Contents

1 Introduction

1.1 Background

Concrete has through the last hundred years established itself as one of the major building materials. The combination of excellent compressive strength, durability and readily available and affordable subcomponents has made concrete a highly demanded construction material and the backbone of our society's infrastructure. Concrete is the essential foundation and building block for strong, reliable and durable infrastructure.

Through the course of concrete history and development, the purpose has always been to improve the performance of concrete structures. It is known that Egyptians were using early forms of concrete in around 3000 BC to build pyramids (1). The ancient Romans made many developments in concrete technology, including the use of pozzolan (1). And since Joseph Aspdin invented the modern Portland cement in 1824 (2), the further development in concrete technology began to flourish, including the discovery of steel reinforced concrete and the use of admixtures and additives.

Since the 1950s, the overall development of concrete technology has improved a lot. New techniques and methods in different aspects have contributed to develop concrete with better performance and properties, and this has kept concrete a competitive material. Also the demands from our societies, such as more durable concrete, more environmental-friendly concrete and creating pleasing, artistic and creative structures, have played a major part in this development. And to further keep concrete a competitive material, research and further development of concrete are important.

One of the goals of any building project is to minimize the construction costs. Löfgren (3) found that roughly 40 % of total construction costs for a concrete building can be related to labor costs, and about 22 % of labor costs can be related to the reinforcement work. The current recession in economy in a lot of countries is an additional motivation to reduce the total costs and it is forcing the construction industry to find new ways to reach that goal. Through research done within concrete technology over the years, there are material technologies available that have the potential to significantly reduce the total operational costs. Examples of such materials are self-compacting concrete (SCC) and fiber-reinforced concrete (FRC). These materials will reduce some of the labor activities at the construction site, such as reinforcing and casting and finishing of concrete.

In addition to the competitiveness of concrete and minimizing construction costs, another motive for the need of SCC and FRC is the better performance and quality achieved in the concrete by the use of these materials. As an example, fibers in combination with self-compacting concrete has shown to achieve much higher loadbearing capacity than corresponding construction elements in conventional vibrated concrete (4).

Fibers are added to enhance the ductility, increase the tensile and flexural strength of the material and to decrease crack widths and retard their propagation. Comprehensive research over the years on fibers has shown that fiber reinforcement has actually sufficient strength and ductility to be used as a complete replacement to conventional reinforcement in some types of concrete structures, such as foundations, walls and slabs on grades. In beams and suspended slabs, fibers are used in combination with conventional reinforcement which increase both the loadbearing capacity and the stiffness of the structure (5). In both cases, from a structural viewpoint, fibers are incorporated to improve the fracture characteristics and structural behavior through the fibers' ability to bridge cracks.

In recent years, the technology has reached a level which makes it possible for fibers to completely replace conventional steel reinforcement in load carrying structures if the fibers are oriented and distributed as expected (4). However, for now, a more comprehensive study and research in this field is necessary to develop an all-round pure fiber-reinforced concrete which can be applied in load carrying structures. This will also help develop standardized guidelines for fiber-reinforced composites.

1.2   Objectives and scope of research

This MSc-thesis is a part of a COIN project called "FA 2.2 High tensile strength all-round concrete". The aim of this project is to develop a ductile high tensile strength concrete with residual flexural tensile strength in the range of 10-15 MPa. The goal is to replace conventional steel reinforcement completely with fibers in load carrying structures.

To reach the above mentioned objectives, experimental work will be done in this thesis which includes investigating and evaluating the fresh and hardened properties of self-compacting concrete reinforced with different types and contents of fibers, namely steel fibers and basalt fibers. Also, a comparison between steel and basalt fibers will be taken to find which of the two fiber types gives the better overall performance.

This thesis consists of an important first part; a literature study where different fiber types and their effect on the fresh and hardened concrete properties is gone through. Also the test methods which are applied to determine the fresh and hardened properties of fiber-reinforced concretes are focused on. Also, previous work conducted in the project FA 2.2 has been summarized in order to make it easier for the reader to understand earlier work done in this field.

2 Fiber-reinforced concrete

2.1 General

Portland cement concrete is considered a relatively brittle material. When subjected to tensile stresses, non-reinforced concrete will crack and fail. Since mid-1800's steel reinforcement has been used to overcome this problem. As a composite system, the reinforcing steel is assumed to carry all tensile loads.

Fiber-reinforced concrete (FRC) is Portland cement concrete reinforced with more or less randomly distributed fibers. Thousands of small fibers are dispersed and distributed randomly in the concrete during mixing, and thus improve concrete properties in all directions, including the post peak ductility performance, pre-crack tensile strength, fatigue strength and impact strength. In comparison to conventional reinforcement, the characteristics of fiber reinforcement are that:

1. The fibers are generally distributed throughout a cross-section, whereas steel bars are only placed where needed.
2. The fibers are relatively short and closely spaced, whereas the steel bars are continuous and not as closely placed.
3. It is generally not possible to achieve the same area of reinforcement with fibers as with steel bars.
4. It is much tougher and more resistant to impact than plain concrete.

The fibers are not added to improve the strength, though modest increases in strength may occur. Rather, their main role is to control the cracking of FRC, and to alter the behavior of the material once the matrix has cracked, by bridging across these cracks and so providing some post-cracking ductility.

2.2 Development of Fiber-reinforced concrete

Since Biblical times, fibers have been used to strengthen brittle materials, for example straw and horsehair mixed with clay to form bricks and floors. The concept of fiber reinforcement was developed in modern times and brittle cement-paste was reinforced with asbestos fibers in early 1900's (6). Because of health issues, the need to replace asbestos fibers in the early 1950's gave rise to the development of composite materials. Glass-fibers were introduced for reinforcement of cement paste by Biryukovichs, while steel fibers were for the first time proposed as dispersed reinforcement of concrete by Romualdi in his two papers in 1963 and 1964 (7). By the 1970's, steel fiber reinforcement had been accepted as a viable alternative to traditional reinforcement. No standards or recommendations were available at that time which was a major obstacle for the acceptance of this new technology. The evolution into structural applications was mainly the result of the progress made in fiber technology; a steady buildup of knowledge and understanding of its use into a wide range of applications as well as the research carried out at different technical institutes and universities in order to understand and quantify the material properties. Table 1-1 shows the chronological development of matrix and fibers since the 1970's, presented in a conference held in March 2012 in Kassel, Germany (8).

Decade	Cementitious Matrix and Concrete	Fiber
1970's	• Better understanding of hydration reactions; gel structure; • Better understanding shrinkage, creep, porosity, … • High strength concrete to 50 MPa in practice • Development of water reducers • Advances in concrete treatments and curing conditions	• Smooth steel fibers; normal strength • Glass fibers • Some synthetic fibers
1980's	• Increased development of chemical additives: HWRA, etc… • Increased utilization of fly ash and silica fume, and other mineral additives, etc… • Increased flowability (flowable concrete) • Reduction in W/C ratio; • High-Strength-Concrete terminology: up to 60 MPa; special high strength: up to 80 MPa; exotic high strength (special aggregate and curing): up to 120 MPa • High-Performance-Concrete terminology: high-strength-concrete with improved durability properties.	• Deformed steel fibers: normal and high strength • Low-modulus synthetic fibers (PP, nylon, etc..) • Increased use of glass fibers • Micro fibers • High performance polymer fibers (carbon, Spectra, Kevlar, etc..)
1990's	• Increased development in chemical additives: superplasticizers; viscosity agents; etc…. • Increased use of supplementary cementitious materials as cement replacement • UHPC: application of concept of high packing density; addition of fine particles; low porosity; lower water to cementitious ratio; • Self consolidating concrete; self compacting concrete;	• New steel fibers with a twist (untwist during pull-out) • PVA fibers with chemical bond to concrete • Improved availability of synthetic fibers
2000's	• Increased developments of proprietary and non-proprietary UHPC/UHP-FRC • UHPC: improved understanding of high packing density; application of nanotechnology concepts	• Ultra high strength steel fibers: smooth or deformed with diameters as low as 0.12 mm and strengths up to 3400 MPa • Carbon nano-tubes; carbon nano-fibers
2010's	• Increased understanding of the cementitious matrix at the nano-scale • …???...	• Carbon nano-fibers, graphene, … • …???...

Table 1-1 Chronological advances in matrix and fibers since the 1970's

Today most of the fiber types incorporated into concrete are steel, glass, synthetic and natural based. Accordingly, the concrete in which they are applied is denoted as follows:

- Steel fiber reinforced concrete (SFRC)
- Glass fiber reinforced concrete (GFRC)
- Synthetic fiber reinforced concrete (SNFRC)
- Natural fiber reinforced concrete (NFRC)

These types of fibers vary considerably both in properties and effectiveness. In Table 1-2, some common fibers and their typical properties are listed (9).

Fibre type	Relative density	Diameter (μm)	Tensile strength (MPa)	Modulus of elasticity (MPa)	Strain at failure (%)
Steel	7.80	100-1000	500-2600	210,000	0.5-3.5
Glass					
E	2.54	8-15	2000-4000	72,000	3.0-4.8
AR	2.70	12-20	1500-3700	80,000	2.5-3.6
Synthetic					
Acrylic	1.18	5-17	200-1000	17,000-19,000	28-50
Aramid	1.44	10-12	2000-3100	62,000-120,000	2-3.5
Carbon	1.90	8-0	1800-2600	230,000-380,000	0.5-1.5
Nylon	1.14	23	1000	5,200	20
Polyester	1.38	10-80	280-1200	10,000-18,000	10-50
Polyethylene	0.96	25-1000	80-600	5,000	12-100
Polypropylene	0.90	20-200	450-700	3,500-5,200	6-15
Natural					
Wood cellulose	1.50	25-125	350-2000	10,000-40,000	
Sisal			280-600	13,000-25,000	3.5
Coconut	1.12-1.15	100-400	120-200	19,000-25,000	10-25
Bamboo	1.50	50-400	350-500	33,000-40,000	
Jute	1.02-1.04	100-200	250-350	25,000-32,000	1.5-1.9
Elephant grass		425	180	4,900	3.6

Table 1-2 Typical properties of fibers

The character and performance of FRC changes with varying concrete binder formulations as well as the fiber material type, fiber geometry, fiber distribution, fiber orientation and fiber concentration.

2.3   Fiber types

The individual fibers can be subdivided into two groups: discrete monofilaments separated one from the other (Figure 1-1) and fiber assemblies made up of bundles of filaments (Figure 1-2). The monofilament fibers rarely assume the ideal cylindrical shape, but are deformed into various configurations (Figure 1-1). The bundled fibers often maintain their bundled nature in the composite itself, meaning they do not disperse into the individual filaments.
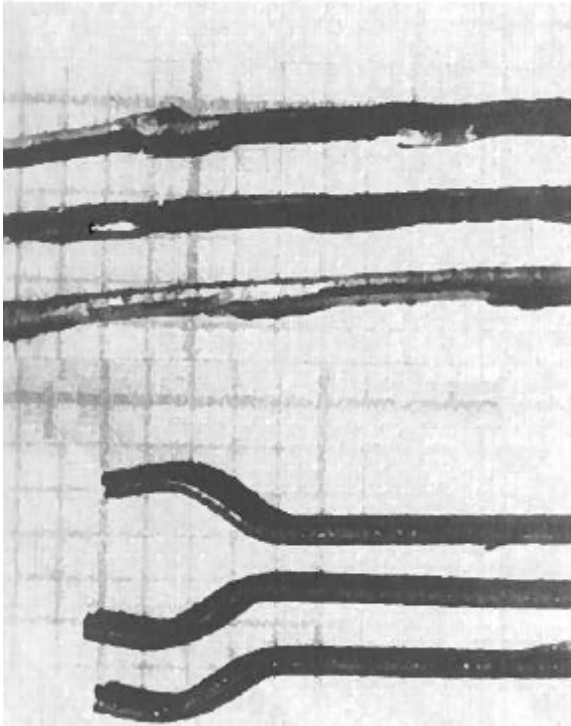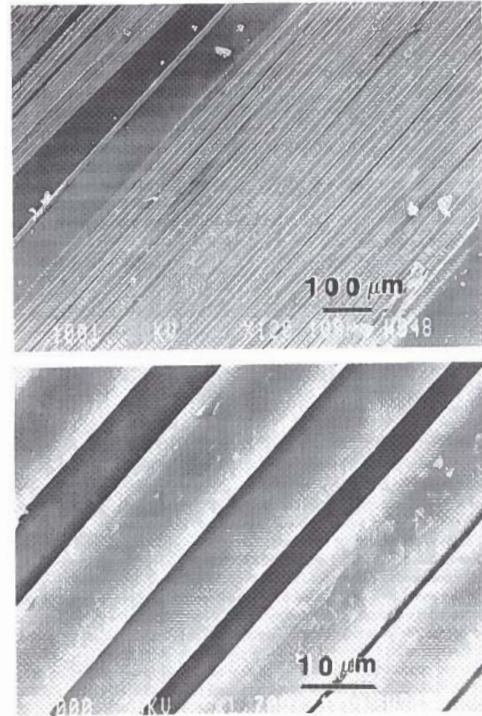
Figure 1-1 Monofilaments

Figure 1-2 Bundled filaments

2.4 Fiber classification and geometry

2.4.1 Classification

Fibers used in cementitious composites may be classified as: 1) macro-fibers, when their length exceeds the maximum aggregate size (for coarse aggregates: at least by a factor of two) and if their diameter is much greater than that of the cement grains (which typically means less than 50 μm); and 2) microfibers, when the diameter is the same as the cement grains and the length is less than the maximum aggregate size.

Fibers can also be characterized in other ways. According to Naaman (10), the classification can be based on the fiber material: natural organic (cellulose, sisal etc.), natural mineral (asbestos, rock-wool) or man-made (steel, basalt, glass etc.). Furthermore the classification can also be based on their physical or chemical properties, such as surface roughness, density, chemical stability, flammability etc. Also it can be based on their mechanical properties, such as tensile strength, elastic modulus, stiffness, ductility etc.

2.4.2 Geometry

Some important terms related to fibers are going to be used further in this thesis. They are defined as follows:

- The length, l, is measured and defined as the distance between the fiber endpoints. The length is determined by equipment with accuracy of 0,1 mm. If the fiber is bent, the total length of the fiber shall also be measured and this is given as the length of the fiber after it is straightened out.
- The diameter, d, is measured in two directions, perpendicular to each other. The fiber's diameter is the average of these two measurements.

- The aspect ratio, l/d, is calculated by dividing fiber length by its diameter.
- The concentration of fibers within a concrete mix is measured as a percentage of the total volume of the composite (concrete and fibers) termed volume fraction (V_f).
- The fiber factor (which by the way is also used to characterize and compare the properties of different fiber-reinforced mixtures) is defined as V_f × aspect ratio = V_f × (l/d)

The effectiveness of fibers in improving the mechanical performance of the brittle matrix is dependent on the fiber-matrix interactions. Three types of interactions are particularly important:

1. Physical and chemical adhesion
2. Friction
3. Mechanical anchorage

The adhesional and frictional bonding between a fiber and matrix are relatively weak and for conventional fibers not sufficient for developing adequate reinforcing efficiency. For this reason the fibers are sometimes deformed to overcome this limitation. The induced deformation in the fiber provides great anchoring effects and the bonding achieved has been shown to be much greater than the one achieved by interfacial effects (6). Hence, fibers can be smooth, crimped, coiled, twisted, with end hooks, deformed, indented, paddles or other, see Figure 1-3.
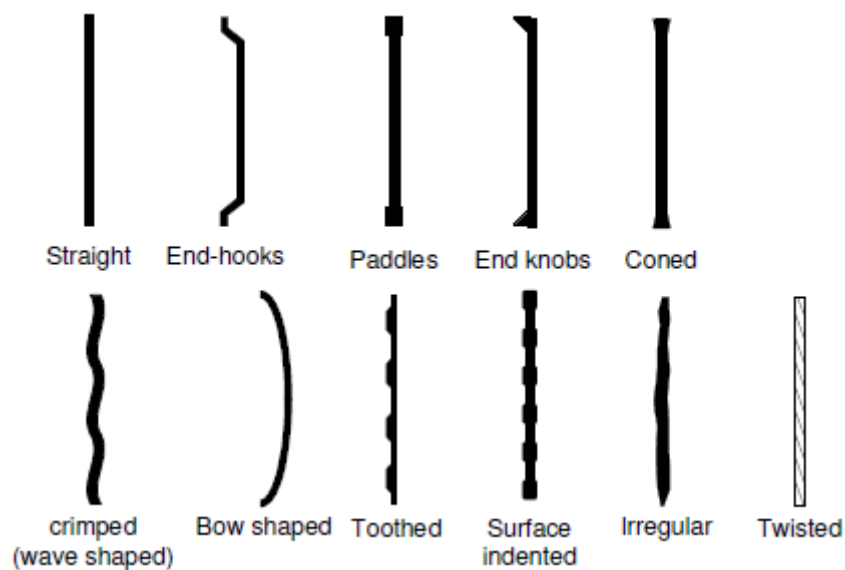
Figure 1-3 Examples of some typical fiber geometries

The cross-section of the fibers comes also in a variety of shapes, as shown in the figure below:
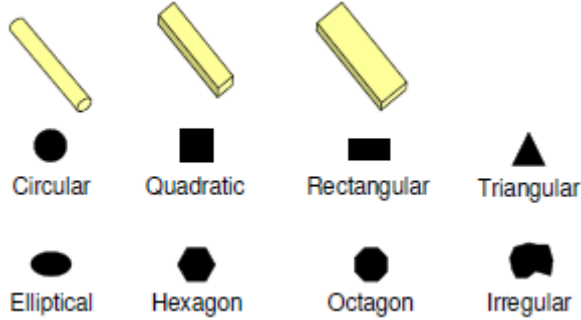
Figure 1-4 Examples of cross-sectional geometries of fibers

2.5   Fiber orientation and distribution

The mechanical performance of fiber-reinforced composites is influenced by the orientation of the fibers. The fibers can be dispersed in a direct or a random orientation in the concrete body. The more they are aligned into the direction of the tensile stress, the more effective they are. The number of fibers bridging a crack is given by the following equation (11):

$$N_f = \frac{V_f}{A_f} * \alpha$$

Where

N_f is the number of fibers per unit area

V_f is the volume% of fibers

A_f is the cross-section area of a single fiber

α is the orientation factor

Direct orientation is characterized by a one-dimensional system (1-D), see Figure 1-5. Here, the fiber efficiency (the orientation factor) is quite simple to determine since all the fibers are oriented in the direction of the load. Therefore, for a 1-D system, the orientation factor equals one.

Figure 1-5 Fiber orientation in 1-D

Plane-random orientation is characterized by distribution of fibers in a two-dimensional system (2-D), see figure. Random orientation is characterized by distribution of fibers in a three-dimensional system (3-D), see figure. The efficiency number can be calculated theoretically for both systems. According to Li and Stang (12), the orientation factor is $2/\pi$ (0,637) for a 2-D system, while for the 3-D case it is 0,5.

Figure 1-6 Fiber orientation in (a) 2-D (b) 3-D
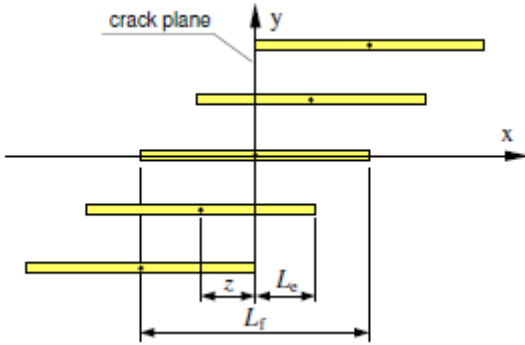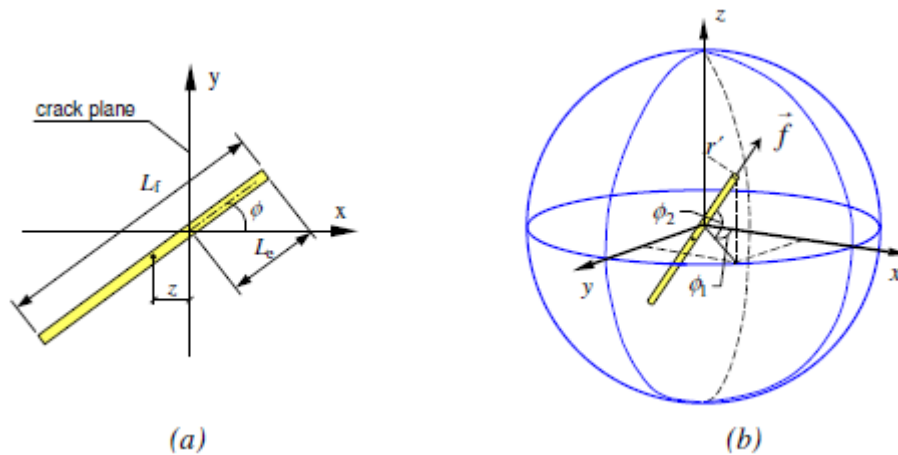
Geometerical boundaries affect the orientation to various degrees. The smaller the cross-section of a beam for instance, the more restricted the possibilities of free orientation of the fibers. According to Kooiman (13), the constrained orientation of fibers affect the orientation factor when the dimensions of a member are less than five times the length of the fibers.

Also, other factors affect the orientation factor; method of placement, the equipment used and the properties of the fresh concrete.

2.6 Fiber material

2.6.1 Steel fibers

Steel fiber reinforced concrete (SRFC) is the most commonly-used fiber concrete, though it is fast being overtaken by synthetic fiber reinforced concrete. Steel fibers were originally used as secondary reinforcement for crack control in flat slabs, pavements and tunnel linings. Today, their use has been stretched out to also include truly structural applications, either to replace conventional steel bars, or to act in a complementary fashion with it as a secondary reinforcement.

The use of steel fibers is popular due to the many favorable properties of this fiber type: high modulus of elasticity, high strength, high ductility and a very good durability in the alkaline environment of the concrete.

Steel fibers greatly increase the toughness (toughness is a measure of the ability to absorb energy during deformation) of cements and concretes. This increase can prevent, or at least minimize, cracking due to changes in temperature or relative humidity. As mentioned earlier in section 1.1, that increase in strength due to fiber additions are very modest (except for high fiber volumes) and the main purpose for adding fibers is to improve the post-peak load carrying capacity of the concrete (i.e. toughness). Figure 1-7 (14) shows that increasing volume of fibers doesn't increase the strength

noticeably, while the toughness increases rapidly with even the slightest increment of fibers. For example, when the fiber volume is increased from 0,5% to 1%, the toughness in relation to plain concrete rises from approximately 5 times to 15 times.
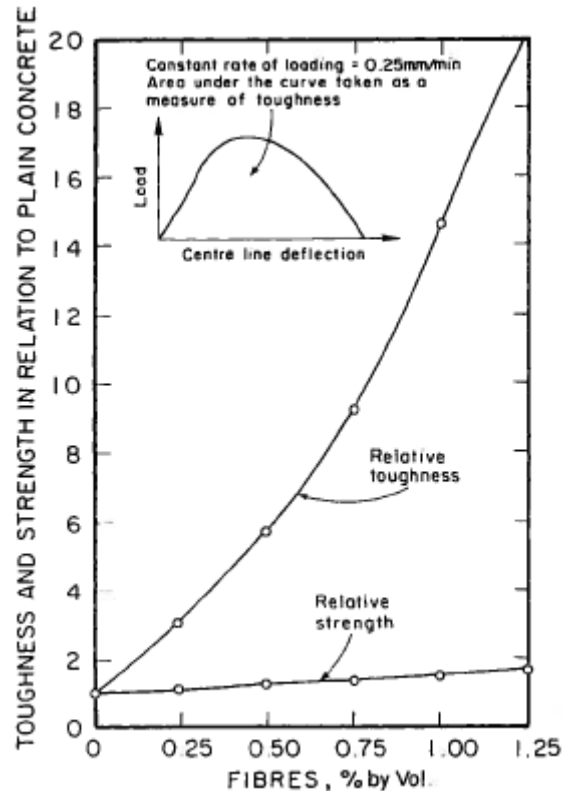
Figure 1-7 Effect of the volume of steel fibers on the strength and toughness of SFRC

Steel fibers are generally produced from carbon steel and stainless steel and their tensile strength varies from 345 to 2100 MPa. In Norway, the specifications, definitions and requirements for steel fibers in concrete are given in NS-EN 14889-1, while in the US the standard ASTM A820 is used. Five general types of steel fibers are identified in this standard based upon the product or process used as a source of the steel fiber material (15):

- Type I, cold-drawn wire
- Type II, cut-sheet
- Type III, melt-extracted
- Type IV, mill cut
- Type V, modified cold-drawn wire

When steel fibers are incorporated into a concrete mix, the packing density (see section 1.10.2) of the aggregates decreases. This effect limits the maximum fiber content (16). For example, the maximum packing density is obtained with about a 40% volume of fine aggregate for plain concretes. To achieve maximum packing density, in for instance a concrete containing 2% fibers, about 60% fines content is required. This is shown in Figure 1-8.

To achieve a uniform fiber distribution in SFRC is difficult due to the tendency of steel fibers to ball or clump together. This tendency of clumping is caused by several factors:

- The Fibers are already clumped together before addition into the mix; the mixing action is not able to break up the clumps
- There are too short time intervals between each addition of fibers, not allowing them to disperse in the mixer
- Even if fibers are not clumped together prior to mixing, they may be added with too high volumes
- The mixer itself could be too worn of inefficient to disperse the fibers
- If the fibers are added into the mixer before the other ingredients then they will clump together
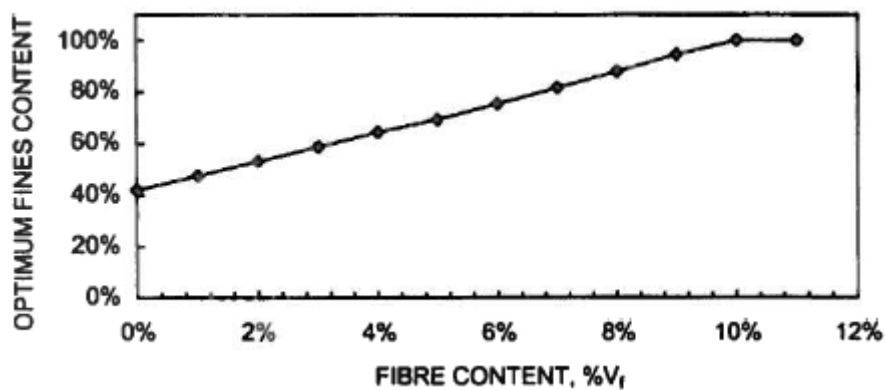
Figure 1-8 Fines content vs. fiber content for determination of optimum packing density (16)

2.6.2 Glass fibers

Glass fibers have been developed mainly for the production of thin sheet components. They are produced and marketed as either continuous or chopped roving (Figure 1-9), or they can be formed into a mat (Figure 1-10). Originally the first types of glass fibers used in cement were so called E- and A-glass. Due to the low alkali resistivity in these types, the fibers deteriorated rapidly in the highly alkaline environment of the cementitious matrix (17, 18). Hence, the strength of the concrete was reduced. Continued research resulted in alkali-resistant glass fibers (AR-glass), which improved long-term durability. However, other sources of strength-loss were observed. Still today, the long-term performance of GFRC is the major criterion by which its quality is assessed. It is known that ageing of glass fiber reinforced cement (GRC) composites leads to a change in properties, as seen from the stress-strain curves in Figure 1-11. The most significant change is the marked reduction in the ultimate strain in natural weathering and water storage, and an increase in the first crack stress and a reduction in the tensile strength (19, 20). However, the properties are kept intact for composite kept in dry air. The same trend is observed for flexural properties, showing stability in dry air but a decline in flexural strength and toughness for water stored specimens, as seen in Figure 1-12 (21). It should be noted that de decline in flexural strength tends to level off, as seen on the same figure.

Figure 1-9 Continuous roving
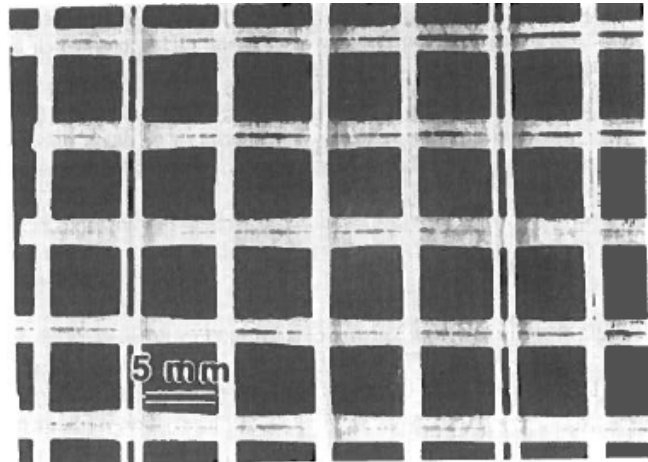
Figure 1-10 Woven mat
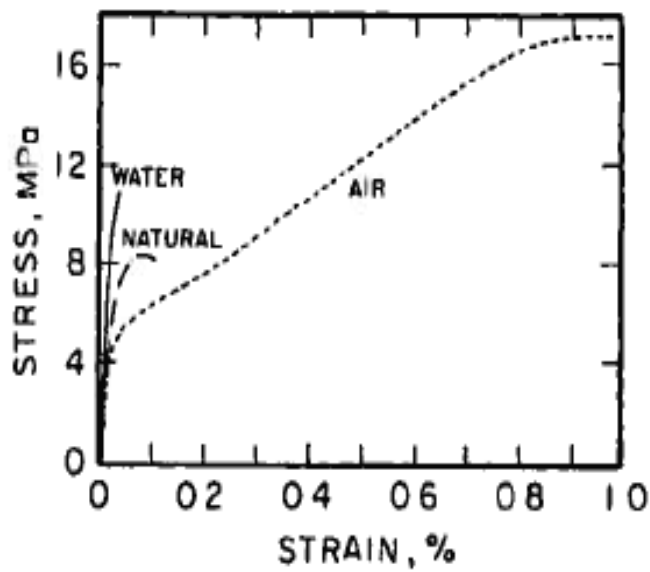
Figure 1-11 Effect of ageing for 5 years on the stress-strain curves of AR-GRC composites
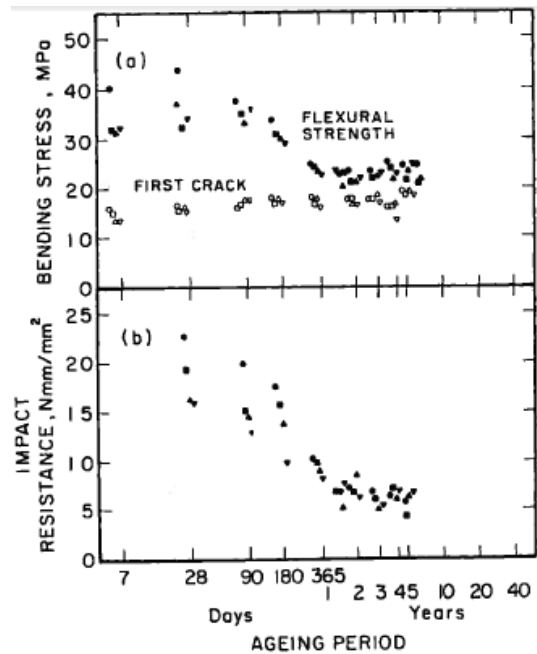
Figure 1-12 Changes in the properties of AR-GRC after water storage

2.6.3   Asbestos fibers

As mentioned in section 1.2, Asbestos fibers were the first ones used for fiber reinforcement in modern times. In the 1960s and 1970s, it became evident that this fiber type posed great health hazards. Irving Selikoff (22), an American industrial physician, showed in a study that asbestos can cause asbestosis, lung cancer and mesothelioma. He found that several former US naval industry workers died because of asbestos induced illnesses. They used asbestos as insulation and fire protection material on ships, where it was sprayed on boilers, incinerators, hot water pipes and steam pipes. The fibers were inhaled, causing damage and disease.

The risk of getting exposed to asbestos is particularly high when the fibers are in a loose form and inhalable, which is the case during the production process. However, after the fibers are mixed with the cement matrix, the risk may occur again during various constructional operations, for instance maintenance and removal. For these reasons several countries have banned the use and production of asbestos (23).

Bentur and Mindess (6) point out that the asbestos research done over the years and the gained information is still important and of great scientific and engineering value. Due to this information of asbestos, other similar composites and other composite systems where the fibers are of similar size as the asbestos are developed and being applied. Also similar performance is gained using other fibers which pose no health hazards. Bentur and Mindess write: "*For such systems, the understanding of the "reference" of asbestos-cement composite is of considerable value. In view of these considerations, it was decided to keep this chapter in the revised book, to serve as a source of valuable information.*"

Asbestos fibers are produced in a Hatschek process; the Hatschek machine and schematic description presented in the figure below (24):

1. Slurry vats	5. Vacuum box	9. Take-off conveyer
2. Sieve cylinders	6. Breast roll	10. Whipper
3. Running felt	7. Formation cylinder	11. Suction box (felt drying)
4. Couch rolls	8. Cutting wire	12. Lamina
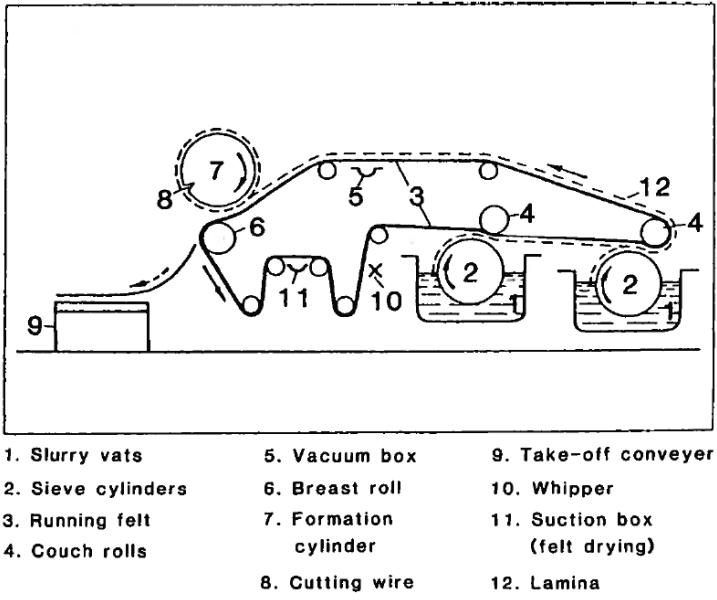
Figure 1-13 Schematic description of the Hatschek process

Asbestos fibers are made of natural crystalline fibrous materials. Though the fibers are initially bundled, they tend to be split up after mixing with the cement matrix. Still a considerable portion of the fibers remain bundled. The high modulus of elasticity, strength and a natural attraction to Portland cement allows effective dispersion of large fiber volumes (10% and more) and strengthens the fiber-matrix bond.

Compared to fiber reinforced plastics, the matrix of asbestos cement is a relatively brittle and hard substance. Table 1-3 (25) shows different properties of cement with and without the addition of asbestos, clearly showing increment in strength.

	Flexural strength N/mm²	Tensile strength N/mm²	Elastic modulus kN/mm²	Tensile strain to failure %
Cement	7–8	5–6	15	0.04
Asbestos cement	30–40	17–20	28–35	0.4–0.5
Chrysotile asbestos	–	3600	150	0.1–0.3

Table 1-3 Mechanical properties of Portland cement, asbestos cement and chrysotile asbestos fibers

For an asbestos-cement composite, the strength and modulus does not increase with the fiber content and length. The maximum strength appears at intermediate fiber content and at an intermediate length, while the modulus of elasticity decreases with increasing fiber content (Figure 1-14, Figure 1-15, Table 1-4, Table 1-5).
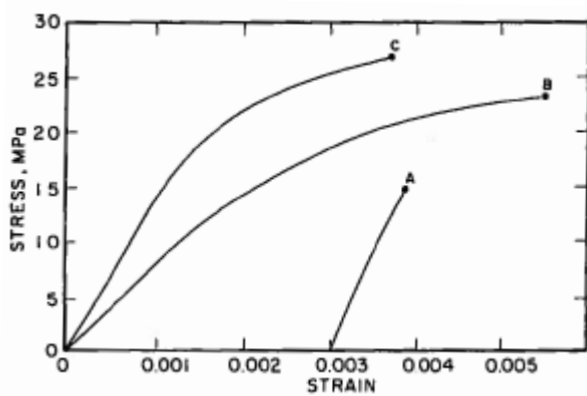
Figure 1-14 Stress-strain curves of asbestos-cement composites with different fiber contents. A-low, B-high and C-intermediate (26)
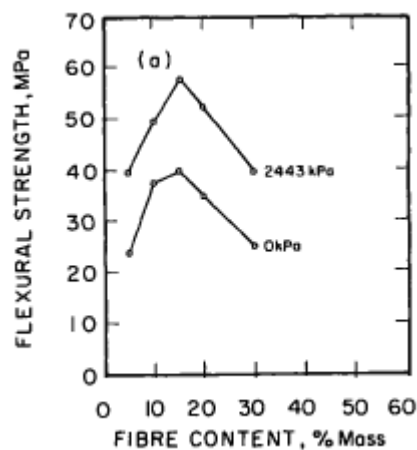
Figure 1-15 Effect of fiber content and compaction pressure on the properties of asbestos cement composites (27)

Fibre content (% vol.)	Matrix void content (% vol.)	Modulus of elasticity[a] (GPa)	Tensile strength[a] (MPa)	Ultimate elongation[a] (%)
2.91	14.3	17.29	14.6	0.95
5.10	26.7	16.09	20.3	2.32
7.32	32.3	14.73	25.4	3.70
14.85	60.4	8.45	21.3	5.06

Table 1-4 Effect of fiber content on properties of asbestos-cement composites(26)

Fibre length	Fibre content (% vol.)	Matrix void content (% vol.)	Modulus of elasticity[a] (GPa)	Tensile strength[a] (MPa)	Ultimate elongation[a] (%)
Short	5.70	17.9	16.93	17.8	1.28
Medium	5.10	26.7	16.09	20.3	2.32
Long	4.72	32.6	13.05	16.1	2.54

Table 1-5 Effect of fiber length on the properties of asbestos-cement composites (26)

As mentioned above, there has been an effort to develop other fibers which are called asbestos-free fibers or substitutes where the goal has been to have similar or better properties, while preserving the unique asbestos properties. But the combination of high strength, high modulus of elasticity, great bond and stability in the alkaline cement environment is difficult to match with any one type of fiber.

2.6.4 Basalt fibers

Basalt fiber is a unique product derived from basalt rock, a natural material that is found in volcanic rocks originated from frozen lava. The rock itself is extremely hard and it has been used as crushed rock in construction since ancient times. This rock has excellent strength, durability and thermal properties.

The fibers are created by melting the basalt rock between 1500 and 1700 °C and forcing it through in platinum/rhodium crucible bushings (28). These fibers are manufactured as chopped fibers and continuous fibers. They are very similar to glass fibers, but better in terms of thermal stability, heat and sound insulation properties, vibration resistance, as well as durability (more stable in strong alkalis than glasses). Basalt fibers also have good resistance to chemical attack and in seawater environment (29). For these reasons they are a good alternative to glass fibers as reinforcing material and combined with the lower cost of basalt, this fiber type could potentially replace glass fibers in various fields; aerospace, automotive, transportation and shipbuilding for instance . They can be used from very low temperatures (about -200 °C) up to high temperatures in the range of 700-800 °C (28), which makes them an excellent economic alternative to other high-temperature-resistant fibers. They are typically applied in heat shields, composite reinforcement, and thermal and acoustic barriers. In the mechanical properties of basalt fibers are compared with Kevlar, high-strength carbon and glass, see Table 1-6.
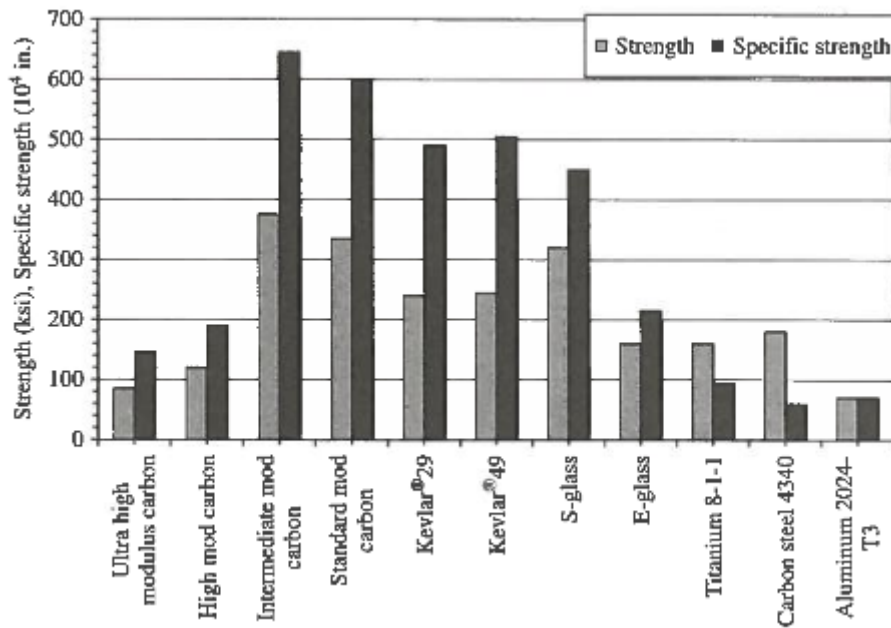
Table 1-6 Tensile strength of typical fibers and metals

2.6.5 Synthetic fibers

Different types of synthetic fibers have been developed and are increasingly being used as reinforcement, especially polypropylene. Their strength and modulus of elasticity vary widely as shown in Table 1-7. It should be noted that the values in the table are for fibers that are commercially available. They may vary considerably from manufacturer to manufacturer.

Fibre type	Diameter (μm)	Specific gravity	Tensile strength (GPa)	Elastic modulus (GPa)	Ultimate elongation (%)
Acrylic	20–350	1.16–1.18	0.2–1.0	14–19	10–50
Aramid (Kevlar)	10–12	1.44	2.3–3.5	63–120	2–4.5
Carbon (PAN)	8–9	1.6–1.7	2.5–4.0	230–380	0.5–1.5
Carbon (Pich)	9–18	1.6–1.21	0.5–3.1	30–480	0.5–2.4
Nylon	23–400	1.14	0.75–1.0	4.1–5.2	16–20
polyester	10–200	1.34–1.39	0.23–1.2	10–18	10–50
Polyethylene	25–1000	0.92–0.96	0.08–0.60	5	3–100
Polyolefin	150–635	0.91	275	2.7	15
Polypropylene	20–400	0.9–0.95	0.45–076	3.5–10	15–25
PVA	14–650	1.3	0.8–1.5	29–36	5.7
Steel (for comparison)	100–1000	7.84	0.5–2.6	210	0.5–3.5
Cement matrix	–––	1.5–2.5	0.003–0.007	10–45	0.02

Table 1-7 Typical properties of synthetics fibers (6)

There are some issues associated with synthetic fibers, the main one being the low modulus of elasticity for most synthetic fibers. This property must be higher than that of the matrix in order to increase the strength of the composite. However, even with low modulus fibers, considerable improvements can be achieved, for example better strain capacity and toughness.

2.6.5.1 Polypropylene fibers

Polypropylene fibers are produced from homopolymer polypropylene resin and presented in three different geometrical forms: monofilaments, film and tape. There are several advantages of these fibers; they are alkali resistant, they have a relatively high melting point and their price is low. On the other hand their disadvantages, which for instance include low modulus of elasticity, sensitivity to sunlight and oxygen and low matrix-bond, are also present.

Polypropylene fibers are utilized mainly to enhance the shrinkage cracking resistance. They are not expected to increase the strength of concrete, but to improve its ductility and toughness, and impact resistance. Tests using ACI committee 544 recommendation (drop-hammer method) have indicated that the number of blows required to obtain the first crack and the ultimate failure was increased by the addition of polypropylene fibers (30, 31).

For commercially available polypropylene fibers, the modulus of elasticity is in the range of 3-5 GPa and the tensile strength is about 140-690 MPa (32). These values are relatively low. For these reasons, fibers with special properties had to be developed for cement and concrete applications. In Denmark a polypropylene fiber called Krenit has been developed which has a relatively high modulus of elasticity (7-18 GPa) and tensile strength (500-1200 MPa) (33). Another example of a synthetic fiber developed to overcome the disadvantages is the STRUX® fiber (shown in Figure 1-16). This fiber was developed by Trottier and Mahoney (34) by mixing polypropylene and polyethylene in the extrusion process. In addition to a high elastic modulus, it has a high tensile strength and increases the bonding capacity with the matrix. This reduces the plastic shrinkage cracking and may increase the ductility and toughness of the concrete, according to Trottier ad Mahoney (34).
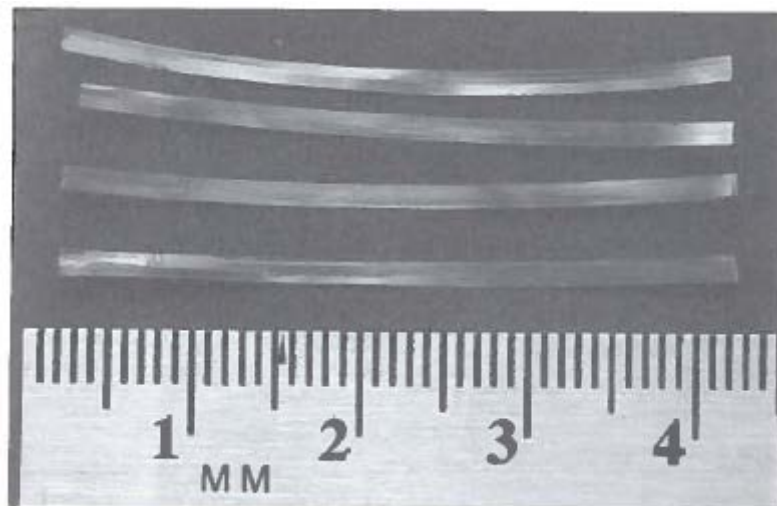
Figure 1-16 STRUX® fiber

Polypropylene fibers are used mainly in two ways to reinforce concrete. They are either used as the primary reinforcement (as in thin sheet components where the volume content is relatively high), or as the secondary reinforcement where the volume content is low. These fibers with low modulus have been used to control the plastic shrinkage cracking, being effective in suppressing most of the cracking and reducing its extent by an order of magnitude when the content is about 0,1% by

volume. Figure 1-17 and Figure 1-18 show tests results of such fibers. However, not all polypropylene fibers are equally effective in reducing plastic shrinkage cracking. According to Kraii (35) who tested seven different polypropylene fibers, some of them did not provide mentionable improvement.
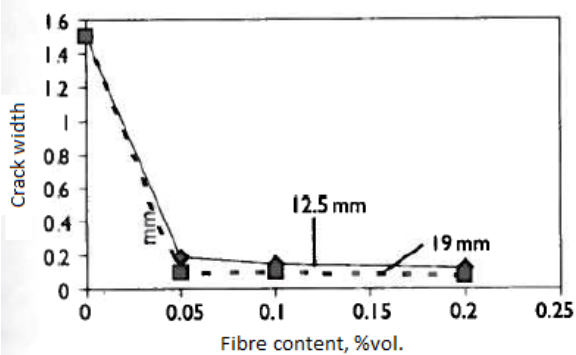
Figure 1-17 Effect of fibrillated polypropylene fiber content and length on plastic shrinkage cracking (36)
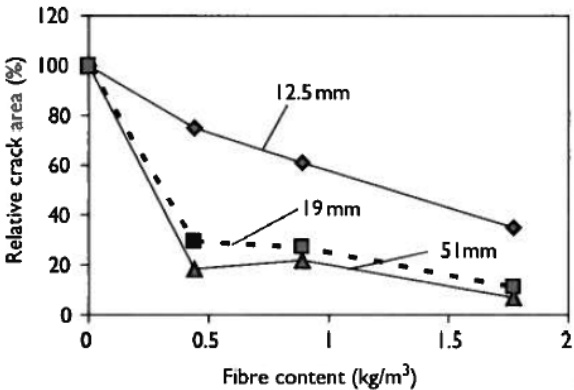
Figure 1-18 Effect of monofilament of polypropylene fiber content and length on plastic shrinkage cracking relative to control (37)

Kovler (38) found out that the low modulus PP (polypropylene) fibers at about 0,1% by volume are not effective for crack control of hardened concrete. Krenchel and Shah (39) found that higher modulus fibers, at a larger content, is needed for crack control of hardened concrete.

Low modulus PP fibers do not increase the compressive and tensile strengths of hardened concretes any significantly from those of the unreinforced matrix (40). However, it is reported that PP fibers are effective in increasing the flexural strength (40). If PP fibers are to be used in concrete pavements or floor systems, it must be considered that they have an adverse effect on the abrasion resistance of concrete (41).

An important effect of low volume fiber reinforcement is to increase the energy absorption capacity in tension or bending. This is shown in both static testing (Figure 1-19) and impact (Figure 1-20). A small increase in impact resistance was reported for fiber content 0,1% by volume, while an increase of about 30-80% were found for fiber content in the range of 0,3-0,5% by volume (42).
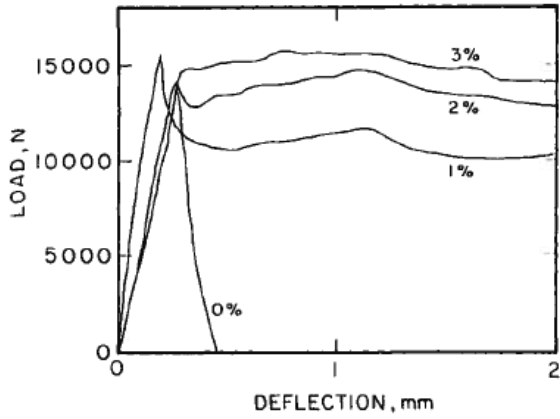
Figure 1-19 Effect on the content of PP fibers on the load-deflection curve (43)
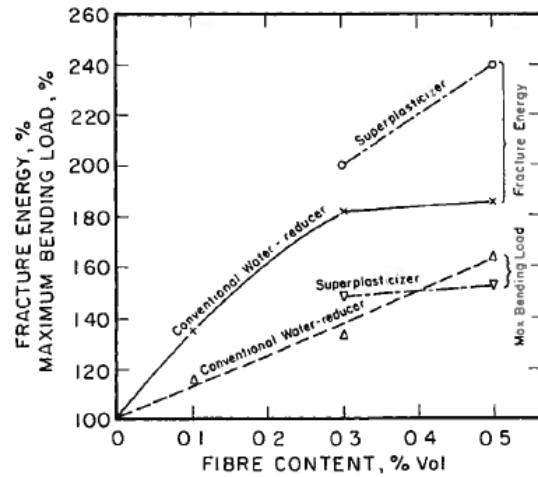
Figure 1-20 Effect on the content of fibrillated PP fibers on the maximum bending load and fracture energy of concretes in impact, expressed as a percentage of the values for beams with no fibers (42)

2.6.5.2   Acrylic fibers

Acrylic fibers were first developed in the mid-1940s but were not produced in large quantities until the 1950s. They are often used for sweaters and tracksuits and as linings for boots and gloves. These types of acrylic fibers have a tensile strength in the range of 200-400 MPa and they are not alkali resistant (44) and therefore not suitable for use in FRC. However, recently high modulus acrylic fibers with high tensile strengths (up to 1000 MPa) have been developed and are being used in FRC. The stress-strain curves of these fibers are shown in the figure below where they are compared with conventional textile acrylic fibers, showing higher tensile strength and elastic modulus.
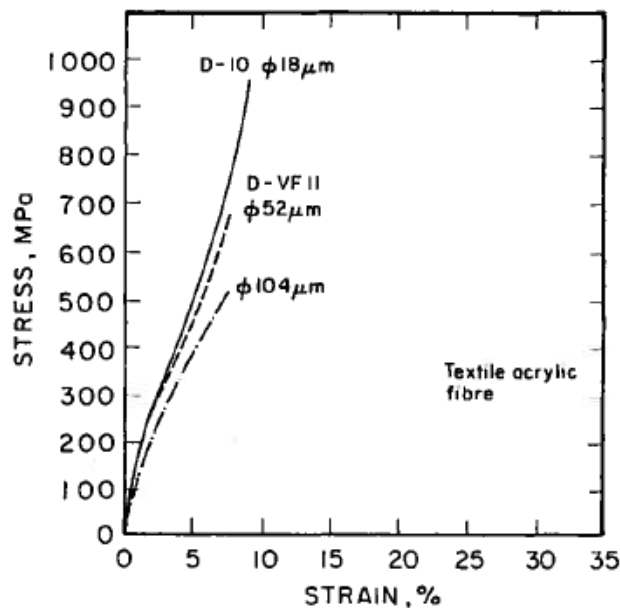
Figure 1-21 Stress-strain curves of acrylic fibers and conventional textile acrylic fibers

Although the properties of acrylic fibers are not as good as those of asbestos, they have been found to be the most promising replacement for asbestos fibers (Figure 1-22) (45). The best result in replacement is achieved when acrylic fibers are used in combination with processing fibers.
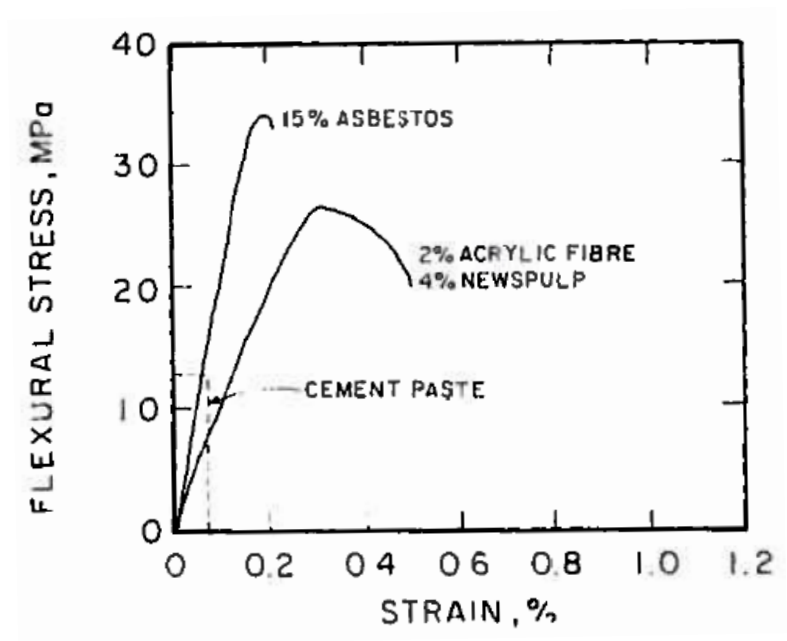
Figure 1-22 Stress-strain curves of asbestos cement and acrylic-cement composite produced to replace asbestos cement

2.6.5.3   Nylon fibers

Nylon was the first truly synthetic fiber to be commercialized in 1939. These fibers are spun from nylon polymer and transformed through extrusion, stretching and heating to finally form a crystalline fiber structure (Figure 1-23).
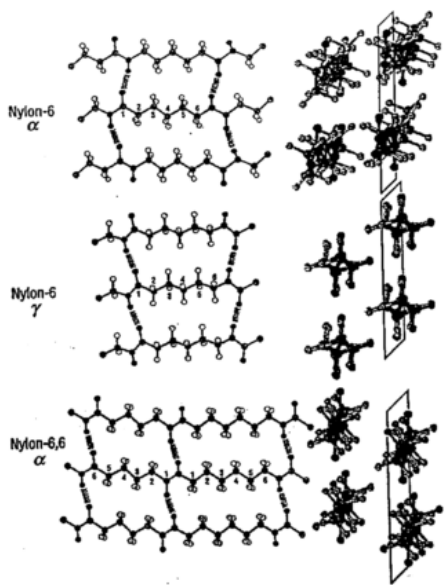
Figure 1-23 Crystal structure of Nylon 6 and Nylon 66

28

Nylon fibers come only in monofilament form. Unlike polypropylene and polyester fibers, the nylon fibers have a hydrophilic nature with a natural moisture balance of 4,5% (9). Due to this strong affinity to water, nylon fibers are bound chemically to the matrix, though the bond is of low strength (in comparison: the bond of polypropylene and polyester fibers is mechanical). Nylon is chemically stable in the alkaline cement environment.

A typical nylon fiber has a tensile strength of about 800 Mpa while the elastic modulus is about 4 GPa. Manufacturers of nylon fibers report that the nylon fibers can be added in smaller dosages to produce the same reinforcing effects as the polypropylene fibers due to nylon fibers having higher aspect ratios (46).

2.6.5.4   Polyester fibers

These fibers come only in monofilament form and belong to the thermoplastic polyester group. They are temperature sensitive and above normal service temperatures their properties may be altered. Like the conventional acrylic fibers described in section 1.6.5.2, the polyester fibers cannot be used in FRC due to their instability in the alkaline cement environment.

2.6.5.5   Polyethylene fibers

Polyethylene fibers have been produced for concrete in monofilament form with wart-like surface deformations, which improve the mechanical bond. Polyethylene in pulp form (a continuous network of fibrillated fibers) can be used as asbestos replacement. The tensile strength is in the range of 80-590 Mpa and the elastic modulus is about 5 GPa for polyethylene fibers currently being used as concrete reinforcement. However there are fibers available with higher elastic modulus (15,4-31,5 GPa) (47).

Concrete reinforced with short, dispersed polyethylene fibers at contents between 2 and 4% by volume have been evaluated and they show linear flexural load deflection behavior up to first crack, followed by an apparent transfer of load to the fibers, permitting an increase in load until the fibers break. Thus, these fibers seem to be very effective for crack control. Figure 1-24 (48) shows that at 4% the maximum load in the post-cracking range exceeds the stress at first crack.
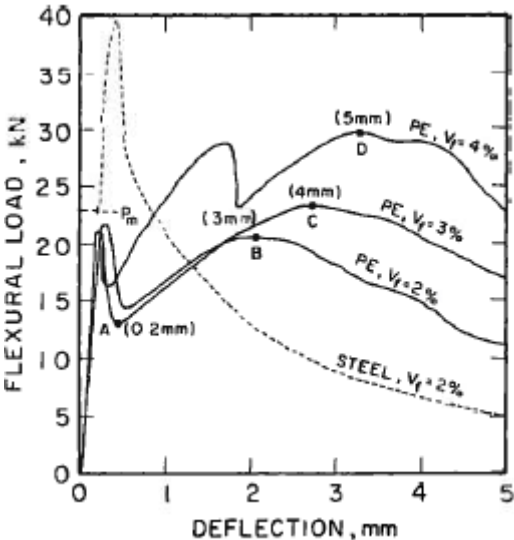
Figure 1-24 The effect of the content of short polyethylene fibers on the load-deflection curves of concretes

2.6.5.6   Carbon fibers

The structure of carbon atoms is shown in Figure 1-25 where the atoms are arranged in a hexagonal array. Numerous filaments (about 10 000) form a tow and carbon fibers consist of these tows. Originally carbon fibers were developed for applications within the aerospace industry due to their high strength and elastic modulus and stiffness properties. Today they are being used in general structural engineering applications. They are more expensive than other fiber types and therefore their commercial use has been limited.
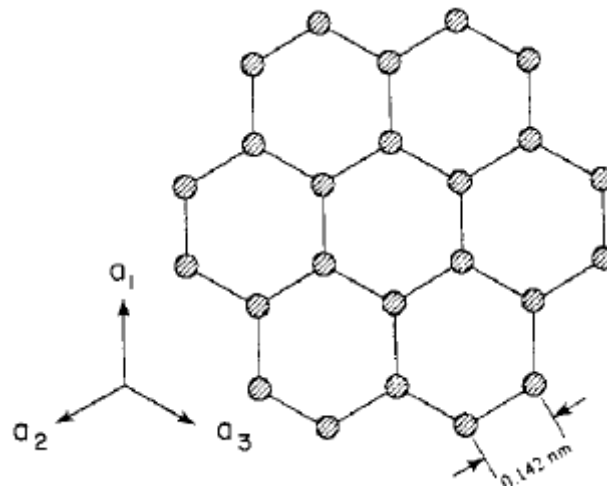
Figure 1-25 Arrangement of carbon atoms in graphite layer

Carbon fibers are produced in two ways; either by baking acrylic fibers with resulting high modulus and high strength (PAN carbon fibers), or from pitch contained in petroleum or coal (pitch carbon fibers). Table 1-8 shows typical properties of both.

	PAN		Pitch
	Type I	Type II	
Diameter (μm)	7.0–9.7	7.6–8.6	18
Density (kg/m^3)	1950	1750	1600
Modulus of elasticity (GPa)	390	250	30–32
Tensile strength (MPa)	2200	2700	600–750
Elongation at break (%)	0.5	1.0	2.0–2.4
Coefficient of thermal expansion $\times 10^{-6}$ °C^{-1}	−0.5 to −1.2 (parallel) 7–12 (radial)	−0.1 to −0.5 (parallel) 7–12 (radial)	—

Table 1-8 Properties of carbon fibers

The PAN carbon fibers are of higher quality and cost and they are manufactured as either Type I (high modulus) or Type II (high strength) (49). The pitch carbon fibers are much less expensive and have superior properties to most other synthetic fibers. They have a lower elastic modulus and strength

than the PAN fibers but the modulus is high enough to exceed that of the cement matrix. This, combined with the low price and the superiority, has made them more attractive for cement reinforcement.

Figure 1-26 (50) shows that the pitch and Pan carbon fibers greatly increase the tensile strength of the composite, while Figure 1-27 (51) shows that carbon addition does not give any significant increase in compressive strength, just a slight increase up to fiber volumes of about 3%. The strength begins to decline for volumes higher than 3%. Figure 1-28 (52) shows the improvement in flexural strength and post-cracking behavior with the addition of carbon fibers.
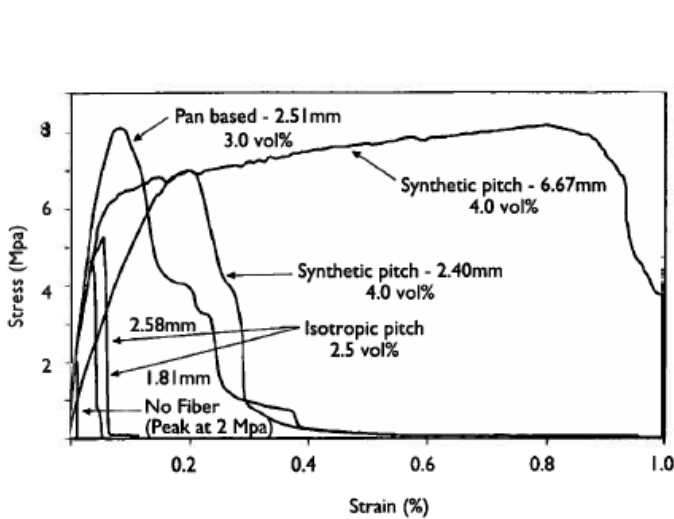
Figure 1-26 Uniaxial tensile testing of carbon fiber reinforced cement
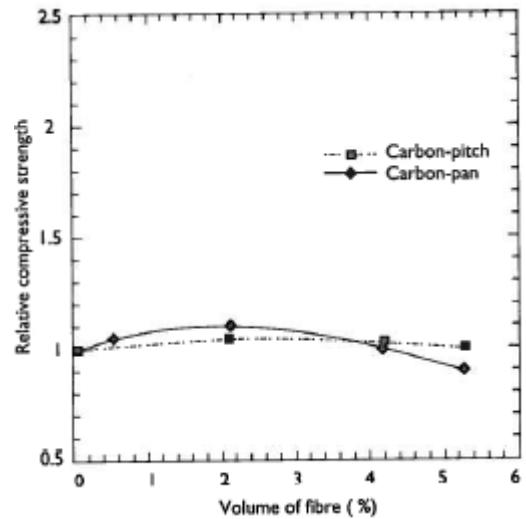
Figure 1-27 Effect of carbon fiber content on compressive strength
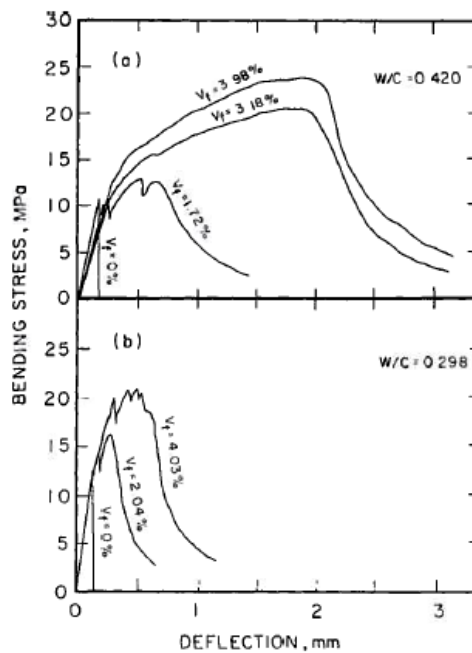
Figure 1-28 Effect of pitch fiber content on the load-deflection curves in bending of mixes with paste matrix.
a) 0,420 w/c
b) 0,298 w/c

Nishioka (49) evaluated the effect of the quality of the fibers on the flexural strength and toughness of the composite and found that they were increased as the fiber strength increased. Pitch fibers with tensile strengths and elastic moduli in the range of 440-764 MPa and 26,6-32,4 GPa, respectively, were used. The result is shown in Figure 1-29. Nishioka (49) further suggested a correlated figure where the average fiber length *after* mixing is plotted against the same properties, see Figure 1-30. This figure shows a better correlation for the data in Figure 1-29 because the fibers tend to breakdown into shorter lengths during mixing. The resulting average fiber length is 0,5 to 0,25 of the original value, according to Bentur (6). Nishioka (49) claims that the originally 10 mm long pitch carbon fibers are broken down to 0,8-1,4 mm during mixing.
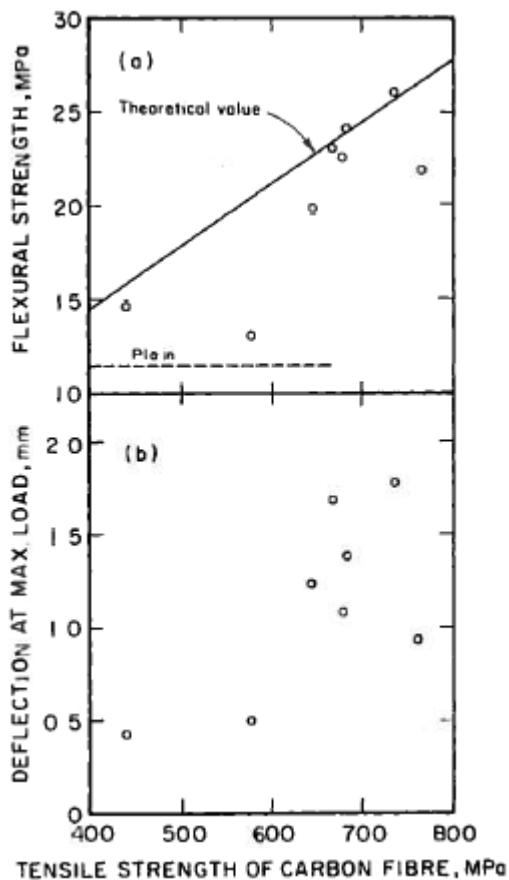
Figure 1-29 Effect of pitch carbon fiber strength on the flexural strength (a) and the deflection at maximum load (b) of a composite with 3% short fibers, 10 mm long and 18 µm in diameter (49)
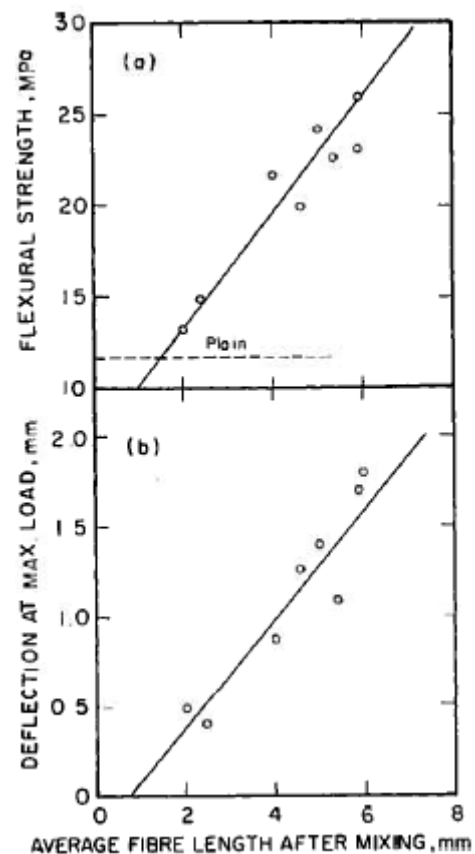
Figure 1-30 Effect of pitch carbon fiber length after mixing on the flexural strength (a) and the deflection at maximum load (b), of a composite with 3% fibers which were 10 mm long prior to mixing (49)

Carbon fiber composites are dimensionally stable, meaning that the fibers (both PAN and pitch carbon fibers) are effective in decreasing strains due to swelling and shrinkage (53, 54). Briggs (55) found that the shrinkage was reduced by a factor of 10 for a 5,6% fiber volume composite, while the creep was reduced by a factor of 6 for a 2% fiber volume.

Carbon fibers composites are also very effective in durability, being inert to most chemicals. After a prolonged testing for alkali resistivity of carbon FRC, it was found that most of the strength and toughness were retained (56).

2.6.5.7 Aramid fibers

Aramid fibers also go by the name Kevlar in the commercial business. They are two and a half times as strong as glass fibers and five times as strong as steel fibers, per unit mass. They have high tensile strength and high tensile modulus. The modulus of elasticity can be as high as 130 GPa depending on the alignment of the molecules to the fiber axis during production. Table 1-9 shows properties of some aramid fibers produced in the US and in Japan. The structure of the aramid fiber and the chemical formula of the aromatic polyamide of aramid fiber are shown below:

Property	Kevlar 49[a]	Kevlar 29[a]	HM-50[b]
Diameter (μm)	11.9	12	12.4
Density (kg/m³)	1450	1440	1390
Modulus of elasticity (GPa)	125	69	77
Tensile strength (MPa)	2800–3600	2900	3100
Elongation at break (%)	2.2–2.8	4.4	4.2

Notes
a Produced by DuPont Company, USA.
b Produced by Teijin Ltd., Japan.

Table 1-9 Properties of aramid fibers
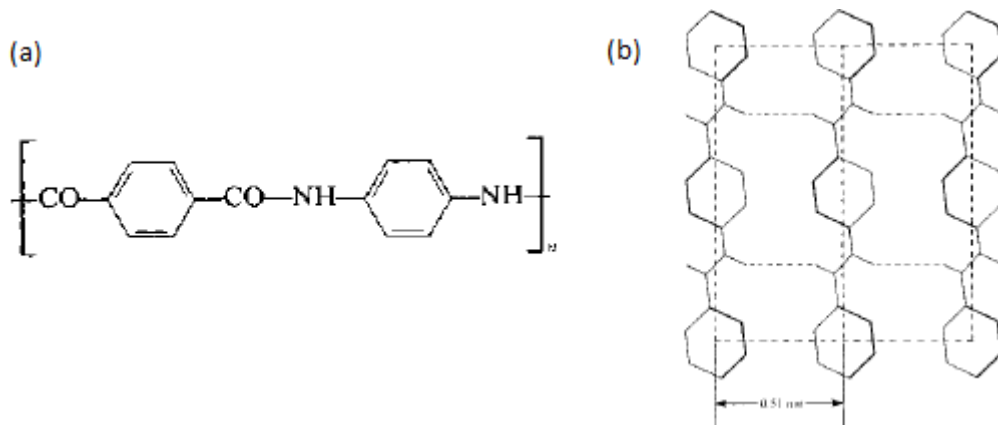
Figure 1-31 (a) Chemical formula (b) Structure of aramid fiber molecules

Aramid fiber-reinforcement enhances the ultimate strength and strain over the first crack strength and strain, leading to a tough composite (Figure 1-32). The figure shows the results found by Walton and Mujamdar (57) after testing composites with short and randomly dispersed fibers with a content in the range of 1-5% by volume. Furthermore they found that the composites retained much of the strength and toughness after two years of ageing but it should be noted that these fibers still are susceptible to alkaline environment even though the rates of attack are low. Ohgishi (58) found that the aramid fibers kept 90% of the initial strength after 10 000 hours of immersion in a pH=12,5 solution. In comparison, the AR glass, carbon and steel fibers kept 42,5%, 41,5% and 99,6%, respectively, of the initial strength. The effect of fiber length and content on the flexural strength and toughness is shown in Figure 1-33, leading to an expected increment.
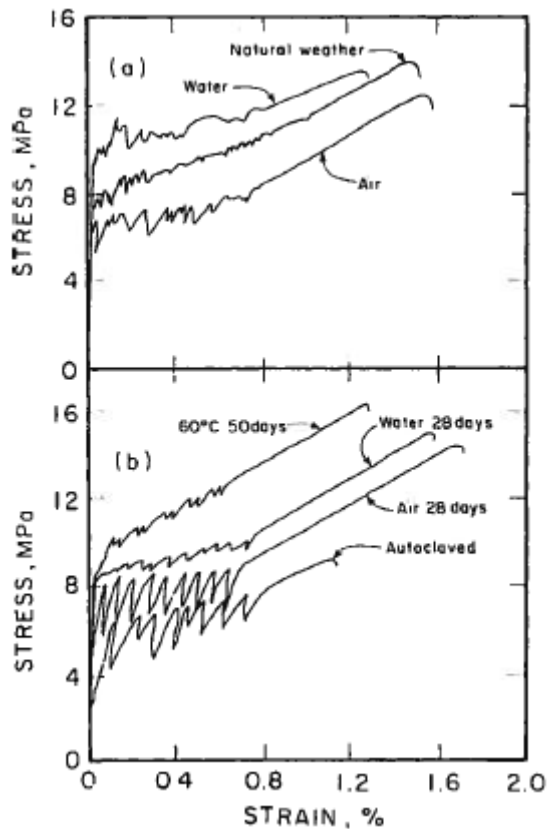
Figure 1-32 Stress-strain curves of cementitious composites reinforced with aramid fibers produced by the spray method. (a) Effect of 2 years weathering (b) Effect of temperature treatments
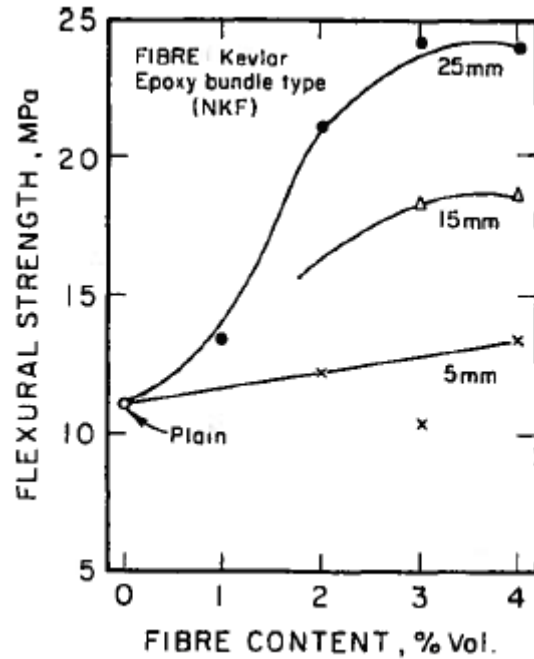
Figure 1-33 Effect of fiber length and content on the flexural strength of mortars reinforced with aramid fibers (58)

2.7   High performance systems

In recent years, extensive efforts have been made to develop new FRC systems with enhanced performance. These composites are not classified after the composition of the reinforcing fibers. Rather, they are defined in terms of the performance and the strategy to achieve it.

Bentur and Mindess (6) write: " *High performance-high ductility FRC composites are usually defined as materials with a strain hardening behavior in tension or deflection hardening in bending. This implies that upon reaching the first crack during loading (either in tension or bending) additional straining of the composite (increase in strain in tension and increase in deflection in bending) will require an increase in load"*. In other words, a concrete exhibiting a strain hardening behavior after cracking gets a higher tensile capacity. It means that the fibers stitch the concrete together when it cracks. If a strain softening behavior is shown, the maximum tensile capacity decreases after the crack opening. It means that the fibers do not contribute in holding the cracks together. The schematic description of the softening/hardening behavior of the composite is shown in Figure 1-34 (59).

To obtain a strain hardening FRC, the fiber content needs to exceed the critical volume (below which the load-bearing capacity of the fibers is smaller than the first crack stress) which is shown in Figure 1-35 (6). It may seem like a basic and simple "rule", but it is difficult in practice due to for example difficulties of incorporating large volumes of fibers in the matrix.
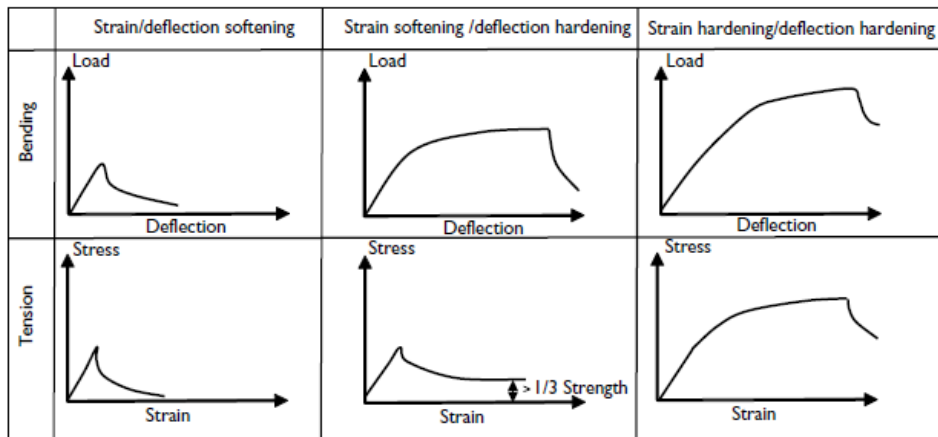
Figure 1-34 Schematic description of strain softening, strain hardening (in tension) and deflection hardening (in bending) in FRC composites
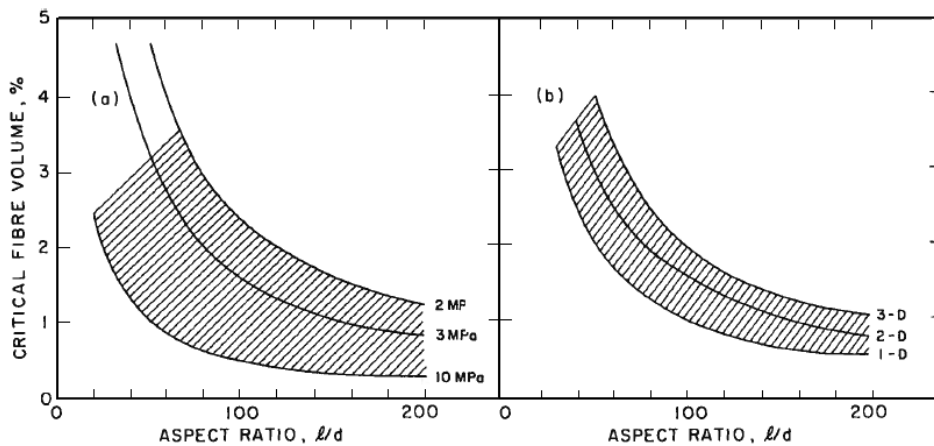
Figure 1-35 Plots of calculated critical fiber volume, $V_{f(crit)}$ vs. aspect ratio l/d for short fibers: (a) composites with different fiber-matrix bond strength (b) Composites of different fiber orientations

Some of the high performance composites which are developed will be outlined in the following sections.

2.7.1 SIFCON and SIMCON

The conventional FRC contains a fiber volume fraction in the range of 1-3% (9) when mixing process is used. With the Hatschek process or spraying, the volume content could rise to about 5-12% with short fibers. Another production method was developed by Lankard (60-62) in which he infiltrated a preplaced steel fiber bed with a fluid cement slurry, leading to a high volume-high aspect ratio fiber-cement composite known as SIFCON (Slurry Infiltrated Fiber Concrete). Maximum fiber volume is a function of several parameters; shape, diameter and aspect ratios of fibers, fiber orientation, the method used in packing, mold size and the extent of vibration (63). Lankard (61) reported fiber contents as high as 20% which leads to great increment in the flexural strength and toughness. Figure 1-36 shows the effect of fiber content in SIFCON product compared with a conventional FRC with a low fiber volume. Homrich and Naaman (63) found that the orientation of the fibers also affected the properties of the composite (Figure 1-37). In another study of SIFCON by Homrich and Naaman, they found that the mode of failure was by fiber pull-out without fiber fracture and the tensile properties are listed in Table 1-10 (64).
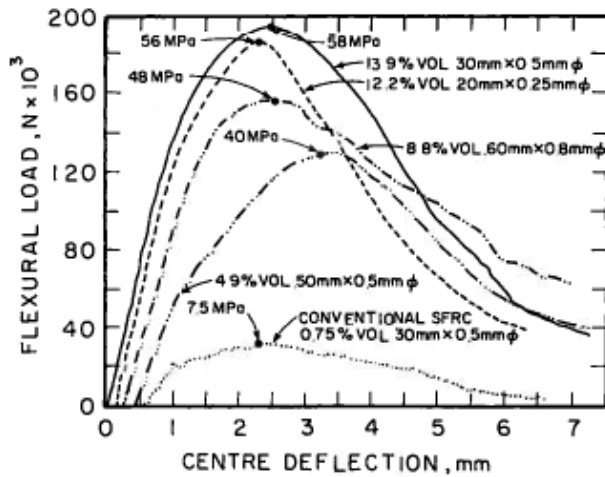
Figure 1-36 Effect of fiber content in SIFCON product on the load-deflection curve of the composite (61)
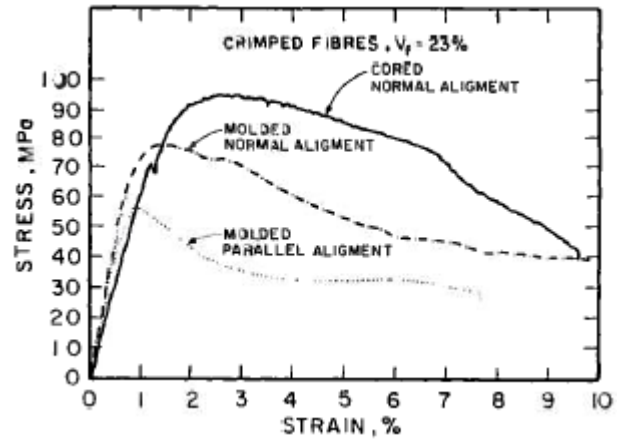
Figure 1-37 Effect of fiber orientation on the behavior of SIFCON product under compression (63)

Type of fibre	Fibre content % vol.	Modulus of elasticity GPa	Maximum stress, MPa	Strain at maximum stress, %	Stress at 2% equivalent strain, MPa
Hooked	12.1	4.6	15.7	1.21	13.7
Deformed	13.8	13.9	16.1	0.68	11.6

Table 1-10 Tensile properties of SIFCON composites with hooked and deformed fibers in a 0,26 w/c ratio matrix

SIMCON (Slurry Infiltrated Mat Concrete) was developed by Hackmann (65). The quest of easier handling of SIFCON at the construction site led to this new technology. SIMCON is fabricated by placing a steel-fiber mat in a mold and infiltrate the slurry onto the mat. With such mats, it is easier to control the orientation and alignment of the fibers. The steel-fiber mats consists of

- Steel wool
- Conventional steel fibers

The mats used in SIMCON consist of conventional steel fibers such as those used in SIFCON. The steel wool has high aspect ratios (in the range of 400-500) which is much greater than for the conventional steel fibers (66). Bentur in a still unpublished work (67) infiltrated steel wool with a 0,3 w/c slurry, which gave a fiber volume of 2-3% of the composite. This gave a flexural strength of about 25 MPa. However, he found that an increase in the fiber volume resulted in reduction in properties due to difficulties in compaction. This can be seen in Figure 1-38. For SIMCON (conventional steel fibers) the relations between fiber content and mechanical properties are shown in Figure 1-39. Krstulovic-Opara and Malak (68, 69) found that SIMCON has much greater efficiency than SIFCON. For example, for 3-5% fiber content in SIMCON, they got a tensile strength in the range of 10-16 MPa. For SIFCON to get the same tensile strength (16 MPa), the fiber content needs to be about 14%.
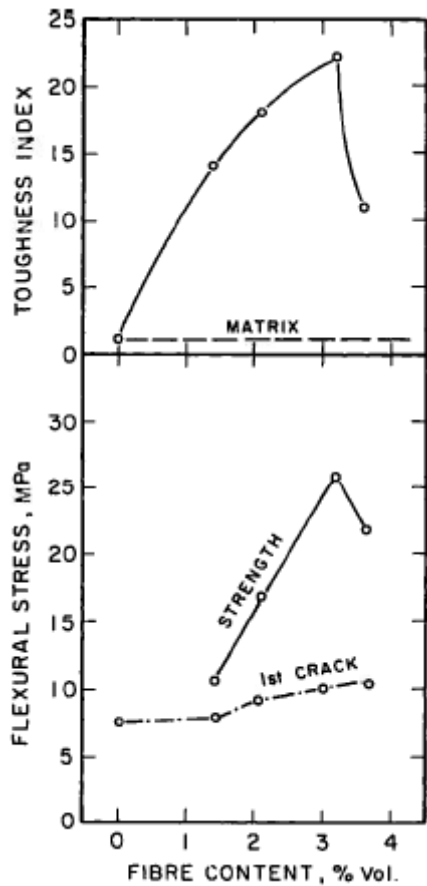
Figure 1-38 Effect of steel wool content on the flexural properties of the composite
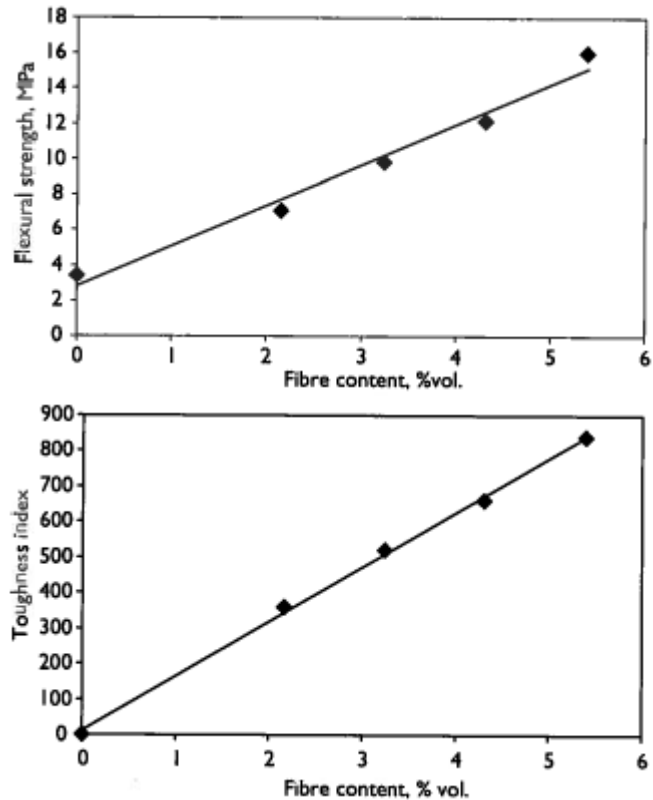
Figure 1-39 Relations between fiber content and mechanical properties in SIMCON system (68)

The main difference between SIFCON and SIMCON is the fiber type. Short fibers are generally used in SIFCON, while a mat with long fibers is used in SIMCON, allowing higher aspect ratios in the latter composite.

SIFCON and SIMCON both exhibit high strengths and contain a high volume percentage of steel fibers compared to SFRC. The ultimate flexural strength is very high and is in the order of magnitude higher than that of SFRC. Also, these composites show excellent ductility and extremely high abrasion and impact resistance when compared with plain concretes and SFRC. Even though these composites possess several desirable properties, they are quite expensive and therefore used only in situations where such unique properties are required or where plain concrete or SFRC cannot perform as expected by the user. These applications include pavement repairs, bridge decks, military applications (for instance under-ground shelters), aerospace launching platforms and others.

2.7.2 Systems with high density matrix

These high performance fiber reinforced systems have extremely dense matrixes. A variety of these composites have been developed, such as RPC (reactive powder concrete), DUCTAL® (a newer generation of RPC), CRC (compact reinforced composite) and CARDIFRC®. The one feature they all have in common is the extremely dense matrix with w/c smaller than 0,20 and the incorporation of 2-6% of meso-steel fibers with a diameter in the range of 0,1-0,2 mm and length of 5-15 mm. Also, other common features are the use of relatively large cement content (750-1000 kg/m^3) and a compressive strength in the range of 100-160 MPa (the strength can be further increased by thermal curing). Properties of these composites are shown in Table 1-11 (16).

Ingredient	DSP/CRC [12]	RPC, [44]		RPC with range of aggregates, [9]	
		20° and 90°C curing	Autoclave curing	Fillers only	Graded aggregate
Cement	750 kg/m³	I	I	934 kg/m³	937 kg/m³
Silica fume	179	0.23–0.25	0.23	234	235
Filler, < 1.0 mm	572[a]	1.1–1.49[b]	0.89[c]	1030[d]	—
Sand fraction (1–4 mm)	460–690	—	—	—	—
Graded aggregate (up to 8 mm)	—	—	—	—	1031
Water	169	0.17–0.19	0.19	215	200
Fibre content	3–12% vol.	I–3% vol.	I–3% vol.	2.4%	2.4%
w/cm	0.18	0.14–0.15	0.15	0.18	0.17
Compressive strength, MPa — 20°C curing	—	170–230[e]	—	~160	~160
90°C curing	—	—	—	~160	~160
Autoclave curing	—	—	490–680	~190–210	~190–210
Flexural strength, MPa — 20°C curing	~10–40	30–60[e]	—	45.7	35.5
90°C curing	—	—	—	48.3	40.6
Autoclave curing	—	—	45–141	60.1	40.7

Table 1-11 Properties of composites with low w/c, high strength matrices

In the following subsections, the RPC and CRC will be further gone through.

2.7.2.1 Reactive Powder Concrete (RPC)

This composite was first produced in France in the early 1990s, but the concept was first developed by P. Richard and M. Cheyrezy. Reactive powder concrete is an ultra-high-strength and high ductility cementitious composite with advanced mechanical and physical properties. The dense matrix is made of well graded particles with the maximum size of about 0,6 mm in order to yield maximum density (6). Small powder-like particles, the dense matrix and the addition of 2-5% of steel fibers give a compact composite with refined microstructure and homogeneity. Richard and Cheyrezy (70) propose the following principles for developing RPC:

- Elimination of coarse aggregates for enhancement of homogeneity
- Utilization of the pozzolanic properties of silica fume
- Optimization of the granular mixture for the enhancement of compacted density
- The optimal usage of superplasticizer to reduce w/c and improve workability
- Use of pressure (before and during setting) to improve compaction
- Improvement of microstructure by post-set heat treatment
- Addition of steel fibers to improve ductility

By using these principles, it is reported that very high compressive strengths of 200 to 800 MPa can be obtained. For RPC giving about 200 MPa in compressive strength, the flexural strength obtained is in the range of 30-60 MPa. Similarly, for about 800 MPa in compressive strength, the flexural strength is in the range of 45-141 MPa (70). For application of this composite, RPC is seen as a promising material for special prestressed and precast concrete members, including industrial and nuclear waste storage facilities.

2.7.2.2   Compact Reinforced Composite (CRC)

CRC was developed in 1986 at Aalborg Portland cement factory in Denmark. CRC is built up of a very strong and brittle fiber reinforced matrix called DSP (densified small particles). CRC specimens consist of a high concentration of steel fibers and an equally large concentration of conventional steel reinforcing bars which are uniformly and continuously placed. This makes the CRC very ductile and it makes it possible to utilize steel bars much more effectively without having large cracks. Typical mechanical properties could be a compressive strength of 140-400 MPa and a bending strength of 100-300 MPa (71).

CRC is mostly used for slender structures such as balcony slabs, walk-ways and staircases, but also where special properties are required such as high strength lining blocks for mines. Another special application of CRC is for in-situ cast joints between precast members. Figure 1-40 shows a staircase made of CRC.

Figure 1-40 Example of staircase made of CRC. There are no supporting beams for the staircase; the load is carried by the steps

2.8 Fresh concrete properties

The main challenge of FRC is to introduce a sufficient volume of uniformly dispersed fibers to achieve the desired improvements in mechanical behavior, while retaining sufficient workability in the fresh state to permit proper mixing, placing and finishing. Regarding workability, self-compacting concrete (SCC) has been found to give the best possible effect of fiber insertion compared with conventional concrete. In this chapter, the fresh characteristics of SCC are reviewed; segregation resistance, filling ability and passing ability.

2.8.1 Characterization of SCC

Maage (72) writes about SCC: "*A common requirement is a slump-flow larger than 60 cm in order to characterize the concrete as self-compacting.*" Opsahl (73) writes that it is common to require a slump-flow value larger than 650 mm in order for the concrete to be characterized as self-compacting.

Self-compacting concrete homogeneously spreads due to its own weight only, without any additional compaction energy (such as pokers) and spreads without entrapping air. The motivation for applications of SCC has been:

- Elimination of vibration
- Improved working conditions: workers are not exposed to noise and vibration from compaction equipment
- Increased quality: becomes independent of degree of vibration
- Increased productivity: shorter casting periods and less resources needed for producing the concrete
- Improved characteristics in the hardened state
- Larger architectural freedom in structural design

For SCC to homogeneously fill a mold, high demands with regard to segregation resistance, filling ability and passing ability have to be fulfilled.

2.8.2 Segregation resistance

Segregation resistance is the ability of a concrete to remain homogeneous while in its fresh state. This implies concrete stability in dynamic conditions (during transport and placing) and in static conditions (after placing), which is a challenge due to the high flowability of SCC. High segregation resistance can be obtained by using high amount of fine material (filler, limestone powder, ground granulated blast slag, fly ash, silica fume) and/or by adding special stabilizing admixtures that increase the viscosity of the matrix and thus increasing the concrete viscosity and stability. Special attention should be drawn to the addition of silica fume, because too large amounts may lead to increased yield strength, causing the concrete to lose its self-compacting property. Common test methods to determine the segregation resistance are Settlement Column test, Sieve Stability test, Penetration apparatus and visual observation on the slump flow spread (section 1.8.7.4).

2.8.3 Filling ability

The filling ability of SCC is its ability to flow under its own weight (without vibration) into and fill completely all spaces within formwork containing obstacles such as reinforcement. The inter-particle friction between the various solids affects the filling ability. Such solid-to-solid friction increases the internal resistance to flow, limiting the filling ability and speed of flow. The addition of

superplasticizer can disperse cement grains and reduce these inter-particle frictions and enable the reduction in water content while maintaining the required levels of flowability and viscosity. The filling ability is enhanced by reducing the aggregate volume and increasing the paste volume. Test methods for filling ability are for example slump-flow, T_{500}-test and U-Box.

2.8.4   Passing ability

Passing ability is the ability of SCC to flow through openings approaching the size of the mix's nominal maximum-size aggregate, such as spaces between steel reinforcing bars, without segregating or blocking. Blocking develops easily if the size of the aggregate is relatively larger than the size of the opening. Insufficient passing ability can also be caused by the presence of coarse aggregate and a high content of aggregate. Test methods for determining the passing ability are J-ring (in combination with slump flow), L-Box, U-Box, V-funnel, Orimet and filling vessel test.

The test methods proposed to characterize segregation resistance, filling ability and passing ability of SCC are summarized in Table 1-12 (74). Some of these methods will be described in section 1.8.7.

Test	Property			
	Filling ability	Viscosity	Passing ability	Segregation resistance
Slump flow	Total spread	t_{500} time	–	(Paste rim)
J-ring	Total spread[1]	t_{500} time[1]	Stop height, total flow[3]	–
Kajima box	Flow time	–	Visual	–
V-funnel	–	Flow time[2]	(Blocking at orifice)	–
Orimet	–	Flow time[2]	(Blocking at orifice)	–
O-funnel	–	Flow time[2]	(Blocking at orifice)	–
L-box	–	–	Blocking ratio[3]	–
Penetration	–	–	–	Depth
Sieve stability	–	–	–	Percent passing 5 mm
Settlement column	–	–	–	Segregation ratio

[1]If OK passing ability
[2]If no blocking at orifice
[3]If OK filling ability

Table 1-12 Selected test methods for SCC

2.8.5   Rheology as a tool to characterize SCC

Rheology is the study of flow and deformation of materials and it is concerned with the relationships between stress, strain, rate of strain and time. It is generally accepted that the basic property influencing the performance of fresh concrete in casting and compaction is its rheological behavior. Generally for fluids, there are several models available to characterize the rheological behavior, see the figure below.
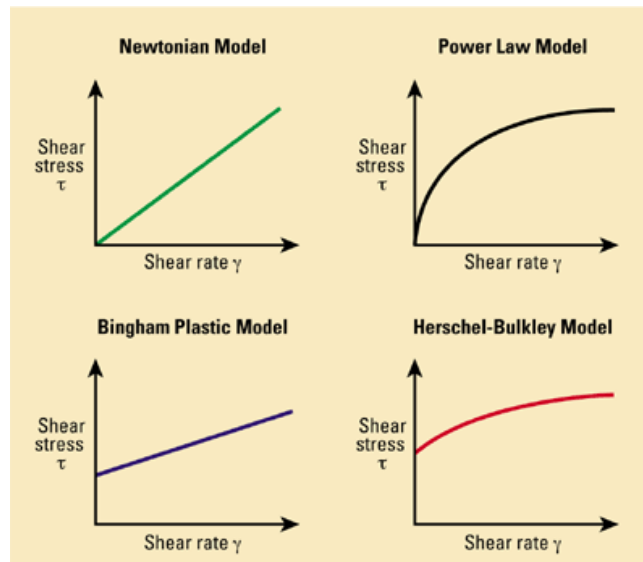
Figure 1-41 Rheological models

The Newtonian model states a linear relationship between the shear stress and the shear rate. Both parameters are linked by a constant factor defined as the plastic viscosity, which is a measure of the resistance to the flow of materials:

$$\tau = \mu \times \gamma$$

Where

τ is the shear stress in Pa or N/mm^2

μ is the plastic viscosity in Pa.s

γ is the shear rate in 1/s

Experimental data has confirmed that the rheology of self-compacting concrete is described by the two parameters of a Bingham model, yield stress and plastic viscosity (75). The Bingham model describes the flow behavior of suspensions more generally and it is defined as:
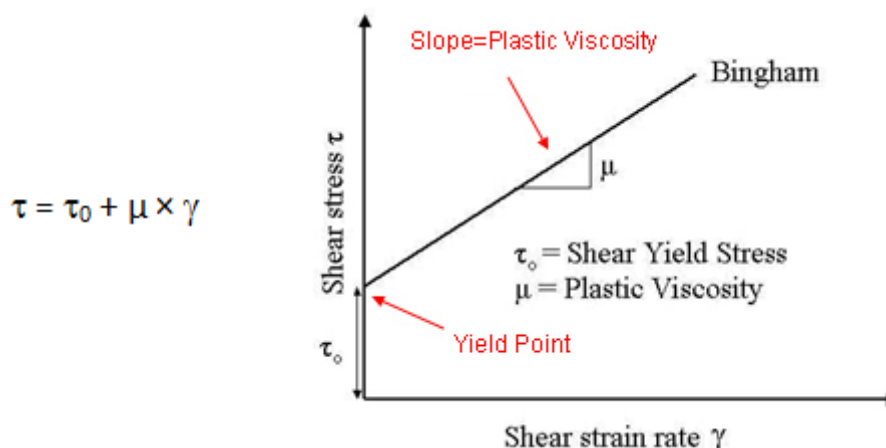
The yield stress (τ_0) is a measure of the shear stress required to initiate the flow. Beyond this value, the shear stress is linearly related with the increase of the rate of shear. The Bingham model reduces to the Newtonian model if the yield stress value is equal to zero.

The rheological behavior is also time-dependent, as mentioned above. SCC has in many cases proven to be thixotropic, which means that the material rapidly loses its flowability when allowed to rest undisturbed, but regains the flowability when energy is applied. At a constant shear rate, the thixotropic material undergoes a structural breakdown while being deformed, whereas the structure rebuilds at rest. Hence, the response is time-dependent.

2.8.6 Optimizing yield stress and plastic viscosity

Proportioning SCC is a balance between obtaining both sufficient flow and stability, which means that the yield stress and the viscosity values have to be low. But too low viscosity will cause instability. Hence, the viscosity value that does not cause instability has to be obtained. The following table shows a very rough estimation of compositions and rheological properties of SCC in selected countries (76).

Country	Powder (kg/m^3)	Water (kg/m^3)	Yield value (Pa)	Plastic viscosity (Pa s)
Sweden	>550	180	0–30	50–100
The Netherlands	>550	190	0–10	60–120
Japan	>550	170	0–30	50–120
France	?	?	0–10	>60
Switzerland	<450	200	0–50	110–20
Norway	<450	170	10–50	30–45
Iceland	<450	180	10–50	20–40
Denmark	<450	160	30–60	<40
UK	>500	210	10–50	50–80
Germany	>500	180	0–10	60–90
USA	>500	190	0–20	40–120

Table 1-13 Composition and rheological properties of SCC

Wallevik (77) suggested a figure showing the plastic viscosity and yield stress that should be obtained to avoid segregation and difficult flow, see Figure 1-42. This was a result of rheological measurements on SCC with a wide range of compositions. The measurements resulted in ranges of plastic viscosities of 7-160 Pa.s and yield values from 0-60 Pa. Restricted flow is observed for concretes with high rheological properties, while segregation is observed for concretes with low rheological property. In a study by Nielsson and Wallevik (78), they combined the values in Figure 1-42 with the related minimum slump flow to achieve SCC. This is shown in Figure 1-43. The target values of SCC concerning yield value and plastic viscosity is marked as the dark grey region.
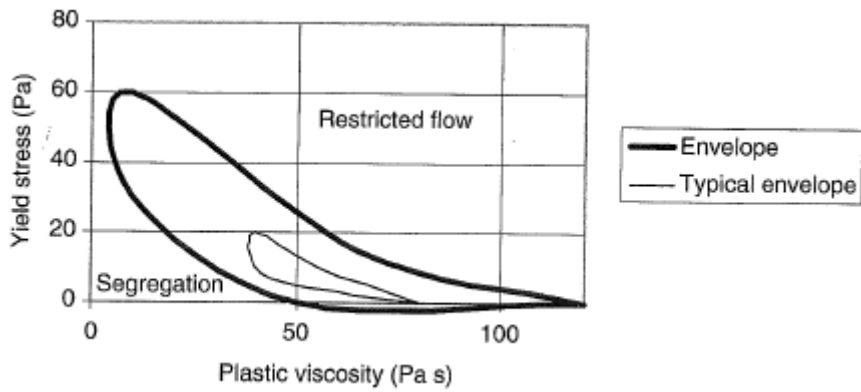
Figure 1-42 Suggested approximate envelope of yield stress and plastic viscosity for SCC
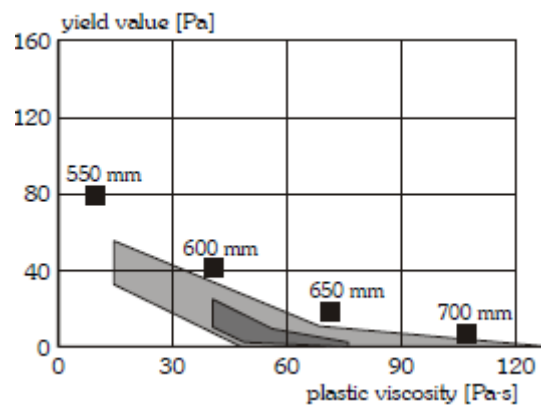
Figure 1-43 Target range of SCC and the related minimum slump flow

There are equations available that can be used to calculate approximate values of the viscosity and the yield stress. The equation proposed by Krieger and Dougherty (79) is based upon the Newtonian model and a homogeneous matrix. It shows that there is an increase in the viscosity of the medium when particles are added. This increase depends on the concentration of the particles:

$$\frac{\mu}{\mu_{matrix}} = \left(1 - \frac{\phi}{\phi_{max}}\right)^{-[\mu]\phi_{max}}$$

Where

μ is the viscosity of the suspension

μ_{matrix} is the viscosity of the base medium

ϕ is the volume concentration of particles

ϕ_{max} is the maximum packing

$[\mu]$ is the intrinsic viscosity of the matrix, which is 2,5 for spheres

If the viscosity of the cement paste along with the concentration of the aggregates are known, and the maximum packing of the particles is determined, then the viscosity of the concrete can be calculated.

Similarly, an equation for the calculation of yield stress was proposed by Coussot and co-workers (80). The matrix is also considered homogeneous:

$$\frac{\tau_0}{\tau_{0,\text{matrix}}} = \left(1 - \frac{\phi}{\phi_{max}}\right)^{-m}$$

Where

τ_0 is the yield stress of the suspension

$\tau_{0,\text{matrix}}$ is the yield stress of the matrix

m   is a constant; m = 1 for ϕ < 0,6 and a broad particle size distribution

Other equations that take the effect of aggregate grading and size distribution into account have been proposed. For the calculation of yield stress, Flatt (81) introduced an equation taking into account the interparticle forces that occur in super-plasticized cement paste:

$$\tau_0 = m_1 \frac{(\phi - \phi_0)^2}{\phi_{\text{max}} (\phi_{\text{max}} - \phi)}$$

Where

m_1 is a function of the particle size distribution

ϕ_0 is the percolation solid fraction

Several test methods are applied to measure the yield stress and the plastic viscosity of SCC, mainly LCPC-Box and different viscometers and rheometers.

In the following section, some common selected test methods applied to characterize the fresh concrete properties will be described.

2.8.7 Test methods on fresh concrete

The most used test method to measure or characterize the workability of fresh concrete is the slump test. It is an imprecise method, but it is used widely because of the simplicity of the method. However, the slump measure is applied for conventional concrete as it is a static test, and this test is not suitable for fiber-reinforced cement composites because it does not give a good indication of the workability of the composite. For such situations, it is recommended that tests in which dynamic effects are involved be used.

2.8.7.1 Slump-flow test

The slump-flow test is developed specifically for self-compacting concrete and is standardized in ASTM C1611 (82). In Norway, this method is standardized in NS-EN 12350-8 (83). This method provides information on filling ability (flowability) and passing ability of SCC. It is actually a new modification and combination of the slump test and the flow board test, both of which are shown in Figure 1-44 below. The base plate is of metal and is marked with two visible diameter circles (300 and 500 mm) (Figure 1-45, also showing other specifications). A reinforcement ring called J-Ring can also be used to simulate the resistance as the concrete flows between the bars (Figure 1-46).
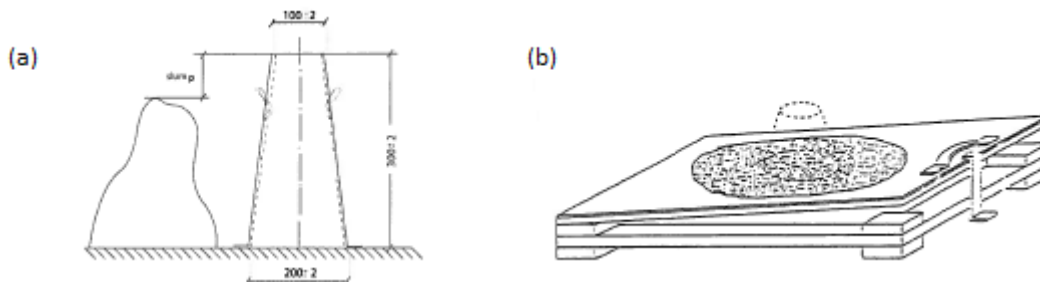
Figure 1-44 (a) Slump measurement (b) Flow board measurement
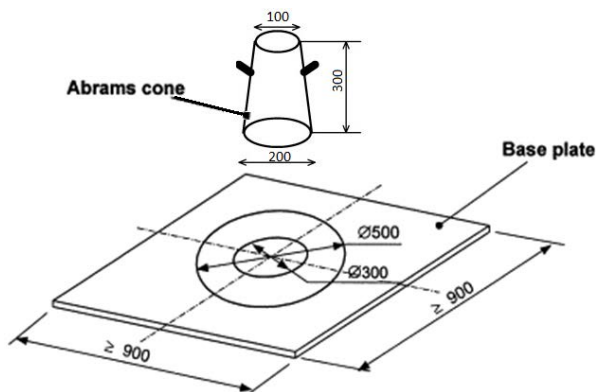
Figure 1-45 Slump-flow test set-up

Figure 1-46 Slump-flow with reinforcement ring (J-Ring)

The test procedure is very simple. Abrams cone is placed in the center of the base plate and a fresh concrete mix is poured into the cone, just like in ordinary slump test. After lifting of the filled and previously moistened cone, the time (T_{500}) required for the concrete to spread over the circle of 500 mm in diameter is measured. When the concrete stops flowing, two diameters (the largest and the one perpendicular to it) of the concrete circle are measured. The final value, which is denoted as the

slump-flow value, is the average of the two. If there are large differences between the two diameters, indicating a non-level surface, then this must be corrected.

2.8.7.2 T_{500} test

As mentioned above, the T_{500} is measured during the slump flow measurement. It is a measure of the viscosity of the SCC. The stopwatch, which has 0,1 second accuracy, is started as the filled cone is lifted and it is stopped when the SCC flow reaches the 500 mm in diameter mark.

2.8.7.3   J-Ring test

This test is standardized in ASTM C1621 (84). In Norway, it is standardized in NS-EN 12350-12 (85). and it is a measure of the passing ability of the concrete, indicating how easily it flows through obstructions, such as reinforcement. The difference in slump flow between a test run with the J-Ring and a test run without the J-Ring, is an indicator of the passing ability of the concrete. A difference greater than 50 mm indicates poor passing ability, while a difference less than 25 mm indicates good passing ability. The ring itself is a cage of rebar, in which the Abrams cone is placed. It consists of a 25 mm thick rigid ring supported on sixteen 16 mm diameter rods equally spaced on a 300 mm diameter circle, see Figure 1-47. The height of the rods is 100 mm.

Dimension	in.	mm
A	12.0 +/- 0.13	300 +/- 3.3
B	1.5 +/- 0.06	38 +/- 1.5
C	0.625 +/- 0.13	16 +/- 3.3
D	2.36 +/- 0.06	58.9 +/- 1.5
E	1.0 +/- 0.06	25 +/- 1.5
F	4.0 +/- 0.06	100 +/- 1.5
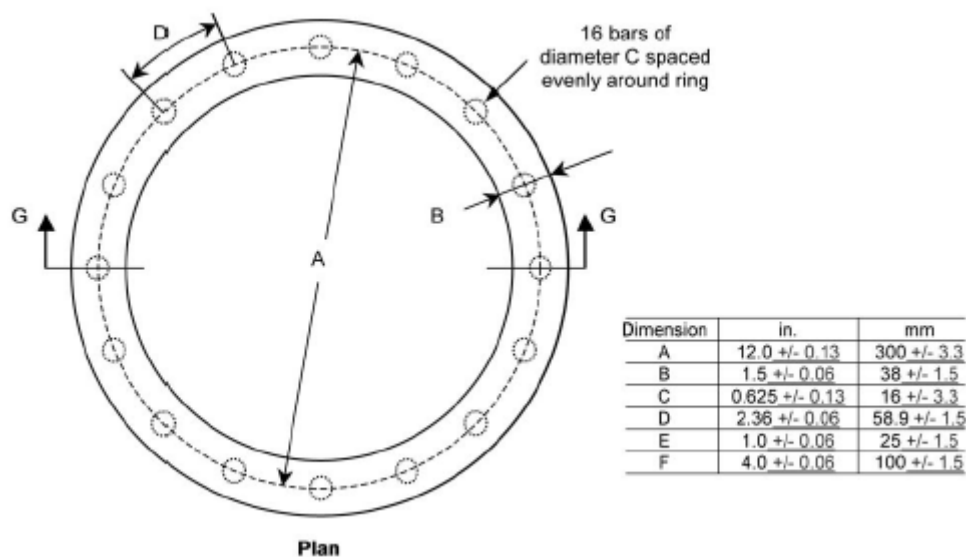
Figure 1-47 Schematics of the J-Ring (84)

The J-Ring test is applied in laboratories to compare the passing ability of different concrete mixtures. It is also applicable in the field as a quality control test.

The J-Ring flow is calculated according to the following equation:

$$J - \text{Ring flow} = \frac{(j_1 + j_2)}{2}$$

Where

    j_1 is the largest diameter of the circular spread of the concrete from the J-Ring test

    j_2 is the circular spread of the concrete at an angle circa perpendicular to j_1

The slump flow is calculated in the same way:

$$\text{Slump flow} = \frac{(d_1 + d_2)}{2}$$

Where

   d_1 is the largest diameter of the circular spread of the concrete from the slump flow test

   d_2 is the circular spread of the concrete at an angle circa perpendicular to d_1

Following these calculations, the difference between slump flow and J-Ring flow is calculated to the nearest 10 mm. Finally the blocking assessment is identified from a table, see Table 1-14.

Difference Between Slump Flow and J-Ring Flow	Blocking Assessment
0 to 25 mm [0 to 1 in.]	No visible blocking
>25 to 50 mm [>1 to 2 in.]	Minimal to noticeable blocking
>50 mm [>2 in.]	Noticeable to extreme blocking

Table 1-14 Blocking assessment (84)

2.8.7.4   Visual Stability Index test

Like the T_{500} test, this test is standardized in ASTM C1611 (the slump-flow test). As the name indicates, it is a test where the stability of SCC is observed visually by examining the concrete mass. This test can therefore be used for quality control of self-compacting concrete mixtures. The test ranks the stability of the SCC on a scale from 0 to 3.

The procedure is very simple. After spreading of the concrete in the slump flow test has stopped, the technician observes the distribution of the coarse aggregate within the concrete mass, the distribution of the mortar fraction, and the bleeding characteristics. From these observations, a Visual Stability Index (VSI) value is assigned to the concrete spread by using the criteria shown in Table 1-15 and by comparing the concrete spread to illustrations given in the standard. These illustrations are given below in Figure 1-48. A VSI of 0 indicates no segregation, while a VSI of 3 indicates obvious segregation and paste separation from the concrete mix. The values of 0 and 1 give a stable mix, while values of 2 and 3 give an unstable mix.

VSI Value	Criteria
0 = Highly Stable	No evidence of segregation or bleeding.
1 = Stable	No evidence of segregation and slight bleeding observed as a sheen on the concrete mass.
2 = Unstable	A slight mortar halo ≤ 10 mm [≤ 0.5 in.] and/or aggregate pile in the of the concrete mass.
3 = Highly Unstable	Clearly segregating by evidence of a large mortar halo > 10 mm [> 0.5 in.] and/or a large aggregate pile in the center of the concrete mass.

Table 1-15 Visual Stability Index values
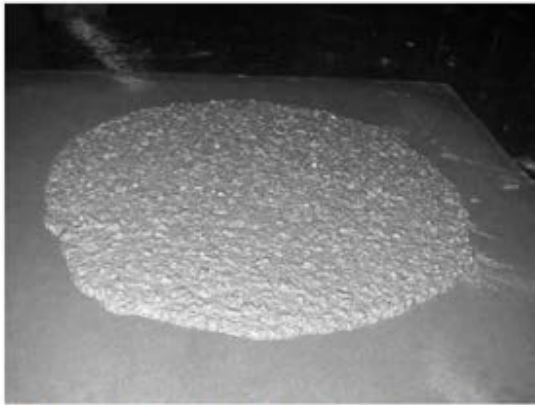
FIG. X1.1 VSI = 0 – Concrete Mass Is Homogeneous and No Evidence of Bleeding.

FIG. X1.2 VSI = 1 – Concrete Shows Slight Bleeding Observed as a Sheen on the Surface.

FIG. X1.3 VSI = 2 – Evidence of a Mortar Halo and Water Sheen.
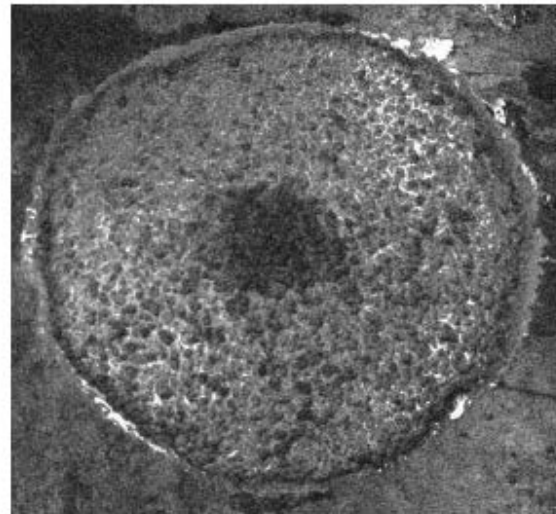
FIG. X1.4 VSI = 3 – Concentration of Coarse Aggregate at Center of Concrete Mass and Presence of a Mortar Halo.

Figure 1-48 Concrete spread in ASTM C1611

2.8.7.5   The LCPC-box

One rheological property that needs to be measured is the yield stress. The slump flow test has some limits in the region of large flows because the thickness of the concrete sample (the concrete spread) starts to become thinner than the thickness of the aggregates. If the fluid mechanics equations are to be applicable, then the thickness of the sample must be at least five times the size of the largest particle (86). This means that the flow is then considered as the flow of a homogeneous mixture. The SCC slump flow, due to its thickness/particle ratio, can therefore not be considered as a homogeneous flow. Due to this, a direct correlation between yield stress and the measured spread does not exist. Hence, the slump flow test cannot be used to measure a value of the yield stress. For example, a higher slump flow cannot automatically mean a lower yield stress. This is shown in Figure 1-49, where two SCC samples are both stable and have the same yield stress. The first sample is composed of a very fluid cement paste and a high volume of small particles, while the second sample is composed of a less fluid cement paste and a lower volume of large particles. Consequently, the slump flow value of the first sample will be higher than the second one. Similarly, Figure 1-50 shows that there is no direct correlation between yield stress and slump flow for SCC with various composition (86).
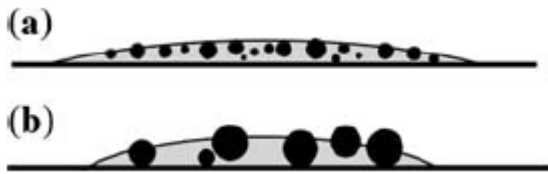
Figure 1-49 Both SCC have the same yield stress, but (a) has a higher slump flow value than (b)
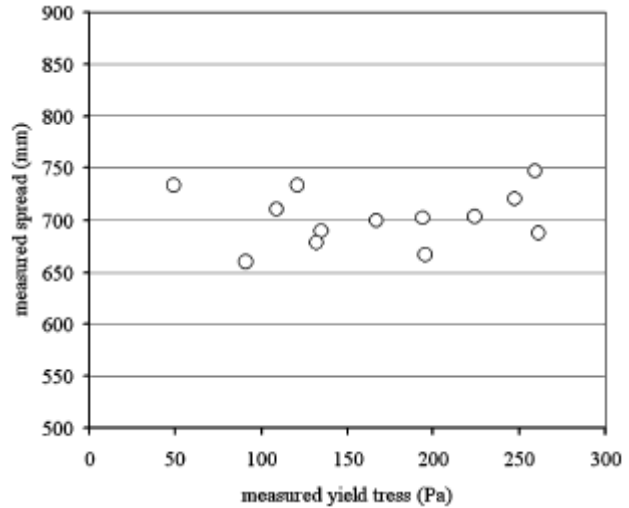
Figure 1-50 Yield stress measured for various SCC, all having a 700 ± 50 mm slump flow

To correlate the measured empirical value to the yield stress, a new method was developed, the LCPC-box. This method allows the measuring of the yield stress. The solution proposed to overcome the issues from slump flow test by pouring the concrete from a 6 liters bucket at one end of a long channel called the LCPC-box. The width of the channel is $l_0 = 200$ mm, the length is 1200 mm and the height is 150 mm, as shown below.
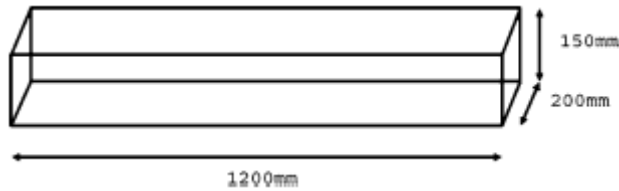
Figure 1-51 LCPS box geometry

In Roussel's research (86), it was showed that the LCPC-box fulfilled the conditions to represent the rheological behavior of the tested SCC and the conditions for a direct correlation between yield stress and the measured spread to exist. It is however not possible to get an explicit solution for yield stress as a function of spread length L. The flow profile in the LCPC-box has been solved for analytically. By measuring the spread length L (showed in Figure 1-52), which is the average of maximum spread length and lateral wall spread length, the ratio yield stress/specific gravity can be read from a figure showing correlation between these two (Figure 1-53). Thus, the yield stress can be calculated.
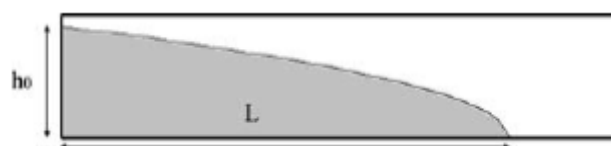
Figure 1-52 Shape at stoppage in the LCPC-box

50
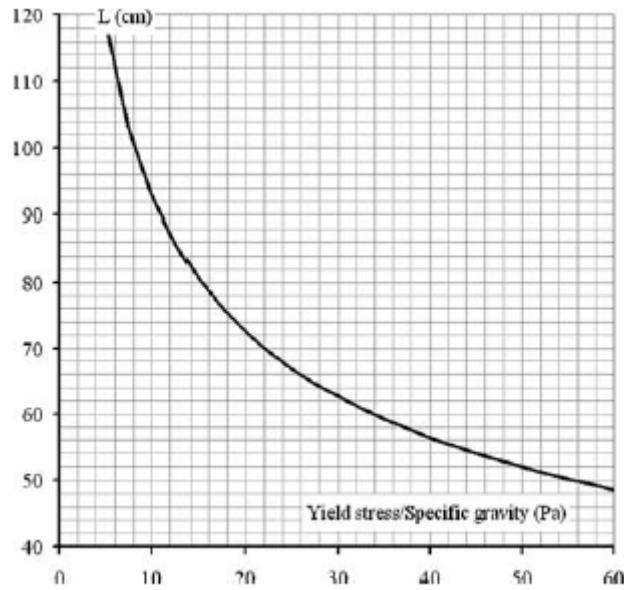
Figure 1-53 Correlation between the spread length L in the LCPC-box and the ratio yield stress/specific gravity for the SCC tested

2.8.7.6   Other test methods

Various workability tests have been devised over the years and only a few of these have been standardized. Grünewald (87) used a lot of different evaluation methods to study the three key properties of SCC (filling ability, passing ability and segregation resistance) in the fresh state. He performed the tests on self-compacting fiber reinforced concrete (SCFRC) and regular SCC. He used the BML-Viscometer to find the yield strength and plastic viscosity. To study the filling ability: the slump flow, T_{500}, V-funnel, Fiber funnel and Mortar funnel tests were performed. Similarly, slump flow with J-Ring, Filling vessel and U-box tests were applied to study the passing ability of the fresh concrete. Also, to study the segregation resistance, the wash-out test was performed. In Table 1-16 the applied test methods for SCC and SCFRC are shown. Similarly, figures of some tests are shown in Figure 1-54.

Test method	SCC series PS/OS	SCFRC series PS/OS	SCC/SCFRC series MS
Slump flow / T_{50}	X	X	X
Segregation test	X (only OS)	X (only OS)	-
Air content[1]	X	X	X
V-funnel	X	-	X
Fibre funnel	X	X	-
BML-Viscometer	X (only OS)	X (only OS)	-
J-ring	X	X	X
Filling vessel test	X	-	-
U-box	X	-	-

Table 1-16 Applied test methods for SCC and SCFRC in the fresh state
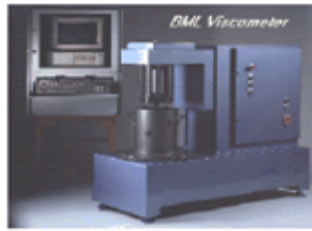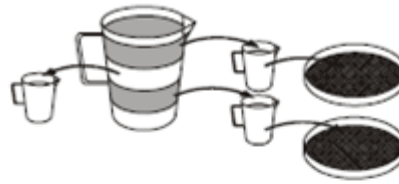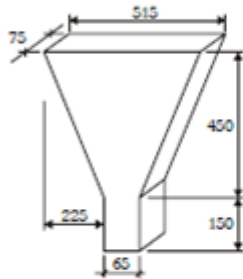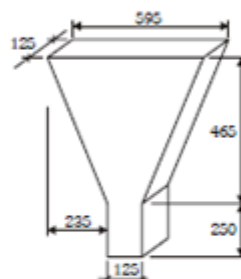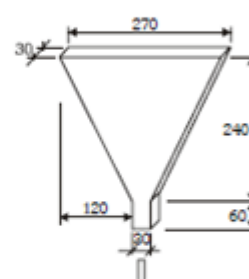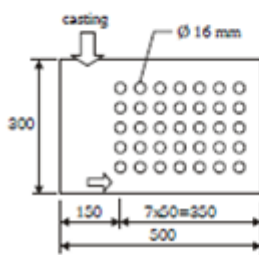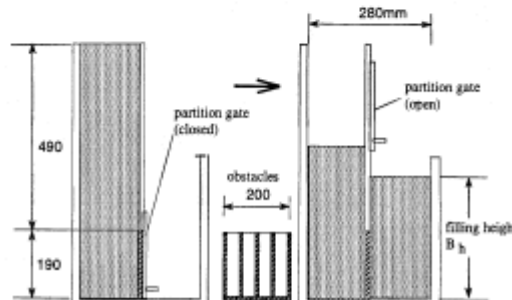
Figure 1-54 Principal pictures/sketches of various tests performed on SCFRC and SCC in fresh state

VeBe test is suitable for the characterization of the workability of fresh FRC in the laboratory, but not for quality control on site. This test is described in NS-EN 12350-3: *Testing fresh concrete-Part 3: Vebe test* (88). The test procedure consists of placing a standard cone in a cylindrical container and filling it with the fresh concrete. The cone is removed and a transparent disc is swung over the top of the concrete, lowering it carefully until it just comes into contact with the concrete. The container is then vibrated until the lower surface of the transparent disc is completely covered with grout. The time from the starting of the vibration until the disc is completely covered is the VeBe time. The test set-up is shown in Figure 1-55.

Inverted slump cone test is standardized in ASTM C995: *Standard Test Method for Time of Flow of Fibre-Reinforced Concrete Through Inverted Slump Cone* (89). This test was developed specifically for FRC and it determines the time required for FRC to flow through an inverted slump cone under internal vibration, thus providing a measure of the consistency and workability of FRC. The procedure consists of placing the cone in a positioning device over a bucket and then filling it with FRC in three layers without compaction. Thereafter, the stopwatch is started when the internal vibrator is inserted. The method requires the vibrator to be inserted vertically and centrally into the top of the sample in the cone and to descend at a rate such that it touches the bottom of the bucket in 3 ± 1 seconds. The stopwatch is stopped when the cone becomes empty and the time is recorded. Figure 1-56 shows the inverted slump cone test set-up (89).
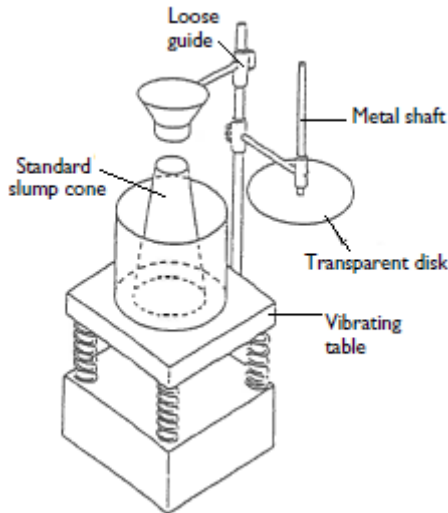
Figure 1-55 Test set-up for VeBe meter
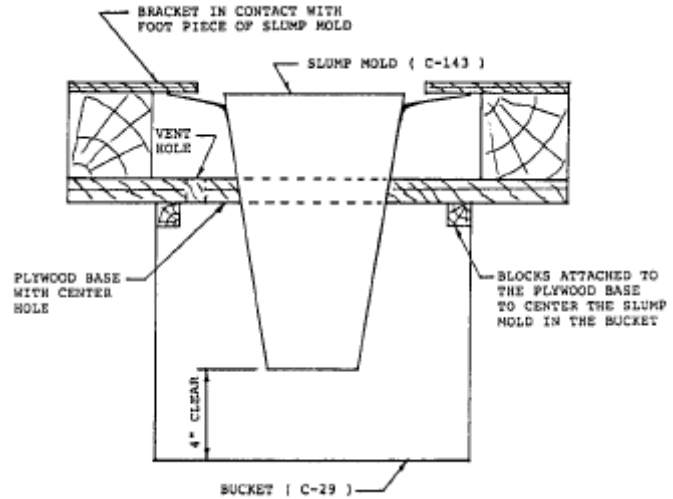
Figure 1-56 Test set-up for the inverted slump cone test

Comparisons of the different test methods have been evaluated by several researchers. The graphs in Figure 1-57 shows the comparison done by Johnston (90) in his work. Figure a shows that the FRC responds well to vibration even at low slump. The linear relationship in figure b shows that the VeBe and the inverted slump cone tests are affected by similar parameters.
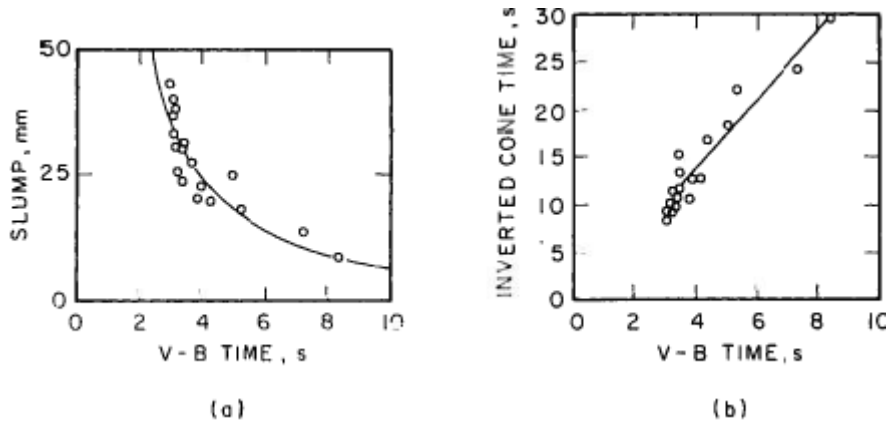
Figure 1-57 Relations between the results in various tests. (a) Slump vs. VeBe (b) VeBe vs. inverted slump cone

2.9   Mechanical properties

Fibers improve the characteristics of cement-based matrices in the hardening and the hardened state, for example they are able to bridge cracks, to transmit stress across a crack and to counteract crack growth. They also improve the fatigue behavior and increase the wear resistance. The mechanical properties of FRC are influenced by several factors:

1.   Fibers: type, geometry, aspect ratio, volume, orientation, distribution
2.   Matrix: strength, maximum aggregate size
3.   Specimen: size, geometry, method of preparation, loading rate

The fibers influence the properties of cementitious composites differently; they are very effective for some properties while for others they are less effective. They are especially effective under tensile loading and flexure, while under compression they are less effective. The main mechanical properties will be described in the following subsections.

2.9.1   Strength in compression

The term toughness was explained in section 1.6.1 as a measure of the ability to absorb energy during deformation. It can be estimated from the area under the stress-strain or load-deformation diagrams. As Figure 1-58 shows, the toughness of the material increases greatly with the addition of fibers. This means that the fiber reinforced concrete is able to sustain load at strains much greater than those at which first crack appears in the matrix. Hence, the fibers significantly increase the post-cracking ductility or energy absorption of the material.
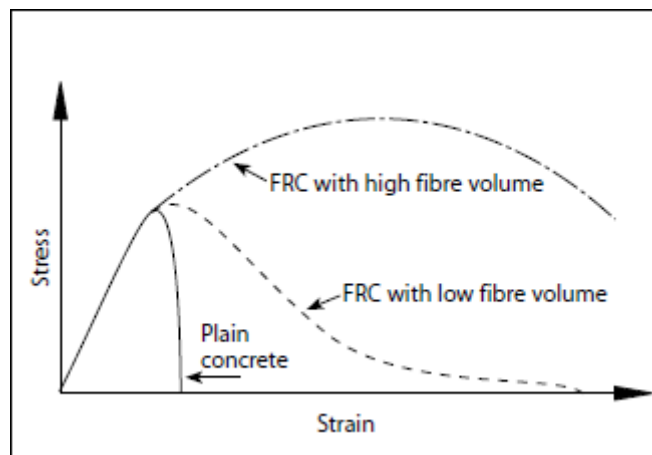
Figure 1-58 Typical stress-strain curve for fiber-reinforced concrete

As already mentioned in section 1.1, the fiber addition in the matrix only gives a very modest increase in strength, if any. As can be seen from Figure 1-59 (91, 92), the effect of the contribution of the fibers to the compressive strength of the concrete seems to be minor. However, as mentioned above, the ductility and toughness increase considerably when fibers are added. This is shown in the same figure and it can be seen how much the toughness (and ductility) increases for increasing volume fraction of the fibers.
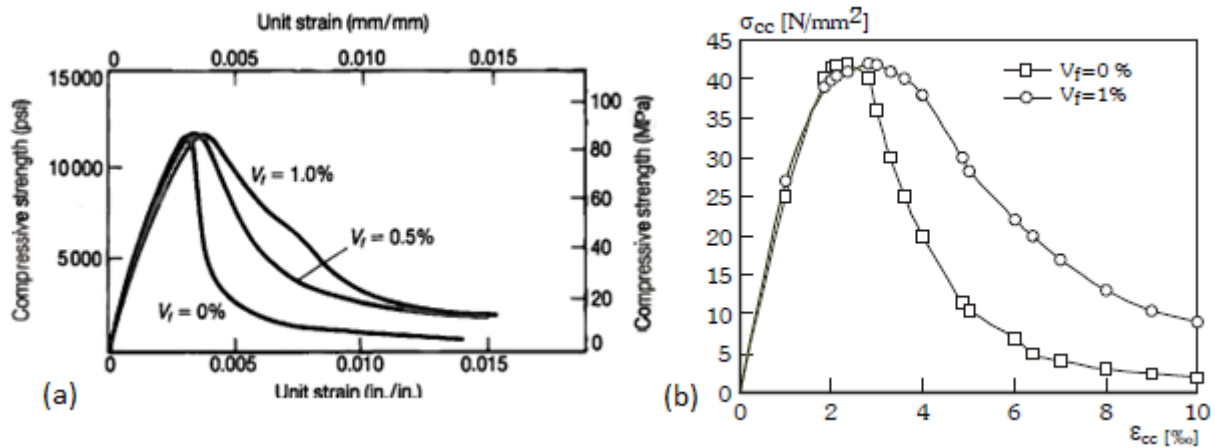
Figure 1-59 Influence of volume fraction of steel fibers on stress-strain behavior for concretes having compressive strength of (a) 90 MPa (b) 42 MPa

A similar trend is shown in a study by Fanella and Naaman (93). The ductility and compressive toughness are considerably enhanced as a response of the increase in the volume fractions and aspect ratios. This is shown graphically in the stress-strain curves in Figure 1-60 and Figure 1-61, respectively. For high fiber volumes used in ultra-high strength concretes, their effect on the compressive strength is less clear. Still some researches show that fibers do increase (to some extent) the compressive strength of these materials. For example Karihaloo and de Vriese (94) reported an 21% increase (from 120 MPa to 145 MPa) on going from no fibers to 4% fibers by volume for a reactive powder concrete. For the same composite, Sun (95) reported an 33% increase (from 150 MPa to 200 MPa) on going from no fibers to 4% fibers by volume.
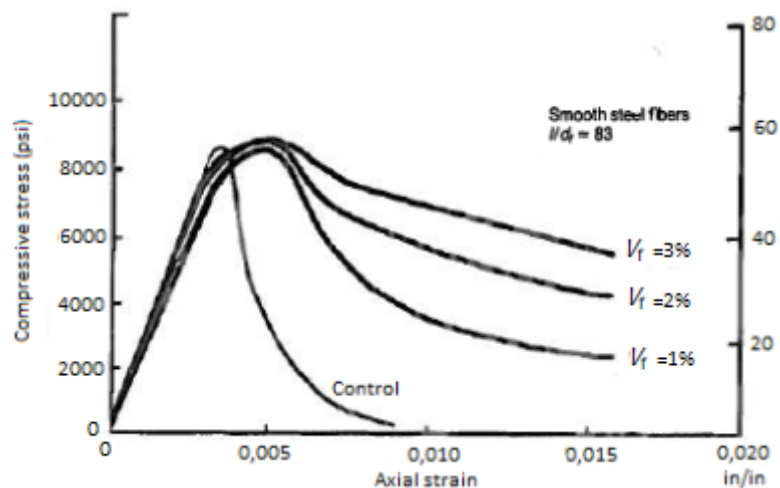
Figure 1-60 Effect of volume fraction of steel fibers on the stress-strain behavior for 62 MPa concrete
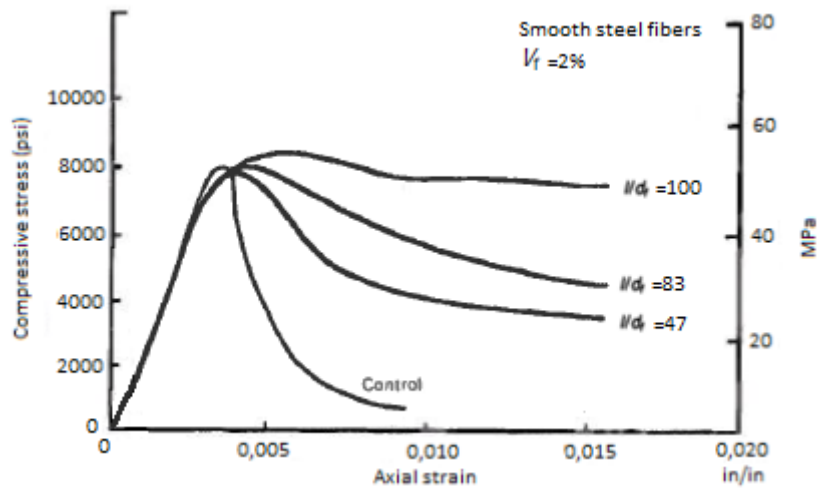
Figure 1-61 Effect of aspect ratio on stress-strain behavior of concrete

2.9.2   Direct tensile strength

It is generally accepted that the behavior of a concrete in tensile loading can be classified as either strain-softening or strain-hardening. Plain concrete is a strain-softening material while fiber-reinforced concretes with low and moderate volume fractions of fibers can also be regarded as strain-softening materials. For the latter material type, there are different opinions among researchers of whether or not the addition of fibers increases the tensile strength. It is reported by Shah and Rangan (14) that fibers aligned in the direction of the tensile stress may give a very large increase in direct tensile strength; 133% increase for 5% by volume of smooth steel fibers. On the other hand, for randomly distributed fibers, the effectiveness of fiber-reinforcement in tension can vary enormously. The increase of strength can vary from no increase at all, to a doubling of strength, see Figure 1-62. For example, Hughes (96) found in his work that there was no increase in ultimate tensile strength in one extreme. At the other extreme, for the same 1,5% volume fraction of steel fibers, he reported that the ultimate load was almost doubled. Also according to a report by Bulletin, the tensile strength may be doubled with the addition of fibers (97). As in compression, the steel fibers lead to major increases in the toughness of the composite (96, 98).

As explained in section 1.7, high-performance fiber-reinforced cement composites are defined as strain-hardening materials. They appear to be more effective in tension than in compression. In a study done by Krstulovic-Opara (99), the tensile strength of SIMCON was increased with about 150% on increasing the steel fiber volume fraction from 2,16% to 5,25%. At the same time tensile strengths of 17 MPa were reported for 5,29% fiber volume. Also Naaman and Homrich (64) reported tensile strengths of up to 28 MPa in a SIFCON composite.
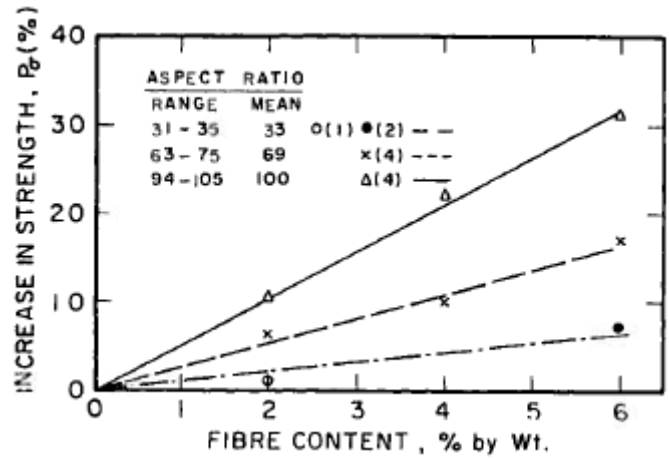
Figure 1-62 Influence of fiber concentration on tensile strength (100)

The effect of the shape of the fibers on the tensile stress behavior is also apparent. Shah and Rangan (14) have demonstrated this effect in the figure below. It can be seen from the descending portion of the plots that the deformed fibers (better anchorage qualities) increase the tensile resistance of the concrete beyond the first crack (increased toughness).
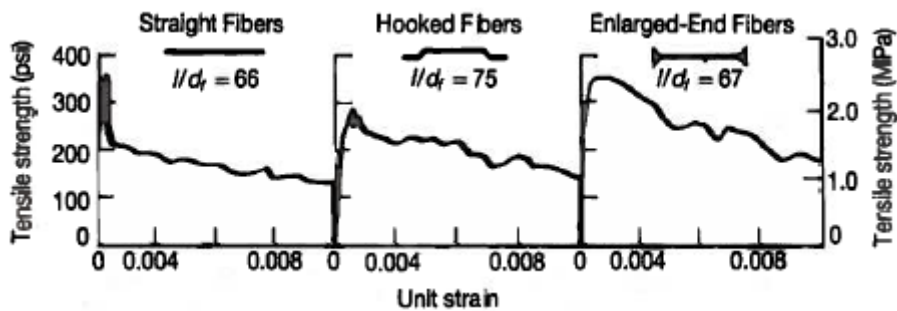
Figure 1-63 Effect of shape of steel fiber on tensile stress in mortar specimens loaded in direct tension

2.9.3   Flexural strength

Fibers seem to affect the flexural strength in concrete to a much greater extent than it affects the compressive and tensile strengths. This increase is affected by the fiber volume and also the aspect ratio of the fibers. There are two stages of determining the flexural strength; cracking load stage in the load-deflection diagram, and the ultimate load stage. Several researchers (101-103) have found that the flexural strength increases with the addition of fibers. Padmarajaiah and Ramaswamy (104) concluded that both cracking load and ultimate flexural load increased as the steel fiber content increased (though this test was for fully and partially prestressed beam specimens). This is shown in the figures below. The ultimate peak load was found to be 104 kN, 112 kN and 117 kN for 0,5%, 1,0% and 1,5% by volume of fibers, respectively.
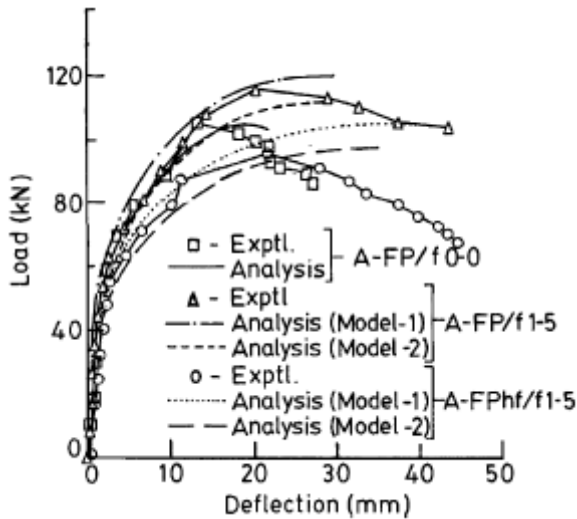
Figure 1-64 Load vs. deflection response for fully prestressed beam specimens
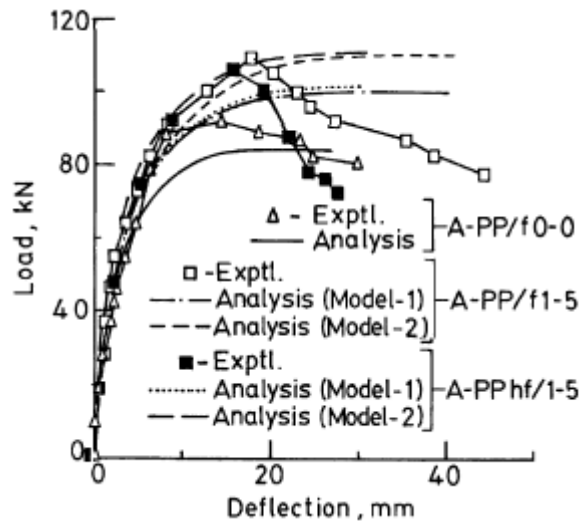
Figure 1-65 Load vs. deflection response for partially prestressed beam specimens

For self-compacting concrete, Pajak and Ponikiewski (102) investigated the flexural behavior of this concrete reinforced with straight and hooked end steel fibers at levels of 0,5%, 1,0% and 1,5%. They drew the conclusion that the increase of fibers volume ratio increased the flexural tensile strength, as shown in Figure 1-66 (plain SCC is described with "0" in the figure). The maximum load increases with an increase of fiber content for both types of steel fibers. The hooked end steel fibers give higher maximum load than the straight ones, and this dependency increases as the fibers volume content increases.

Similarly, Wang (103) obtained enhanced cracking strength and peak strength for SFRC compared to plain concrete. This is shown in Figure 1-67 and Figure 1-68. As expected, SFRC showed ductile behavior with an increase in the volume ratio of fibers. It can be seen in Figure 1-68 that the curves give a smoother transition from first crack for increasing fiber content. Also, the areas under the curves are larger (greater toughness).
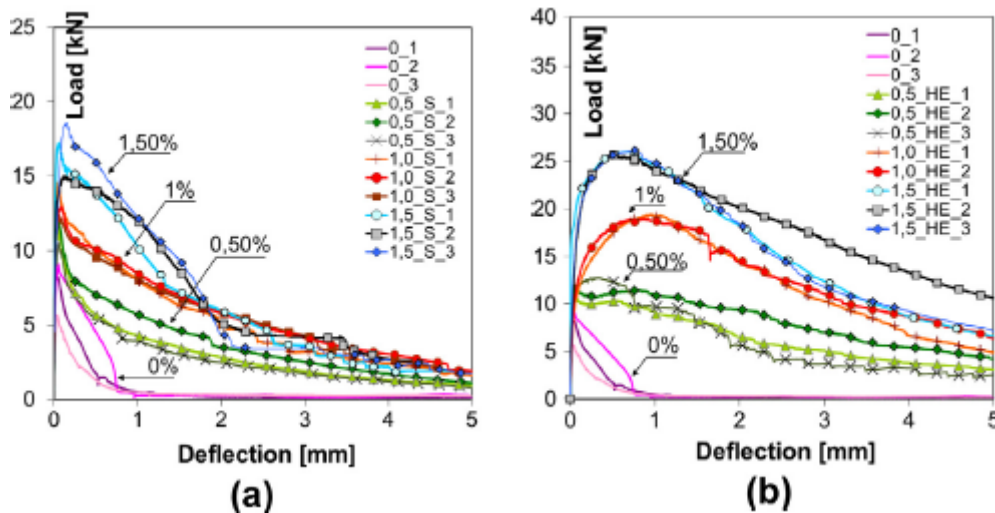
Figure 1-66 Results from three-point bending tests on SCC reinforced with different volume ratio of steel fibers: (a) straight fibers (b) hooked end fibers
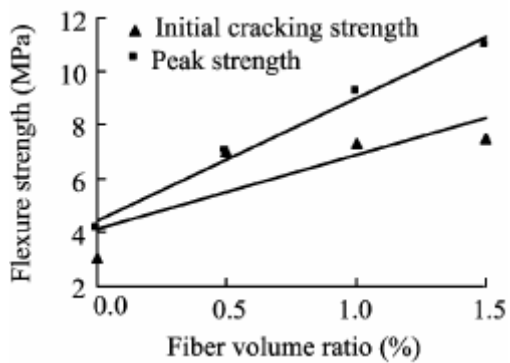
Figure 1-67 Relationship of flexural strength and fiber volume ratio
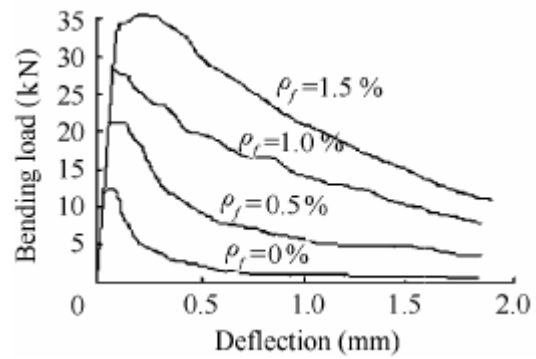
Figure 1-68 Bending strength and deflection curves

2.9.4 Flexural toughness

Toughness is represented by the load vs. deflection curves and it gives an indication of the quality of the material in terms of crack control. This mechanical property is of greater importance than any enhancement of flexural strength that may occur. For instance, Figure 1-69 (105) shows an enormous difference in the post-cracking behavior between different steel fiber reinforced concretes, even though they do not differ much in their flexural strengths. This leads to higher toughness for curves that have a larger area under them. This is also shown in Figure 1-70 (106), in which the high performance steel fiber composite called reactive powder concrete (having a strain hardening behavior) is schematically compared to a conventional low fiber volume SFRC (which exhibit a strain-softening behavior). The RPC will have a much higher toughness than the SFRC.
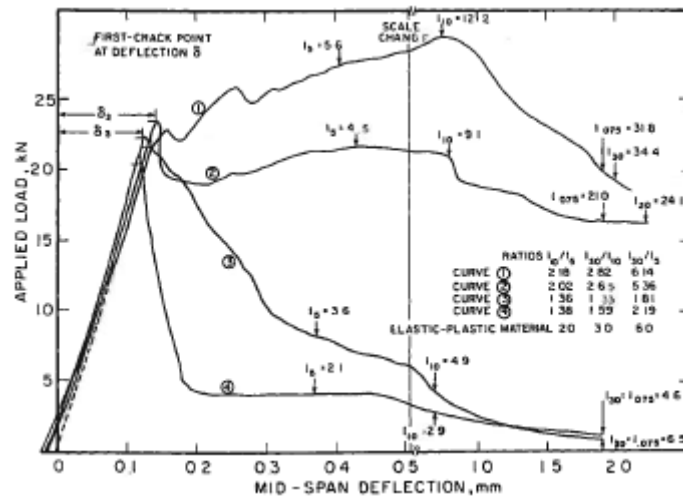
Figure 1-69 A range of load-deflection curves obtained in the testing of steel fiber reinforced concrete
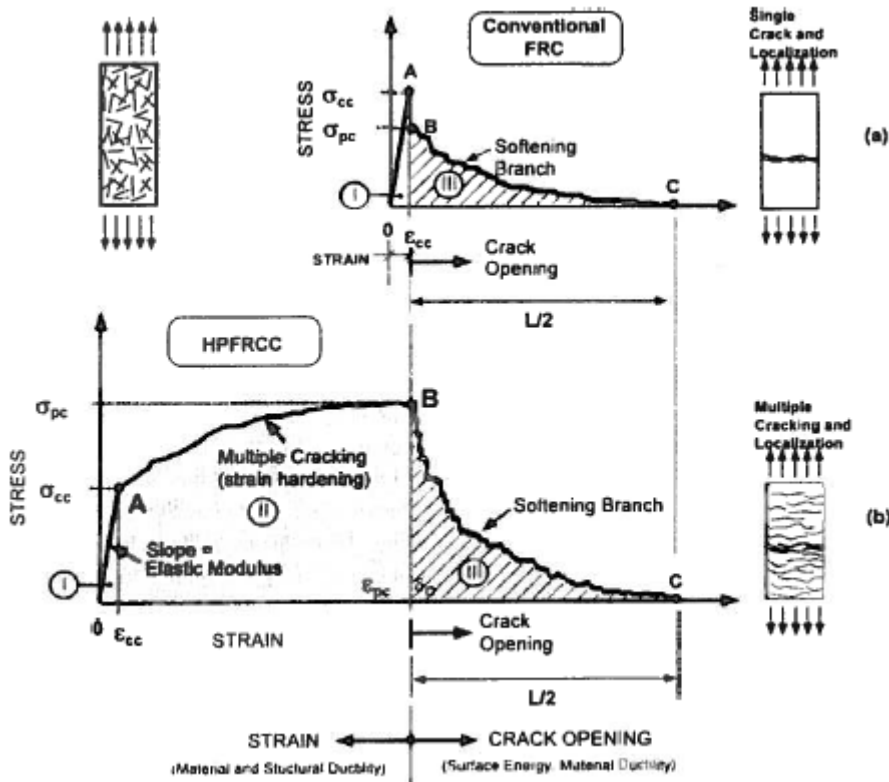
Figure 1-70 Comparison of typical stress-strain responses in tension of high performance fiber reinforced concrete and conventional FRC

Similarly, for synthetic fibers, Soutsos and Lampropoulos (107) found an increase in the flexural toughness. Table 1-17 shows clearly a considerable increase in the toughness of steel and synthetic fiber reinforced concretes. Plain concrete is described with "PC" in the figure. The synthetic fibers achieved almost comparable flexural toughness values to the lowest values obtained with steel fiber dosage of 30 kg/m^3.
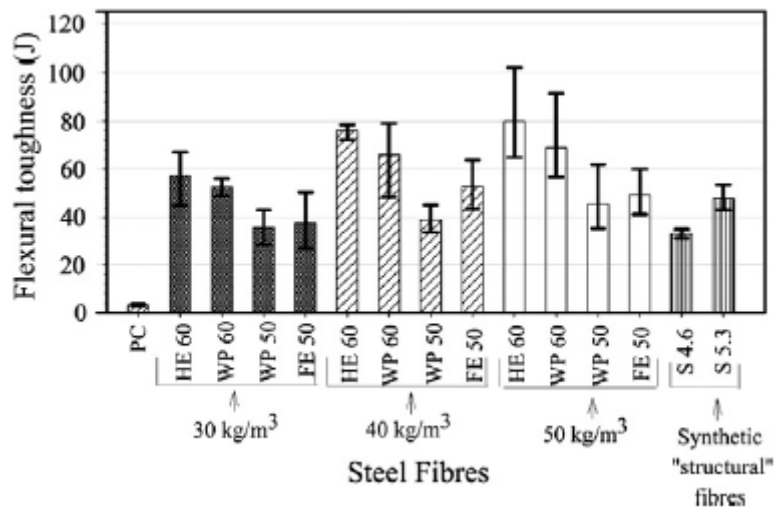
Table 1-17 Flexural toughness of steel and synthetic fiber reinforced concretes

2.9.5 Shear strength

Randomly distributed fibers in the matrix in combination with vertical stirrups enhance the shear capacity of concrete beams. Williamson (108) reported an increase of 45% in shear capacity over beams without stirrups when 1,66% by volume of straight steel fibers were used. When 1,1% by volume of deformed-end steel fibers were used, the shear capacity increased by 45-67%. And when crimped-end fibers were used, the capacity increased by almost 100%.

Other works indicate the shear toughness to increase as well. Valle and Buyukozturk (109) found a significant increment in the shear strength and ductility of concrete with the addition of steel fibers. The better properties were particularly true for high strength concrete, due to the improved bond characteristics of the fibers in a high strength matrix. Also, Mirsayah and Banthia (109) concluded with significantly improved shear strength and shear toughness. A fourfold increase in shear strength, from 4 MPa to 16,6 MPa, was found by Sun (110) going from plain concrete to SFRC with 2,5% of fibers by volume.

However, Barr (111) did not find any mentionable improvement in shear strength in his studies and concluded that the shear strength of SFRC was independent of fiber content. He did find the shear toughness to increase with increasing fiber content though.

2.9.6 Test methods of hardened composite

The evaluation of the properties of fiber-reinforced concrete is of great importance because then the composites can be used effectively and economically in practice. While some properties can be evaluated by the same procedures commonly used for conventional concrete (for example compressive strength), other properties need to be evaluated by test methods which are different from those used for conventional concretes.

The most common test methods applied for concretes in general are given by American and European standards organizations and publications, such as ASTM International (American Society for Testing and Materials) and RILEM (Reunion Internationale des Laboratoires et Experts des Materiaux). Also Japanese based test methods are often utilized.

2.9.6.1 *Testing in compression*

Within the practical limits of fiber content given by requirements for the workability of FRC, it is generally agreed among researchers that the compressive strength is not affected by the addition of fibers (as was shown in section 1.9.1). However, Kanstad (4) suggests that the compressive strength of the FRC should be experimentally determined if the steel fiber volume exceeds 1% (0,5% for synthetic fibers).

There are in general no special test methods for determining the compressive strength of FRC. The same methods used for conventional concrete can also be used for fiber-reinforced concrete. The most common methods applied are for instance ASTM C39: *Standard Test Method for Compressive Strength of Cylindrical Concrete Specimens* (84); BS 1881-116: *Method for determination of compressive strength of concrete cubes* (112).

However, there are some test methods developed for the determination of the compressive toughness of FRC. The Japan Concrete Institute names this method as JSCE SF5: *Method of test for Compressive Strength and Compressive Toughness of Steel Fiber-Reinforced Concrete.* The set-up of this test is shown in Figure 1-71 (113). The test may be carried out using an open-loop testing machine but it is recommended to use closed-loop machine for compressive strengths higher than 60 MPa.
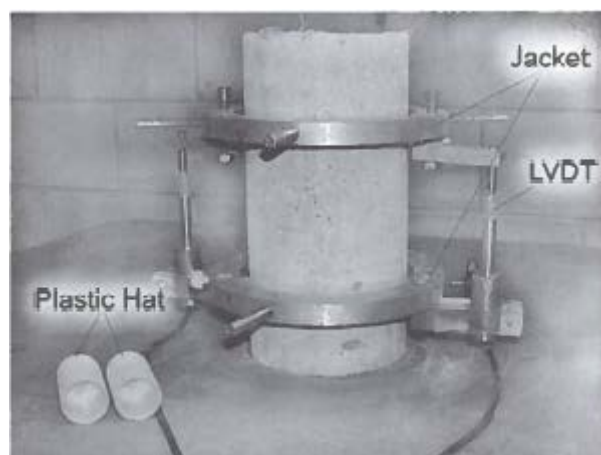
Figure 1-71 Test set-up for compressive toughness according to JSCE SF5

A similar test to the Japanese one is developed by RILEM-TC called 148-SCC: *Test method for the measurement of the strain-softening behavior of concrete under uniaxial compression* (114). It measures the complete compressive stress-strain curve of plain concrete (works also for FRC).

In Norway, the most commonly used standard for determination of compressive strengths is called NS-EN 12390-3 *Testing hardened concrete-Part 3: Compressive strength of test specimens* and it requires the compression testing machine to be in compliance with NS-EN 12390-4 (115, 116). The principle is very simple: load the specimen with the highest compressive force possible until failure. The maximum load sustained by the specimen is recorded and the compressive strength of the concrete is calculated by the equation:

$$f_c = \frac{F}{A_c}$$

Where

f_c is the compressive strength, in MPa or N/mm^2

F   is the maximum load, in N

A_c is the cross-sectional area of the specimen on which the compressive force acts

The test specimen shall be a cube, cylinder or core. It is voluntary to use packing between the specimen and the platens of the testing machine (they are primarily used to protect the platens and are often the same size as the specimen being tested). Other packing than auxiliary platens or spacing blocks are not allowed. If auxiliary platens are used, they shall be aligned with the top and bottom face of the specimen. The surfaces of the specimen are wiped off of excess moisture before placing them in the testing machine. The specimens are positioned so that the load is applied perpendicularly to the direction of casting. The loading rate is constant and within the range of 0,6 ± 0,2 MPa/s. NS-EN 12390-3 defines the tests as satisfying or unsatisfying if the shapes of the specimens after failure are looking like the ones shown below (Figure 1-72).

Satisfactory failures of cube specimens

Satisfactory failure of cylinder specimen

Some unsatisfactory failures of cube specimens

Some unsatisfactory failures of cylinder specimens
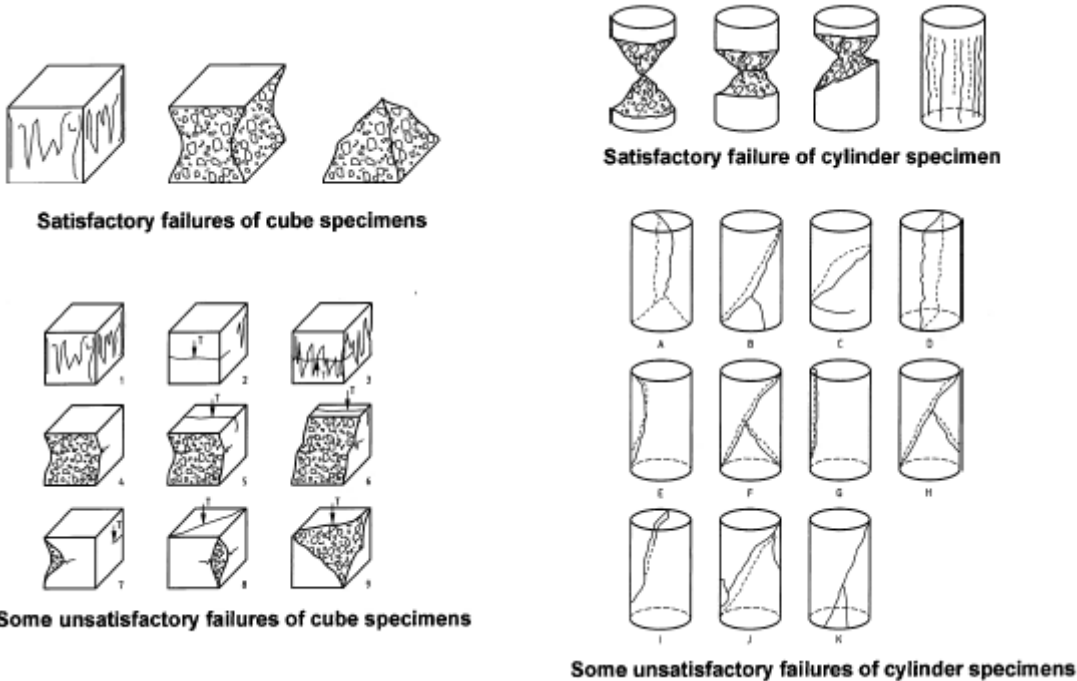
Figure 1-72 Shapes of the specimens after failure

According to NS-EN 12390-4, the testing machine shall be provided with

- dials or digital displays which allow the force to be read to the required accuracy
- a system which allows the maximum force sustained to be read after completion of the test, until reset
- displays that are readable from the operating position

A picture of the closed-loop test machine is shown below.

Figure 1-73 Closed-loop compressive strength test machine

2.9.6.2   Three-point bending test

The most important mechanical test for the FRC composite is the flexural (bending) test. It is necessary to measure the complete stress vs. strain (or load vs. deflection) curves to characterize the flexural behavior of FRC, from which the effect of fibers on the toughness and on the crack control is reflected. Several standardized test methods haven been published, which include

- ASTM C1018: test method for flexural toughness and first-crack strength of fiber reinforced concrete (third point loading)
- ASTM C1399: test method for obtaining average residual strength of fiber reinforced concrete
- ASTM 1550: standard test method for flexural toughness of fiber reinforced concrete (centrally loaded round panel)
- JSCE SF-4: method of test for flexural strength and toughness of fiber reinforced concrete
- RILEM TC162-TDF: test and design method for steel fiber reinforced concrete-bending test

The different test methods often give different results when compared with each other (117). There could be a lot of reasons for that, for instance more clumping (balling) of fibers in one test compared to another test, different test set-up, different dimensions of the test specimen, different equipment etc. Therefore, there is no agreement on which of these tests best represents the seeked properties of FRC.

In Norway, a method based on sawn un-notched beams for determining the flexural behavior has been used the last years. Another test method given by the European Standard, intended to provide values which can be used for the structural design of FRC beams, is being considered for being used in the current proposal for Norwegian fiber guidelines. This standardized test method is given in NS-EN 14651 (118) (also known as three-point bending test on notched beams) and can be used only if the maximum aggregate size is not larger than 32 mm and/or metallic fibers are not longer than 60 mm. The method provides for the determination of the limit of proportionality (LOP, the point at which the load vs. deflection curve first departs significantly from linearity) and of a set of residual flexural tensile strength values. The beams are cast in molds with Figure 1-74 showing the procedure for filling the mold; the size of shape 1 should be twice that of shape 2. After the casting, the beams are cured and thereafter they are notched using wet sawing.

The test set-up is given in Figure 1-75, showing two supporting rollers and one loading roller. A more detailed test set-up is shown in Figure 1-76.
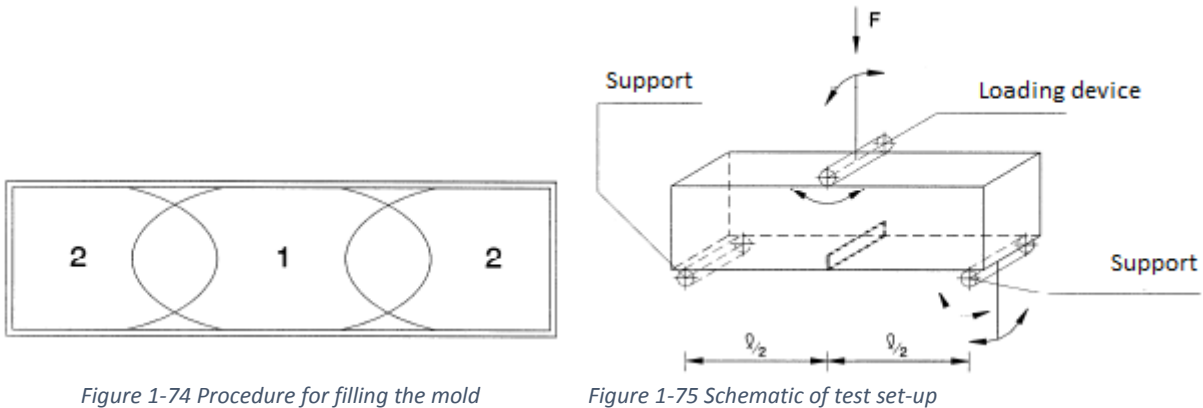
Figure 1-74 Procedure for filling the mold

Figure 1-75 Schematic of test set-up
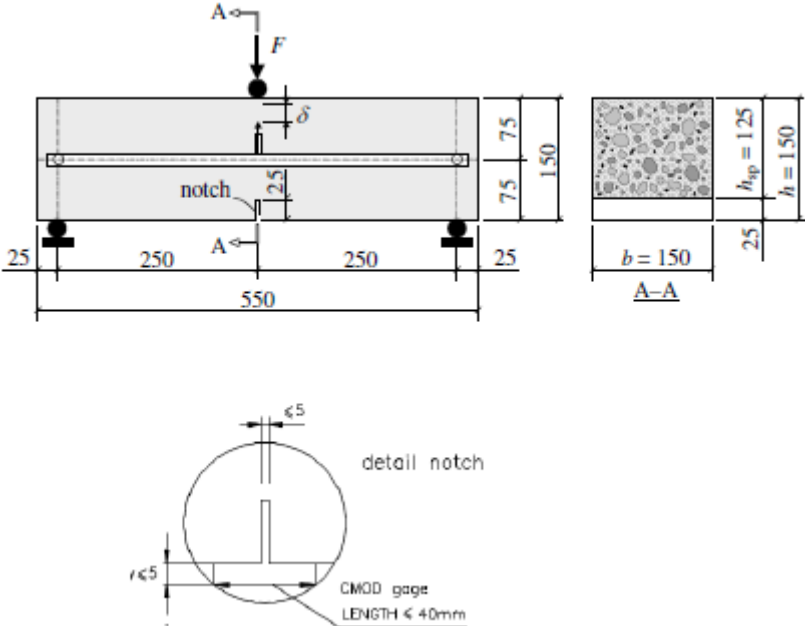
Figure 1-76 Detailed specimen dimensions, arrangement of displacement monitoring gauges and details of sawn notch

The notch is introduced so that the crack mouth opening displacement (CMOD) may be measured. This test might be controlled either by the deflection at mid-span or by the crack opening at the notch tip. A data recording system, coupled directly to electronic outputs of load and CMOD or deflection, measures the CMOD and the deflection. The relation between CMOD and deflection is given by:

$$\delta = 0.85 \, CMOD + 0.04$$

Where

δ is the deflection in millimeters

CMOD is the CMOD value in millimeters

A linear stress distribution (Figure 1-77) is assumed in the tests, and by this assumption the LOP and the four residual flexural tensile strength values (Figure 1-78) are calculated.
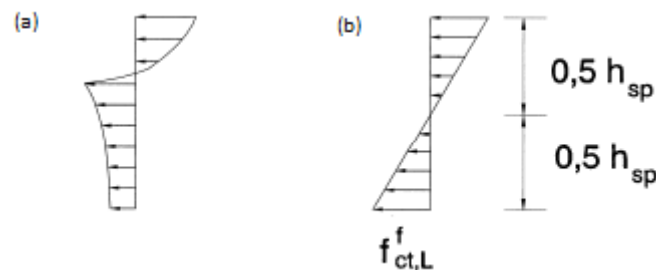
Figure 1-77 (a) Real stress distribution (b) Assumed stress distribution
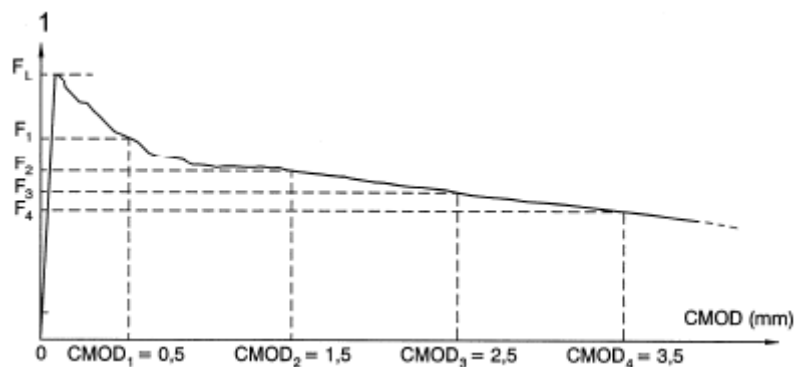
Figure 1-78 Typical load-CMOD diagram from tests

The LOP (limit of proportionality, the point of first crack) is given by (118):

$$f_{ct,L}^{f} = \frac{6M_{L}}{bh_{sp}^{2}} = \frac{3F_{L}l}{2bh_{sp}^{2}}$$

The residual flexural tensile strength is given by (118):

$$f_{R,j} = \frac{6M_{j}}{bh_{sp}^{2}} = \frac{3F_{j}l}{2bh_{sp}^{2}}$$

For both expressions:

F_L is the load corresponding to the LOP. It is determined by drawing a line at a distance of 0,05 mm and parallel to the load axis of the load-CMOD or load-deflection diagram and taking F_L as the highest load value in the interval of 0,05 mm

F_j is the load corresponding to $CMOD_j$ or δ_j (j=1,2,3,4)

M_L is the bending moment corresponding to the load at LOP

M_j is the bending moment corresponding to the load F_j (j=1,2,3,4)

b   is the width of the specimen

h_{sp} is the distance between the tip of the notch and the top of the specimen in the mid-span section

2.9.6.3   Four-point bending test

As mentioned in the previous section, this method has been used in Norway for some years now. The main differences between this test and the three-point bending test are

- as the name suggests, this test is based upon four points
- the casting procedure is different
- the beam dimensions are different
- the beam in four-point bending test is un-notched

A panel with dimension 600 × 600× 150 mm is cast and from this panel three beams with dimension 150 × 150 × 600 mm are sawn, see Figure 1-79. The idea is to imitate the casting procedure at a construction site and represent the best possible field conditions. Unlike three-point bending test where the span width is 500 mm, the span width here is 450 mm (Figure 1-80). This test promotes the crack to occur at the weakest point, which will be at a point between the two point loads. The flexural tensile stress at first crack is expected to be smaller than the stress achieved in three-point bending test.
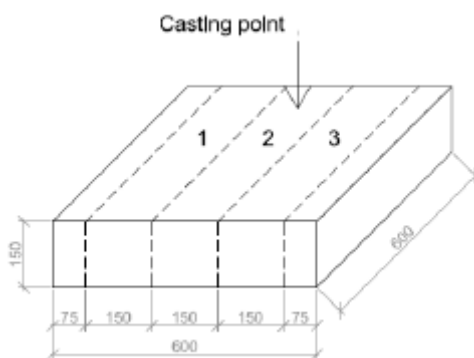
Figure 1-79 Plate elements with three beams
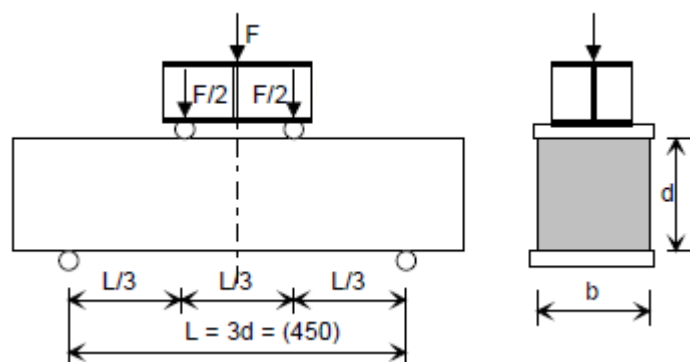
Figure 1-80 Test set-up for four-point bending test

2.9.6.4 South African Water Bed Test

This test is used to evaluate the effectiveness of fibers and mesh in transferring the stresses across construction joints in shotcrete applications. The flexural performance of large shotcrete panels (1600 mm × 1600 mm × 75 mm) is evaluated by fastening the panels in a place over a water bladder, which is then filled with water to apply pressure over the entire specimen. The energy absorbed (the toughness) is the area under the load vs. deflection curve out to a series of given deflections ranging from 25 mm to 150 mm. Figure 1-81 (119) shows a schematic of the South African Water Bed Test apparatus used in this method. Figure 1-82 (119) shows the load vs. deflection curves.
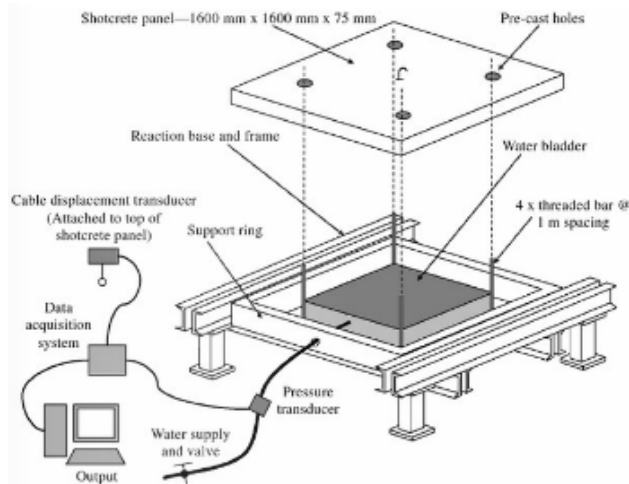
Figure 1-81 Schematic of South African Water Bed Test
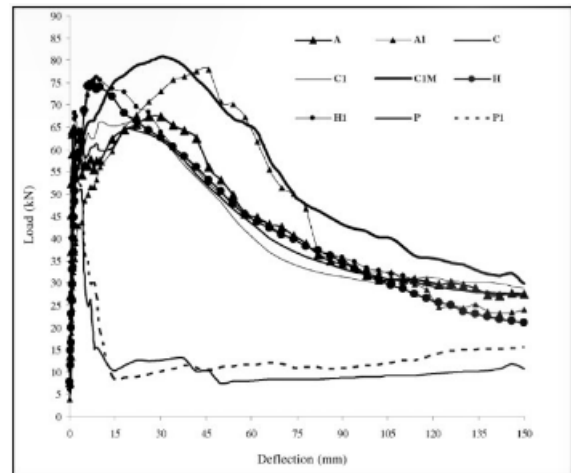
Figure 1-82 South African Water Bed Test load-deflection curves

2.10 Material composition

2.10.1 General

As the case is with any other type of concrete, when proportioning a fiber-reinforced concrete the mix proportions depend upon the requirements for any particular project, in terms of workability, strength, durability and so on. In other words, the mix design of FRC is a compromise between the sought performance in the hardened state and the requirements on workability in the fresh state. The conventional mix designs used for plain concrete, based on the strength and durability considerations, can also be used without modifications for FRC for relatively small fiber volumes (less than ~ 0,5%). However, for larger fiber volumes, the mix design procedures should be based on workability considerations (6). Since the addition of fibers affects the workability negatively, the margins for proportioning are narrower and the optimization of a mix composition is more difficult. Figure 1-83 shows the basic comparison between the mix designs of fiber-reinforced concretes and conventional concretes (8).
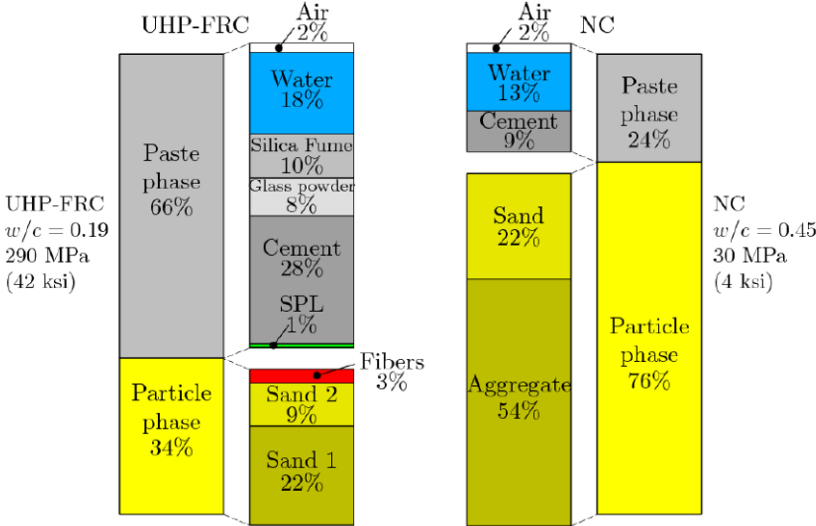
Figure 1-83 Example of mix proportions by volume comparing UHPFRC with normal concrete

Workability and maximum fiber volume are governed by parameters such as

- Maximum aggregate size
- The type and content of the fibers used
- The matrix in which the fibers are embedded
- The properties of the constituents of the matrix on their own
- Fiber addition and mixing process

As mentioned above, it is essential to base the mix design procedures of FRC on workability considerations. Therefore in this chapter, the optimization of material composition of fiber-reinforced concrete based upon the desired workability, flowability and stability characteristics will be described.

2.10.2 Packing density

The matrix of a fiber-reinforced concrete is much denser compared to the matrix of a conventional concrete. In order to produce a dense matrix, it is important to achieve the maximum possible packing density of all granular constituents (120). Grünewald (87) defines the packing density as being the bulk density divided by the density of the solids:

$$PD = \frac{\frac{W_B}{Vol_C}}{\rho}$$

Where

PD   is the packing density [-]

W_B is the weight of solids in a container [kg]

Vol_C is the volume of the container [dm^3]

ρ is the mean specific gravity of the solids [kg/dm^3]

The packing density is a characteristic of the granular skeleton (aggregates and fibers), and it takes into account the packing process, the distribution and shape of the grains and the agglomeration degree of the powders. A densed packed system will require less binder. Therefore, when proportioning FRC it is important that the concrete contains particles of different sizes. The smaller sized particles will fill the voids between the larger sized particles, consequently increasing the packing density. This will give a dense packed system, see Figure 1-84. The inclusion of a large amounts of fine particles will also help obtaining an acceptable flow.
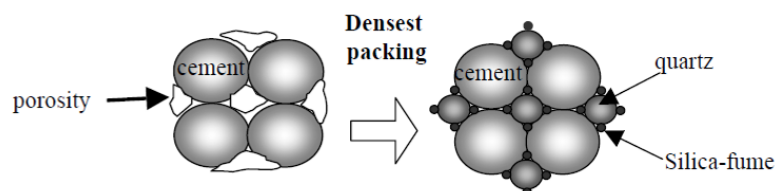
Figure 1-84 Particle packing

The reason for wanting a densed packed system in concrete, lies in the interfacial transition zone (ITZ) around the aggregates. A more densely packed system will decrease the porous and weak ITZ. A more porous structure of the ITZ reduces the tensile and compressive strengths of concrete. Also, the deteriorating processes such as alkali-silica reaction and sulphate attack will increase (121).

A more densely packed system will also affec the bond strength between the matrix and the fibers. The bond will increase considerably due to more contact points between the two (122).

2.10.3 Matrix volume

The fresh concrete is often described as a two-component system consisting of a matrix phase and a particle phase. Matrix is the flowable component which consists of free water, additives and all solid materials with a particle size less than 0,125 mm. This includes cement, silica fume, fly ash and the filler of the aggregates (72).

The matrix envelops the solid particle phase and fill all voids between the aggregate particles. This means that the packing density of the granular skeleton determines the amount of cement paste that is required to fill the voids. The fewer voids the aggregate skeleton contains, the less paste is required to fill them. The excess of the paste will surround and create a lubricated layer around the solids, see Figure 1-85 (87). This will reduce the friction between the fibers and aggregates, leading to improved workability.
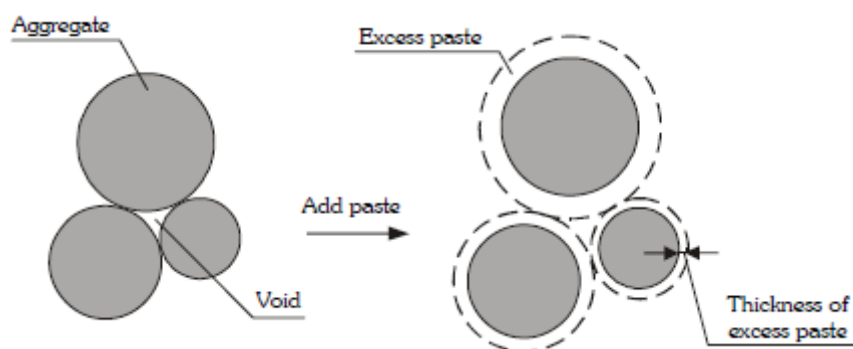
Figure 1-85 Excess paste layer around aggregates

A model applied by Markovic and co-workers (123) for self-compacting fiber reinforced concrete can give the necessary amount of cement paste if the packing density is known. According to this model, the amount of cement paste in SCC consists of two components:

- V_p is the minimum paste content which fills the voids between the fibers and aggregates
- (V_{pa} + V_{pf}) is the additional paste content which covers all aggregate particles (V_{pa}) and all fibers (V_{pf})

The composition of the fiber concrete mixture expressed in volumes may then be represented as:

$$V_a + V_f + V_p + V_{pa} + V_{pf} + V_{air} = 1$$

Where

      V_a is the volume of the aggregates

      V_f is the volume of the fibers

      V_{air} is the air content

This model was applied in their work on concrete mixes with two different fiber types, straight 6 mm long steel fibers and hooked-end steel fibers 60 mm long (123). They concluded that the model was applicable for the short fibers and it worked well for the long fibers with volumes up to 1%.

A large amount of fine particles (cement grains, silica fume, fly ash, filler of aggregate) will make sure that the FRC will obtain an acceptable flow and compactibility. Especially the silica fume which contain particles far smaller than the cement particles, is very effective in filling the voids.

Superplasticizers are used to decrease the porosity of the granular skeleton. They disperse the flocculated cement particels and filler. By adding a superplasticizer, the workability and fluidity of the concrete are substantially increased.

2.10.4 Fiber content

The effect of fibers on the workability is mainly due to four reasons (87):

- The shape of the fibers is more elongated compared with aggregates and the surface area at the same volume is higher, resulting in increased water demand
- Stiff fibers change the internal concrete structure by pushing apart particles that are relatively large compared with the fiber length, while flexible fibers fill the space between them. Stiff fibers increase the porosity
- Surface characteristics of fibers are different from those of cement and aggregates.
- Steel fibers are often deformed in order to provide great anchoring effects between a fiber and the surrounding matrix

It is a known fact that fiber addition decreases the workability of the fresh concrete. Regarding the fibers, the degree to which the workability decreases depends on the type and the content inserted.

Regarding the type of fiber, flexible fibers often have a much higher surface area than that of the stiffer steel fibers. Ando and co-workers (124) found the flow spread of fiber reinforced paste to decrease with increasing specific surface area of the carbon fiber, see Figure 1-86.
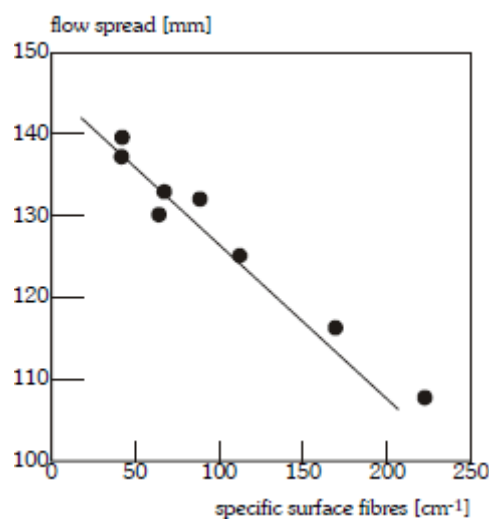
Figure 1-86 Effect of the specific surface area of carbon fibers on the flow spread of fiber reinforced paste

Swamy and Mangat (125) found that the packing density was linearly related with the aspect ratio (l/d) for a given fiber diameter and volume fraction. This was confirmed by studies in Grünewald's work (87), in which the experiments carried out compared the packing density with the steel fibers with different aspect ratios at a given volume fraction. This is shown in Figure 1-87. The first fiber index represents the aspect ratio and the second represents the fiber length. The figure shows the decrease of the packing density at increasing fiber content.
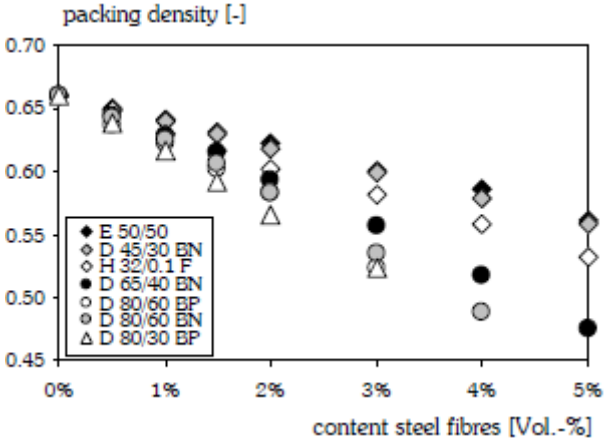
Figure 1-87 Packing density of coarse aggregates (4-16 mm) and different types and contents of steel fibers

Similarly, Edgington and co-workers (126) studied the effect of the aspect ratio and the fiber content on the Vebe-time of concrete mixtures containing maximum aggregate size of 5 mm. Figure 1-88 illustrates the results of this study. The maximum fiber content decreased with increasing aspect ratio.
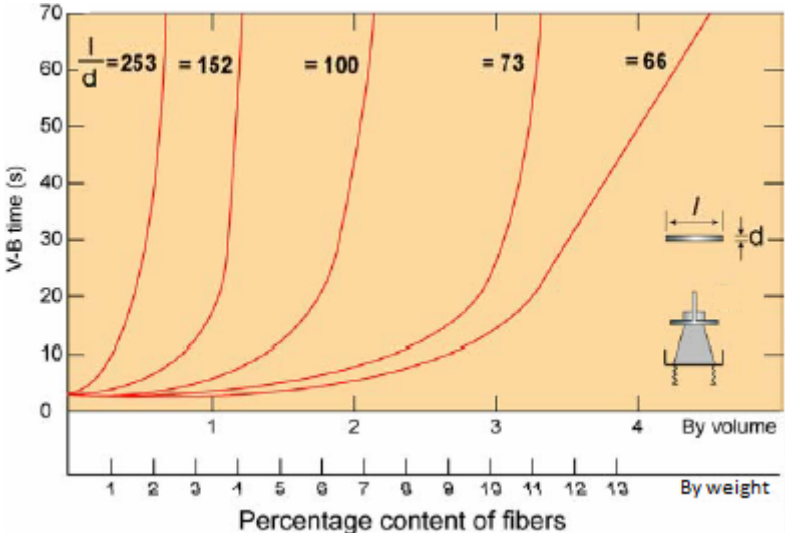
Figure 1-88 Effect of the type and the content of the steel fibers on the Vebe-time of fiber reinforced mortar with maximum grain size of 5 mm

As it has been stated in this section, the type and content of the fibers affect the workability. When proportioning the FRC, it is therefore important to choose the right amount of fibers to achieve sufficient workability in the fresh state to permit proper mixing. At the same time, the chosen amount of fibers have to give the desired improvements in mechanical behavior.

In the next section, the effect on the workability of FRC caused by the choice of aggregates together with the fiber content will be discussed.

2.10.5 Aggregates

The size, the shape and the content of the coarse aggregates affect the workability of the concrete (127). When for instance steel fibers are introduced into a concrete mix, they generally have a detrimental effect on the packing density of the aggregates; the porosity of the granular skeleton (aggregates and fibers) is increased. This increase depends on the relative size of the aggregates to the fiber length as illustrated by Figure 1-89. Johnston (128) recommends that the fiber length should not be shorter than the maximum aggregate size for the fibers to be effective in the hardened state. Grünewald (87) suggested the fiber length to be 2 to 4 times that of the maximum aggregate size.
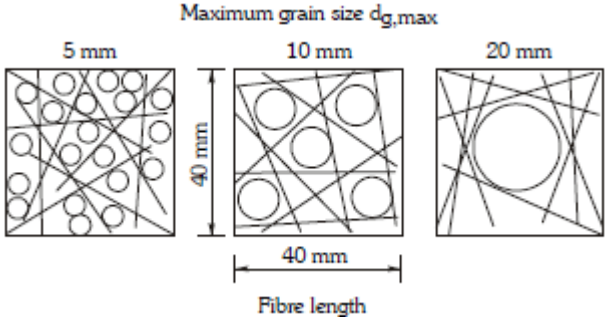
Figure 1-89 Effect of the aggregate size on the fiber distribution (128)

ACI committee 544 suggests that more fibers can be added as the fine aggregate content of the total aggregate content is increased (129). This is supported by findings by Swamy and Mangat (130) in another work. They suggested a figure that shows how the maximum fiber content of the steel fibers decreases at increasing coarse aggregate content, see Figure 1-90. 25 mm long steel fibers and aggregates with a maximum aggregate size of 10 mm were applied in the investigation.
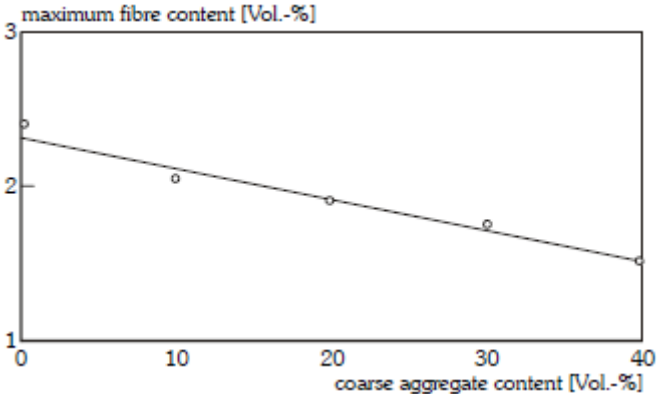
Figure 1-90 Effect of the coarse aggregate content on the maximum content of steel fibers

Similarly, Narayanan and Kareem-Palanjian (131) found that the optimum fiber content (the content of fibers beyond which fiber balling took place) increased at increasing percentage sand of total aggregate. Different steel fiber types with lengths between 25-43 mm were tested and the maximum aggregate size was 14 mm (sand: 3 mm). Similar results were obtained by Hoy and Bartos (16), in which they compared the fines content versus fibre content for determination of maximum packing density. Their results are already mentioned in section 1.6.1 (Figure 1-8).

A design method was proposed by Rossi and Harrouche (132) where the aim was to optimize the granular skeleton of FRC. They made the assumption that the most workable concrete is obtained when the granular skeleton is optimized. Further, they also assumed the optimized granular skeleton to be independent of the nature and volume of the cement paste. Therefore, the content and the composition of the paste were kept constant. The fresh concrete was tested with a LCL-Workabilitymeter that determined the flow time. Figure 1-91 shows how the optimum workability of the FRC depended on the sand content.
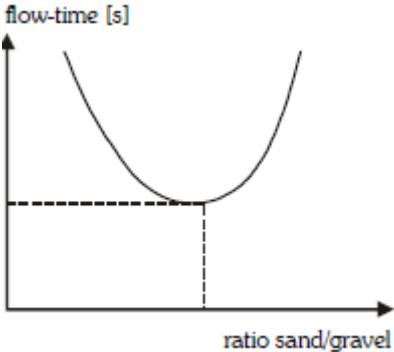
Figure 1-91 Optimization of the granular skeleton

Grünewald (87) investigated how the packing density of the granular skeleton was affected by the content of sand in aggregates. Different types and contents of the steel fibers were tested. Figure 1-92 shows the effect of different sand contents and fiber types (at 1,5% fiber content of the granular skeleton) on the packing density. The effect on packing density is more pronounced at high aspect ratios and low sand contents. At about 75% sand content, the packing density was the same for all types of steel fibers. This trend continued with sand content beyond 75%. This figure shows that the maximum was in the range of sand to total aggregate contents of 50-75%; the packing density decreased towards higher sand contents. Thus, in order to compensate for the effect of the fibers, the mixture composition must be adjusted by increasing the content of grains that are relatively small compared with the fiber length.

Hoy (133) obtained the same results as Grünewald (87). He performed experimental and numerical studies on the packing density of the granular skeleton of SFRC and assumed that the most workable mixture would be that with the highest packing density. Simulations were run with a particle packing program called Solid Suspension Model (SSM) and the resulting optimum composition of the granular skeleton was obtained, see Figure 1-93. The higher the content of the steel fibers, the higher was the required optimum sand content. At a given fiber content, the sand content had to be higher the

higher the aspect ratio was. It should be noted that practical considerations limit the applicability of Figure 1-93; steel fiber contents larger than 2% by volume cause a significant decrease of workability.
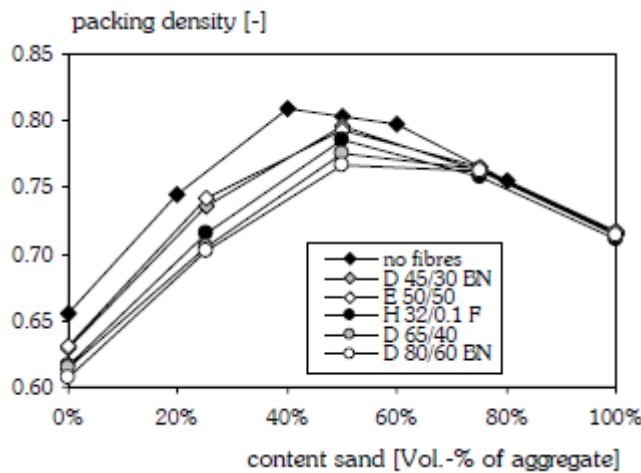
Figure 1-92 Effect of the sand content and the type of steel fibers (at 1,5 Vol.-%) on packing density
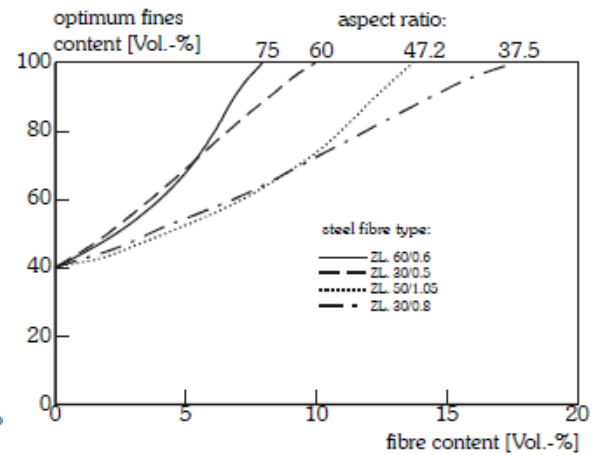
Figure 1-93 Theoretical effect of the type and the content of the steel fibers on the optimum sand content

Edgington and co-workers (126) studied the effect of different maximum aggregate sizes and the fiber content on the Vebe-time. Different reference mixtures were testet and they all contained a steel fiber with aspect ratio of 100. Figure 1-94 shows that the Vebe-time was higher for larger maximum aggregate size for a certain steel fiber content. The presence of aggregate particles less than 5 mm in size had little effect on the compacting properties of the mix. The authors proposed an equation with which to estimate the critical percentage of fibers which would just make the SFRC unworkable:

$$PWc_{crit} = 75 \cdot \frac{\pi \cdot SG_f}{SG_c} \cdot \frac{d}{l} \cdot K$$

PW_{crit} is the critical percentage of fibers. The authors recommended that the the fiber content should not exceed 0,75 PW_{crit} in order to permit proper compaction.
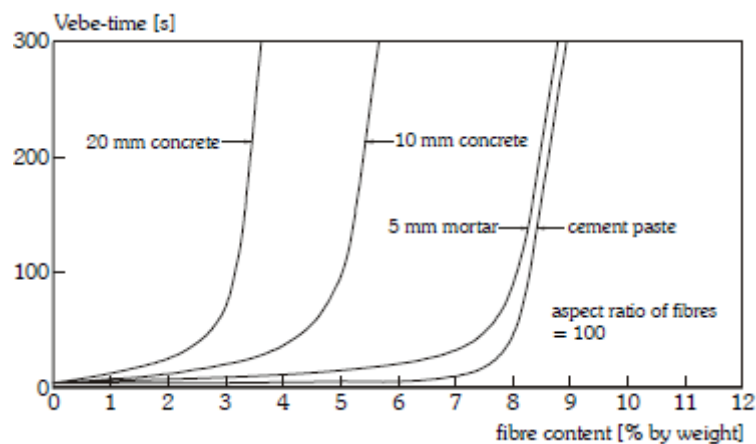
Figure 1-94 Effect of the mixture composition and the fibre content on the Vebe-time

76

2.10.6 Concluding remarks

In general, fiber reinforced concrete mixes contain higher cement contents and higher ratios of fine to coarse aggregate than ordinary concretes, to provide better workability. In addition, to improve workability and to reduce the quantity of cement (to reduce the costs), fly ash is inserted to substitute a large portion of the cement. Also, air entrainment agents in conjunction with water reducing admixtures and, in particular, superplasticizers are often used to improve the workability of high fiber volume mixes. It is important that the mix design procedure should be based on workability considerations.

Further, the mix design of FRC can be approached on a systematic manner; the mix design can be based on optimizing the granular skeleton. This was done by Rossi and Harrouche (132) and Hoy (133). Various particle packing programs can be applied to achieve the most workable mixture, which will give the highest packing density of the granular skeleton. Besides the granular skeleton, the content and characteristics of the paste must also be taken into account to link workability and the mixture composition. It is also important to test the mixtures in laboratories and thus confirm their desired properties before utilizing them in the field.

3 Materials development

3.1 Introductory remarks

This project is a part of an ongoing project called "FA 2.2 High tensile strength all-round concrete" which is a collaboration between Norwegian University of Science and Technology (NTNU) and Concrete Innovation Centre (COIN), a Norwegian based research centre. There are two main objectives within the FA 2.2 project:

- To do research and development work which stimulates and makes use of fibers possible in load carrying concrete structures
- Development and verification of ductile high tensile strength concrete with target tensile strength: 15 MPa

In other words, the main objective is to design a concrete without traditional reinforcement. To reach this goal, efforts in material testing (field and full scale laboratory testing) have been/are being made to achieve the target concrete. The related activities include materials development, fiber type investigations and performance of structures (mechanical properties). Also, a guideline for design, execution and control of fiber-reinforced concrete is being developed.

Based upon previous work, this chapter describes the experimental work done with self-compacting concrete consisting of different fiber types, namely steel fibers and basalt fibers with different dimensions and percentages by volume. The corresponding material properties, fresh and hardened, of the different composites will be evaluated and compared. Then it will be discussed which fiber type shows the overall better performance and whether or not the tested steel- and basalt fiber-reinforced concretes can be applied in load carrying structures.

The experimental part is divided into two series:

- Mixing and testing of self-compacting concrete with different volume fractions of steel fibers
- Mixing and testing of self-compacting concrete with different volume fractions of basalt fibers

First, this chapter will go through the previous work done in the FA 2.2 project and in a master thesis written by a student in early 2013. Afterwards, the new experiments in this thesis will be described; starting with the materials that were used in the experiments and the procedure of mixing and handling the fresh concrete to evaluate the properties of the concrete.

3.2 Earlier work

Fibers in a concrete mix act essentially as rigid inclusions and due to their large surface area and their elongated shape, they affect the workability of the concrete negatively. Self-compacting concrete (SCC) is characterized in its fresh state by high flowability and rheological stability. The addition of fibers into self-compacting concrete takes the benefits from its high performance in the fresh state to achieve a more uniform fiber-dispersion, resulting in a concrete mix with higher flowability than conventional fiber-reinforced concrete (FRC). Consequently, SCC gives the best possible effect of fiber reinforcement compared with ordinary concrete.

3.2.1 Work in 2011-2012

Experiments with ductile fiber reinforced concrete (DRFC) at NTNU in collaboration with COIN over the last two years has resulted in focusing on one specific concrete quality, which was named M60 B35 SCC fiber (134) after durability class M60 and compressive strength class B35. These experiments were a continuation of experiments performed by Sandbakk (5) in his Ph.D. work. Initially, three different concrete qualities were investigated:

- DFRC Medium. Target f_c = 40-45 MPa and f_{res} = 10 MPa
- DFRC High. Target f_c = 65 MPa and f_{res} = 15 MPa
- DFRC Ultra High. Target f_c > 100 MPa and f_{res} = 15 MPa

After trial mixes and testing of these concrete qualities, the experimental program led to one specific concrete, M60 B35 SCC fiber. By utilizing the Andreassen-model, which is a particle packing program developed by Elkem AS and called "EMMA" (135), the goal was to develop a very high flowable and stable SCC before fiber addition. This way, the negative effect of fiber addition on the flowability of the concrete was compensated for. A typical M60 B35 SCC fiber could have the following material composition (showing without fibers):

Material	kg/m^3
Cement (Norcem Standard FA)	225
Free water	200
Silica fume(Elkem Microsilica 920 D)	108
Fly ash (Betofill VK 150)	273
Superplasticizer (Sika Visco Crete FB-2)	10
Aggregates (Årdal 0-8 mm)	1275

Table 2-1 Typical mix design of M60 B35 SCC fiber

The first trial mix was performed with 2% long steel fibers (ordinary Dramix RC BN, 60 mm in length) and 1% short steel fibers (13 mm in length). The results were satisfying and it was decided to repeat the mixture with different fiber types and dosages. Also the mix design was slightly changed for each mix. The following mixes were conducted:

- Series 1
  1. Mix 0: 2% Dramix 65/60 + 1% micro steel fibers
  2. Mix 1.1: 2% Dramix 65/60 + 1% micro steel fibers
  3. Mix 1.2: 2% Dramix 65/60
  4. Mix 1.3: 2% Basalt Gen 3

- Series 2
  1. Mix 2.1: 3% Basalt gen 3
  2. Mix 2.2: 3% Dramix 65/60
  3. Mix 2.3: 2% Dramix 65/60 4D
  4. Mix 2.4: 2% Dramix 65/60 5D

- Series 3: Conducted to develop a more economic defensible mix design
  1. Mix 3.1: 2% Dramix 65/60
  2. Mix 3.2: 2% Dramix 65/60

During the fresh and hardened concrete properties testing, the compressive strength was measured according to NS-EN 12390-3 (116), the flexural strength measured according to NS-EN 14651 (118) and the slump flow according to NS-EN 12350-8 (83).

Fresh properties

As expected, the slump flow was reduced after fiber addition. The following tables show different properties of the M60 B35 SCC fiber concrete in the fresh state (134).

Concrete mix no.	Mix 0	Mix 1.1	Mix 1.2	Mix 1.3
Fibers	2% Dramix + 1% micro	2% Dramix + 1% micro	2% Dramix	2% Basalt
Slump flow before fibers (mm)	780	850	880	820
Slump flow after fibers (mm)	Clod of mortar and fibers	Fiber balling	830* fibers left on the middle of the plate, mortar floating out	470
Density				Not measured

Table 2-2 Fresh properties for series 1

Concrete mix no.	Mix 2.1	Mix 2.2	Mix 2.3	Mix 2.4
Fibers	3% Basalt	3% Dramix	2% Dramix 4D	2% Dramix 5D
Slump flow before fibers (mm)	805	870	795	820
Slump flow after fibers (mm)	360	Failed	575	685
T_{500} before fibers	1,25 s	0,93 s	2,41 s	1,89 s
T_{500} after fibers	Failed	2,15 s	4,63 s	2,17 s
Density before fibers	2200	Not measured	2259	2257
Density after fibers	2165	Not measured	2252	2256

Table 2-3 Fresh properties for series 2

Concrete mix no.	Mix 3.1	Mix 3.2
Fibers	2% Dramix	2% Dramix
Slump flow before fibers (mm)	775	750
Slump flow after fibers (mm)	720	720
T_{500} before fibers	1,25 s	0,93 s
T_{500} after fibers	1,78 s	2,15 s
Density before fibers	2316	2305
Density after fibers	2032	2158

Table 2-4 Fresh properties for series 3

Pictures of Mix 2.1 and Mix 2.2 before and after fiber addition are shown below (134). These are the only mixes with 3% by volume of long fibers, Dramix being 60 mm long while Basalt Gen 3 being 42 mm long.
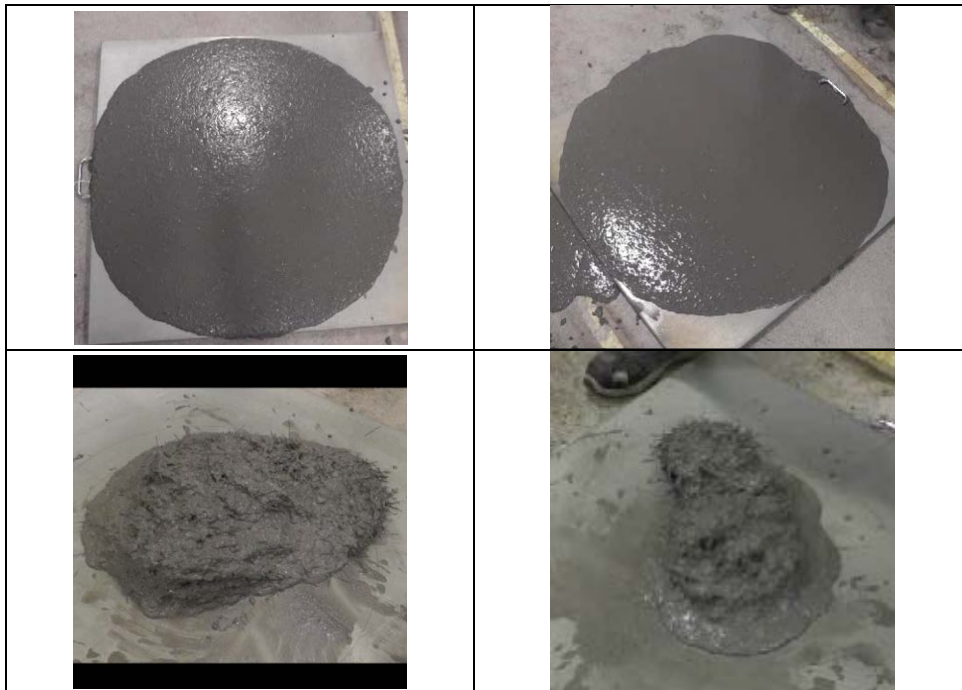
Figure 2-1 Mix 2.1 (left) and Mix 2.2 (right) before and after fiber addition

Hardened properties

The measured compressive strength and flexural strength and stress are shown in the tables below (134). The results from the bending tests are shown in Figure 2-2 as stress vs. CMOD (134).

* Density at demoulding
**Tested at 26 days of age

Concrete mix no.	Mix 0	Mix 1.1	Mix 1.2	Mix 1.3	Mix 2.1
Compressive strength (MPa)	35,8	85,4	70,4	63,3	63,6
F_L (kN)	51,7	61,7	44,9	39,5	35,8
Max flexural strength (MPa)	16,4	18,9	13,9	12,2	11,5
Res. Flex. Str. R1	11,8	16,3	12,4	10,7	10,8
Res. Flex. Str. R2	16,3	18,6	13,6	11,8	11
Res. Flex. Str. R3	16	18,6	13,5	11,3	10,3
Res. Flex. Str. R4	15,1	18	12,9	10,6	9,5
Density	2100	2490	2460	2250	2240
Concrete mix no.	Mix 2.2	Mix 2.3	Mix 2.4	Mix 3.1**	Mix 3.2**
Compressive strength (MPa)	38,7	59,7	54,5	24,2	27,5
F_L (kN)	33,9	39,2	46,4	24,2	16,9
Max flexural strength (MPa)	10,8	12,4	14,7	7,7	5,3
Res. Flex. Str. R1	10,1	11,4	13,2	7,5	5,3
Res. Flex. Str. R2	10,3	12,3	14,4	7,4	4,8
Res. Flex. Str. R3	9,8	11,8	13,7	7,2	4,5
Res. Flex. Str. R4	9,3	10,9	13,2	6,8	4,3
Density	2190	2430*	2410*	2110	2120

Table 2-5 Hardened concrete properties
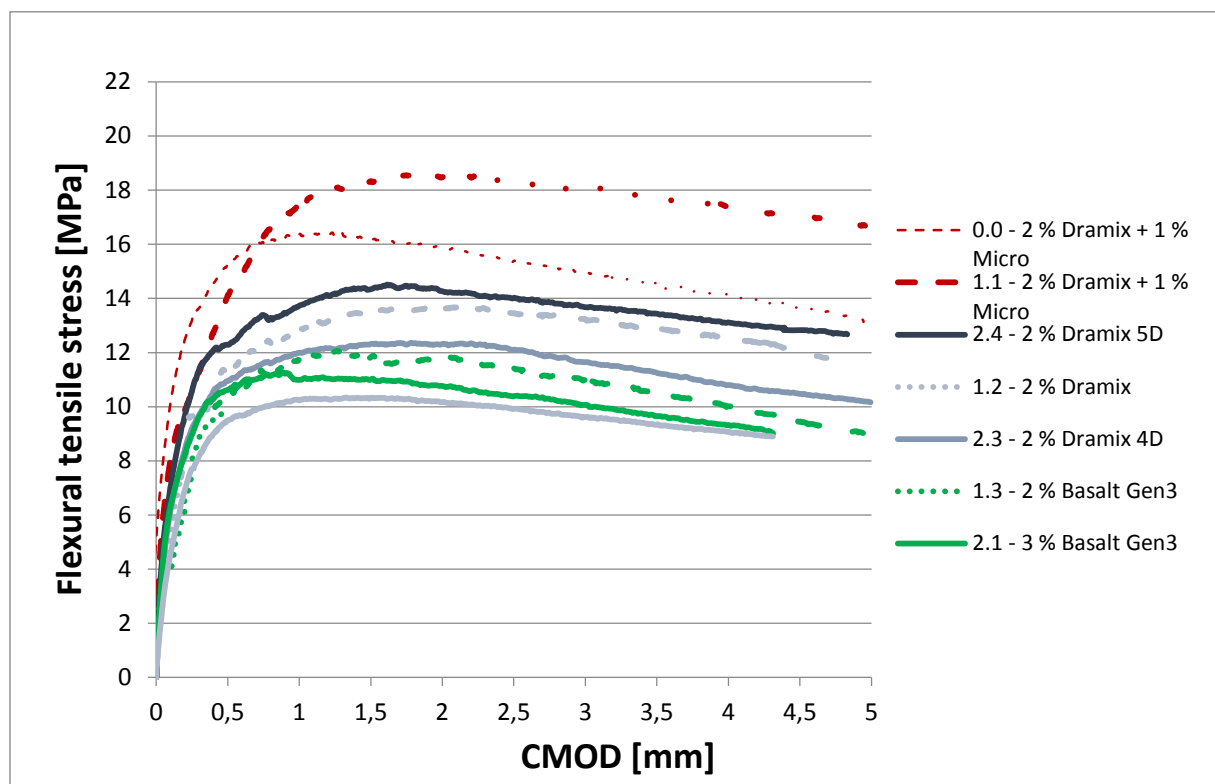
Figure 2-2 Flexural tensile stress and CMOD for all eight mixtures

Results and conclusions

For six of the first mixes, the detailed experimental work is given in (136). Here, only the shallow results are described (the conclusions are not written by this author).

Fresh properties

The flow properties for all mixes before fiber addition were satisfying; high slump flow values (as high as 880 mm, see Table 2-2) were obtained without segregation.

The short fibers were difficult to distribute and fiber balling easily occurred.

After fiber addition, the concretes appeared to have good flow properties when observed during mixing (except for the mixes with short fibers). But the results after the slump flow test showed the opposite; the steel fibers were often left in the middle of the concrete spread, giving an unstable and heterogeneous mix (Figure 2-1). The authors claimed the inadequacy of the test method and too low viscosity of the concretes to be the reasons for this. The short fibers impaired the flowability considerably due to the fiber balling. Concerning the basaltic fiber mixes, the problem with segregation was less, probably due to lower stiffness and shorter length (than steel fibers) and their density being close to the concrete's density.

Hardened properties

The compressive strength varied relatively much. This is due to variation in degree of compaction because of high fiber content. This is especially apparent when comparing Mix 1.2 and Mix 2.2.

The variation in compaction did not seem to affect the flexural strength the same way as it did with the compressive strength. All mixes showed a deflection hardening behavior and a quite high flexural strength and ductility (see Figure 2-2 and Table 2-5). Increasing fiber content with short fibers gave a higher increase in flexural strength than increasing the content with large fibers (Mix 0, Mix 1.1 and Mix 2.2). However, the ductility was not influenced significantly.

The flexural strength was lower for mixes with 3% fibers than the corresponding mixes with 2% fibers.

Conclusions

At least 2% fibers by volume must be included to get a SCC with sufficiently high residual tensile strength in order to replace ordinary reinforcing bars. However, this gives some obstacles:

1. Even though the Andreassen-model provides a very high flowable and stable SCC before fiber addition, the fresh concrete testing demonstrated consistency and flowability problems after fiber addition. The slump flow cone was too narrow to handle the long fibers and it was difficult to take the concrete out from the mixer with a scoop or a pitcher due to the long fibers. Consequently, these obstacles gave a heterogeneous sample and an unrepresentative measure of the flowability.
2. It is difficult to get a representative (homogeneous) sample due to the long fibers. The relatively large fiber content can then lead to large density reductions and insufficient compactions and consequently reduced strength.
3. Large fiber contents reduce the fiber effect on the residual strength due to coupled pullout failure of the fibers crossing the cracks.

In the future work, a more systematically varied fiber content and a more suited casting techniques will be applied to get a better representative of the samples.

3.2.2   Work in 2013

In early 2013, an exchange student named Miguel Roca at NTNU did a follow up of the previous work done in the COIN project FA 2.2 in his MSc-thesis (137). As before, the SCC had resistance class M60 and strength class B35. The main part of the experimental program consisted of investigating different casting techniques for the beam molds and different types and amounts of steel fibers in SCC, with the maximum content being 2% by volume. For the latter, the procedure consisted of starting with 1% by volume of fibers and evaluate the results (the fresh and hardened concrete properties). Accordingly, the fiber content was adjusted and new mixes were tested (section 2.2.2.2).

3.2.2.1   Casting techniques and 1% by volume of fibers

In order to find the best possible casting of concrete into the beam molds, two additional casting techniques were studied as well as their influence on the residual flexural strength:

1. Pour the concrete into the beam molds by the short side using a bucket.
2. Pour the concrete into the beam molds by the short side using a funnel (similarly to a mix truck).

The standard casting technique, as used in the earlier work (FA 2.2), is defined in NS-EN 14651 and shown in Figure 1-74. The pictures below show the procedure of the above mentioned casting techniques as well as the standard casting technique.

Figure 2-3 Standard casting technique

Figure 2-4 Pouring form bucket by short side

Figure 2-5 Pouring from funnel by short side

Also, a new method of filling the bucket/pitcher with concrete was applied. Earlier the pitcher was filled by inserting it directly into the mixer. Now, the mixer was detached from the mixing machine and placed on a small structure by the use of a lift, see Figure 2-6. This allowed the mixer to tilt and fill the bucket with concrete thereby. Thus, the samples were representative for the mixes. Thereafter, the concrete was poured from the bucket and into the beam molds, cylinders and the slump flow cone.

Figure 2-6 New method for filling the bucket

The different casting techniques were studied by testing three mixes. They were called Mix 2, Mix 4 and Mix 5 and they all had the same fiber content of 1% Dramix 65/60 RC BN. Mix 2 and Mix 4 had the exact same recipe (Table 2-6), while the mix design of Mix 5 was slightly different; an anti-washout admixture was added to reduce the original slump flow. The different casting techniques were applied as follows:

- Mix 2: The standard casting technique
- Mix 4: Pouring from bucket by short side
- Mix 5: Pouring from funnel by short side

Material	kg/m^3
Norcem Standard FA	299,4
Elkem Microsilica	29,9
Fly ash	44,9
Fritt vann	197,6
Absorbert vann	6,7
Årdal 0-2 mm	597,3
Årdal 0-8 mm	1106,0
Dynamon SX-N	4,5
Sika demper	0,3

Table 2-6 Mix design of Mix 2 and Mix 4

As before (in FA 2.2) the compressive strength was measured according to NS-EN 12390-3 (116), the flexural strength according to NS-EN 14651 (118) and the slump flow according to NS-EN 12350-8 (83). Additionally the 4C-Rheometer test was used, which automatically determines the yield stress and the plastic viscosity. It should be noted that the flexural and compressive strength tests were made after 14 days, not 28 days as the normal procedure is.

Fresh properties

Here, only the results from slump flow test are shown. The pictures show the state of the concrete spread before and after fiber addition. For test results from 4C-Rheometer, see (137).

	Time of test (min)	Slump Flow (mm)	T 500 (s)	Density(kg/m³)	Air content(%)
Before adding fibres	14	745	1,72	2288	3,4
After adding fibres (1)	36	690	2,5	2325	3,6
After adding fibres (2)	62	590	3,6	-	-

Table 2-7 Fresh properties for Mix 2

	Time of tests (min)	Slump Flow (mm)	T 500 (s)	Density(kg/m³)	Air content(%)
Before adding fibres	17	705	2,4	2290	3,2
After adding fibres	28	690	2,6	2325	3,4

Table 2-8 Fresh properties for Mix 4

	Time of test (min)	Slump Flow (mm)	T 500 (s)	Density(kg/m³)	Air content(%)
Before adding fibres(1)	10	800	1,5	-	-
Before adding fibres (2-Rescon T)	25	680	4,2	2229	5,8
After adding fibres	40	630	5,9	2327	3,9

Table 2-9 Fresh properties for Mix 5
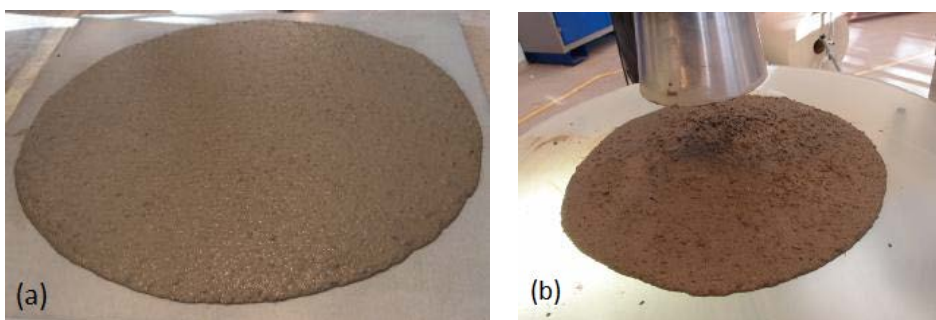
Figure 2-7 Mix 2 (a) before fiber addition (b) after fiber addition

Figure 2-8 Mix 4 (a) before fiber addition (b) after fiber addition
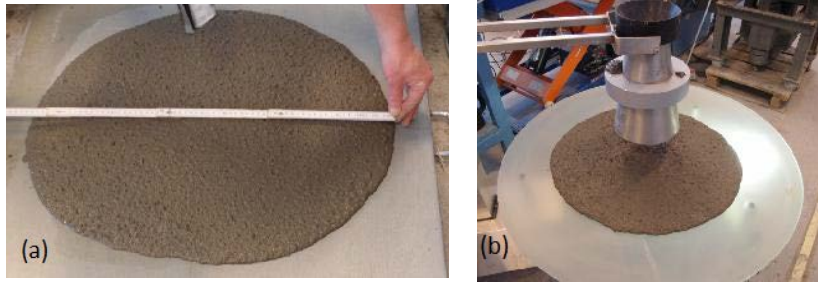
Figure 2-9 Mix 5 (a) before fiber addition (b) after fiber addition

Hardened properties

The following tables and figures show the hardened properties. For the results from fiber counting (fiber distribution), see (137). Also see Appendix F in (137) for detailed results from flexural test.

	Cylinder 1	Cylinder 2	Cylinder 3	Average
fcm at <u>14 days</u> (MPa)	41,1	41,4	41	41,17
Density (t/m³)	2,4	2,39	2,4	2,40

Table 2-10 Compressive strength for Mix 2

	Cylinder 1	Cylinder 2	Cylinder 3	Average
fcm at <u>14 days</u> (MPa)	37,4	37,9	37,7	37,67
Density (t/m³)	2,44	2,43	2,40	2,42

Table 2-11 Compressive strength for Mix 4

	Cylinder 1	Cylinder 2	Cylinder 3	Average
fcm at <u>14 days</u> (MPa)	32,1	32,1	32,1	32,1
Density (t/m³)	2,38	2,39	2,39	2,39

Table 2-12 Compressive strength for Mix 5
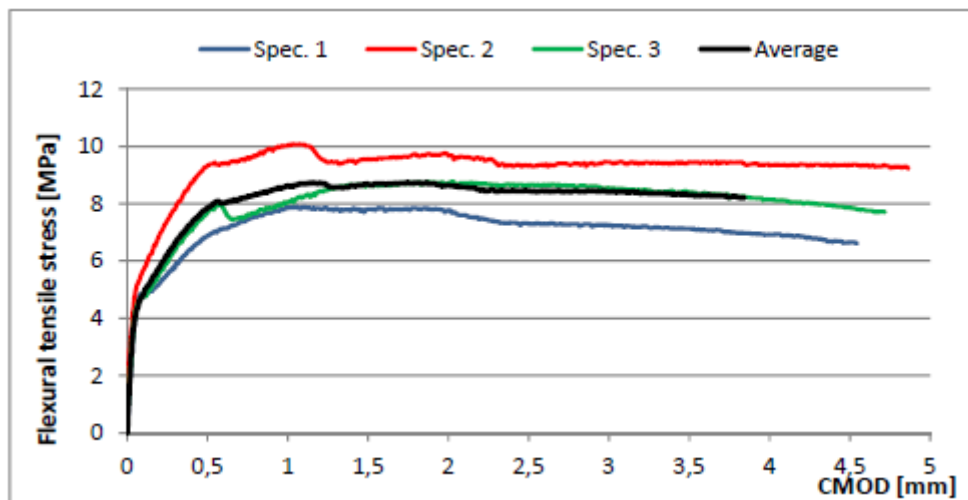
Figure 2-10 Flexural strength for Mix 2
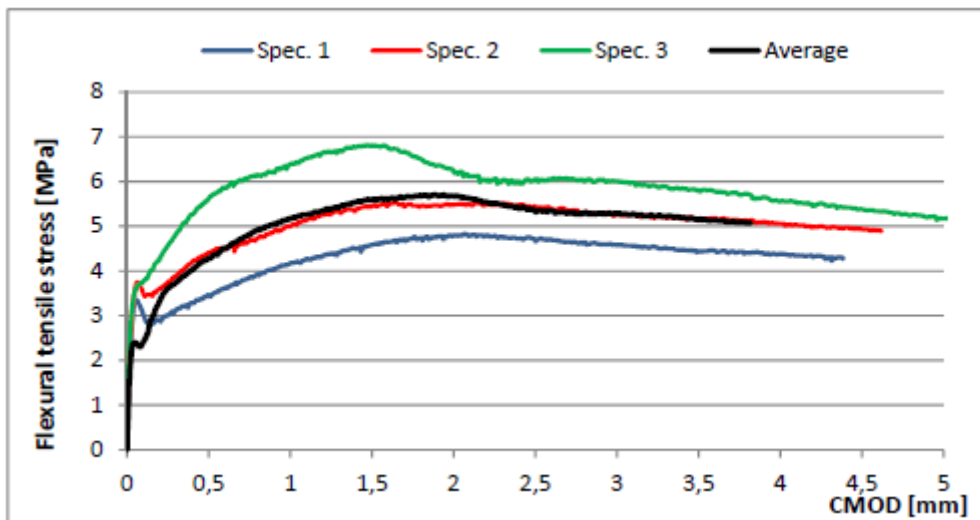
Figure 2-11 Flexural strength for Mix 4
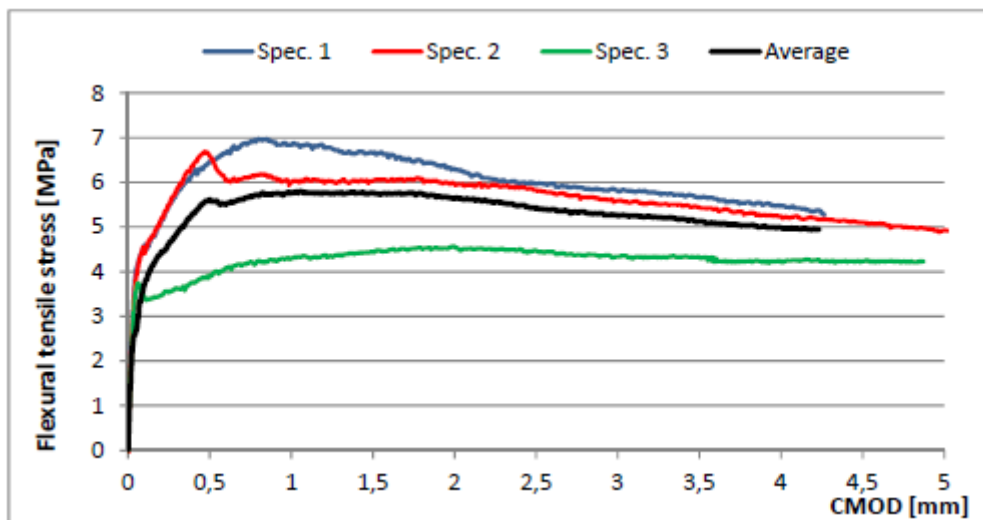
Figure 2-12 Flexural strength for Mix 5

Results and conclusions

Fresh properties

The fresh properties were satisfying for 1% fibers. Unlike in project FA 2.2, all the mixes here showed no segregation and the fibers were spread throughout the concrete spread.

The rheological parameters yield stress and plastic viscosity did not show any important change after adding fibers. This opens up for more volume of fibers. Also, the fact that the density increased in all specimens compared to specimens with 2% by volume of Dramix fibers shows a good compaction process, which strengthened the idea that SCC could be able to handle more volume of fibers.

The new method of filling the bucket proved successful as it did not lead to segregation in the slump flow test. Also, the sample in the bucket seemed more representative of the mix with this new method.

Hardened properties

Mix 2 showed better compressive strength than the other mixes, although Mix 4 obtained a value close to the value in Mix 2. Also, the flexural strength and ductility performances in Mix 2 were a lot better than in Mix 4 and Mix 5.

The better performance in hardened properties for Mix 2 indicates that the casting technique used in this mix (standard casting technique) offers the best results compared to the two additional casting techniques used in Mix 4 and Mix 5. This is also supported by Grünewald and Walraven (138) in their work.

The reason for the worse performances in Mix 4 and Mix 5 compared to Mix 2, is believed to have been due to the orientation factor. The casting techniques used in these mixes did not allow the fibers to be oriented in the favorable direction, which is perpendicular to the load action.

Conclusions

The standard casting technique gives the better performance in the hardened concrete properties and it will be applied for the new mixes (section 2.2.2.2), which will contain maximum 2% fibers by volume.

3.2.2.2   Fiber cocktails

In this part of the experimental program, the various mixes consisted of combinations of Dramix 65/60 RC BN and three other types of steel fibers. The effect of the different combinations on the fresh and hardened concrete properties was investigated.

Dramix 65/60 RC BN steel fibers were combined with the following types of fibers:

- Dramix 65/35 3D BG steel fibers
- Straight 13 mm long steel fibers with 0,16 mm in diameter, aspect ratio = l/d = 81,25
- Straight 6 mm long steel fibers with 0,16 in diameter, aspect ratio = l/d = 37,5

The standard casting technique was applied and the new method of filling the bucket with concrete, as described in section 2.2.2.1, was also applied. The mix designs of the different concretes were basically the same as the one shown in Table 2-6, with the final recipe slightly different for each mix due to the different amount of fibers added. The different mixes were named as follows:

- Mix 6: 1% 65/60 + 0,5% 65/35
- Mix 7: 1% 65/60 + 1% 65/35
- Mix 8: 1% 65/60 + 0,5% 13 mm
- Mix 9: 1% 65/60 + 1% 13 mm
- Mix 10: 1% 65/60 + 0,5% 6 mm
- Mix 11: 1% 65/60 + 1% 6 mm

As before, the compressive strength was measured according to NS-EN 12390-3 (116) and the flexural strength according to NS-EN 14651 (118). This time, the mechanical tests were run after 28 days. The fresh concrete properties were measured with the slump flow test (NS-EN 12350-8) and the LCPC-box (according to Roussel's paper (86)). The 4C-Rheometer test was omitted in these test series.

Fresh properties

The tables below show the fresh properties of the different mixes measured from slump flow test and LCPC–box. Only the pictures from slump flow test are shown in Figure 2-13. For pictures from LCPC-box, see (137).

		Slump Flow (mm)	T 500 (s)	Density(kg/m^3)	Air content (%)
Mix 6	Before adding fibres	790	2,22	2273	3,2
	After adding fibres	465	3,5	2344	3,5
Mix 7	Before adding fibres	775	2,9	2244	3,9
	After adding fibres	450	4,2	2339	4,5
Mix 8	Before adding fibres	805	2,22	2256	3,4
	After adding fibres	435	-	2355	2,7
Mix 9	Before adding fibres	740	3,62	2260	3,6
	After adding fibres	*	*	2294	6,8
Mix 10	Before adding fibres	777	3,4	2270	3,2
	After adding fibres	430	-	2335	3,7
Mix 11	Before adding fibres	756	3,34	2263	3,6
	After adding fibres	*	*	2389	3,2

Table 2-13 Fresh properties from Slump flow test

		After adding fibers
Mix 6	Density (kg/m^3)	2344
	Volume (m^3)	0,006
	h_0 (m)	0,078
	Laverage (m)	0,335
	u_0 (-)	0,780
	τ_0 (Pa)	**82,045**
Mix 7	Density (kg/m^3)	2339
	Volume (m^3)	0,0052
	h_0 (m)	0,078
	Laverage (m)	0,285
	u_0 (-)	0,77
	τ_0 (Pa)	**85,09**
Mix 8	Density (kg/m^3)	2355
	Volume (m^3)	0,006
	h_0 (m)	0,088
	Laverage (m)	0,2775
	u_0 (-)	0,88
	τ_0 (Pa)	**106,53**
Mix 10	Density (kg/m^3)	2335
	Volume (m^3)	0,006
	h_0 (m)	0,083
	Laverage (m)	0,293
	u_0 (-)	0,830
	τ_0 (Pa)	**93,428**

Table 2-14 Fresh properties from LCPC-box

	Before fiber addition	After fiber addition
Mix 6		
Mix 7		
Mix 8		
Mix 9		
Mix 10		
Mix 11		

Figure 2-13 The concrete spread before and after fiber addition

Hardened properties

The tables below show the hardened concrete properties conducted from the compression test and the flexural test. For detailed results from the flexural test and for fiber counting details, see Appendix F and page 88-100 in (137), respectively.

		Cylinder 1	Cylinder 2	Cylinder3	Average
Mix 6	f_{cm} (MPa)	49,74	48,39	49,64	**49,26**
	Density (t/m^3)	2,44	2,47	2,45	**2,45**
Mix 7	f_{cm} (MPa)	45,06	47,69	46,42	**46,39**
	Density (t/m^3)	2,46	2,47	2,46	**2,46**
Mix 8	f_{cm} (MPa)	45,62	48,95	39,74	**44,77**
	Density (t/m^3)	2,43	2,42	2,43	**2,43**
Mix 9	f_{cm} (MPa)	42,3	42,66	44,11	**43,02**
	Density (t/m^3)	2,34	2,34	2,35	**2,34**
Mix 10	f_{cm} (MPa)	50,24	49,41	49,98	**49,88**
	Density (t/m^3)	2,43	2,42	2,44	**2,43**
Mix 11	f_{cm} (MPa)	49,14	49,83	50,42	**49,80**
	Density (t/m^3)	2,46	2,46	2,47	**2,46**

Table 2-15 Hardened properties from compression test

Concrete mix no.	Mix 6	Mix 7	Mix 8	Mix 9	Mix 10	Mix 11
Compressive strength (MPa)	49,26	46,39	44,77	43,02	49,88	49,80
F_L (kN)	32,6	34,3	33,3	41,5	34,3	31,6
Max flexural strength (MPa)	11,8	12,3	11,9	15,0	12,2	11,5

Table 2-16 Hardened properties of the mixes

The results from the bending tests are shown in Figure 2-14 as stress vs. CMOD.
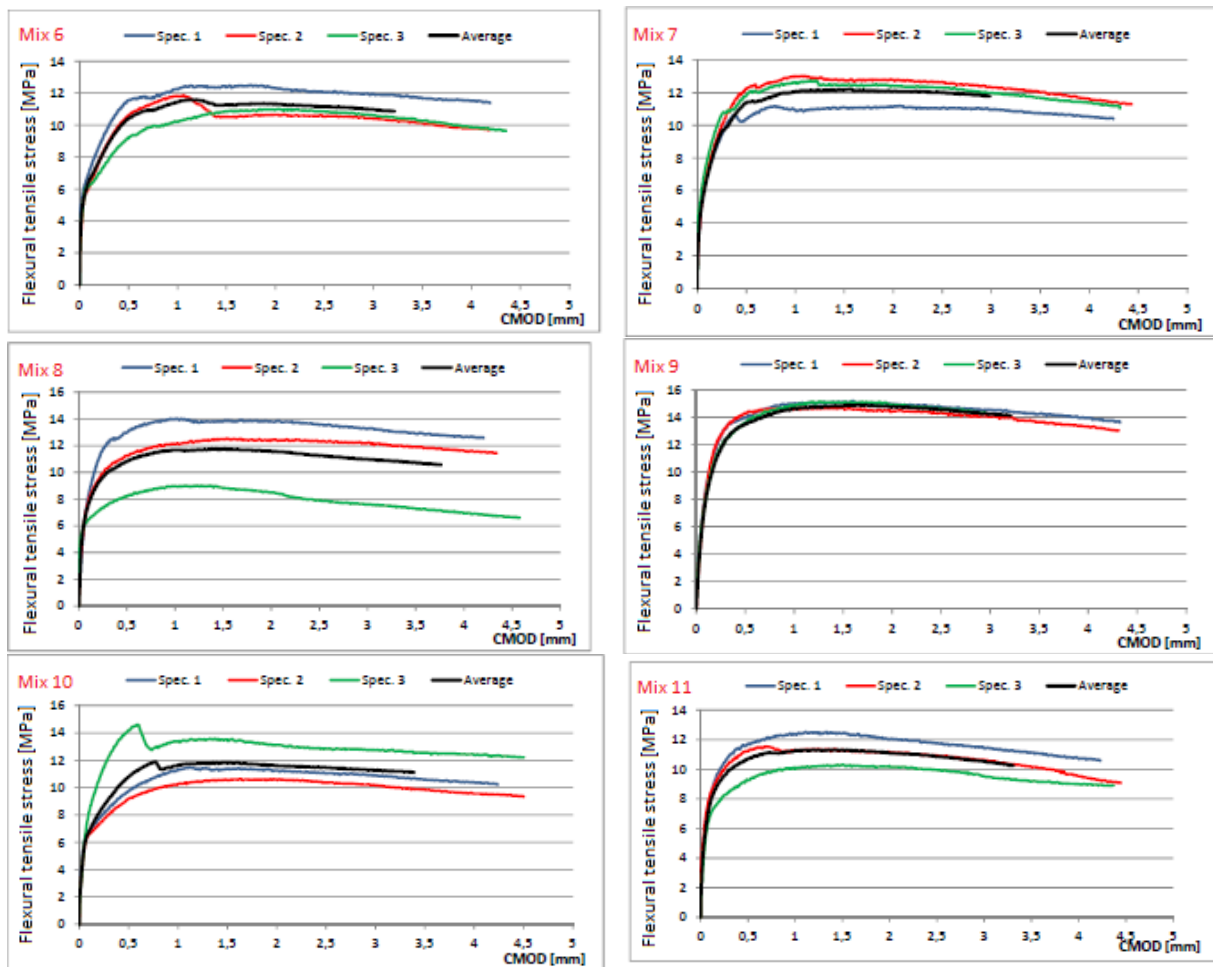
Figure 2-14 Stress vs. CMOD for the mixes

Results and conclusions

Fresh properties

The mixes with 1,5% fibers by total volume were satisfactory. Fluid mixture, good compaction process, no segregation and no fiber balls were observed.

For 2% fibers by total volume, only Mix 7 was satisfying. Mix 9 and Mix 11 did not show segregation and fiber balls did not occur, but the mixes were too stiff, causing no flow.

Hardened properties

The compressive strength values of the various mixes show similar strengths. This emphasizes the common understanding among researchers that fiber addition does not enhance the compressive strength worth of mentioning.

All the mixes showed a quite high flexural strength and ductility. The flexural strength values increase with higher volume of fibers, except for Mix 10 and Mix 11 where it was decreased. As in FA 2.2, increasing fiber content with 13 mm fibers (Mix 9) gave a higher increase in flexural strength than increasing the content with 35 mm (Mix 7) fibers. But Mix 9 showed a totally unsatisfactory behavior in the fresh state, making it irrelevant.

Conclusions

Comparing the flexural stresses with the values in FA 2.2 shows that the beams of one mix in this project have less scattering in their flexural stress values. This is due to the new method of filling the bucket with concrete, which makes the beam specimens of the same mix more homogeneous and similar.

6 mm long fibers offer slightly better performance in the fresh state than 13 mm long fibers but the latter fibers give higher flexural strength.

The compressive strength is not affected by the addition of fibers any mentionably.

3.3   New experiments

This chapter will describe the experiments done in this thesis, which consisted of studying the fresh and hardened properties of self-compacting fiber reinforced concrete with different types and contents of fibers. Based on the previous work, it was chosen to remake some of the mixes in order to reevaluate the properties and compare the results with the results from the previous work. Additionally, new mix designs were prepared and investigated. Hence, the experimental part was divided into two series:

- Steel fibers
  - Mix 1: 1%   Dramix 65/60
  - Mix 2: 1,5%   Dramix 65/60
  - Mix 3: 1%   Dramix 65/60   +   0,5%   Dramix 65/35
  - Mix 4: 1%   Dramix 65/60   +   1%   micro 13 mm

- Basalt fibers
  - Mix 5: 0,5%   Generation 3
  - Mix 6: 1%   Generation 3
  - Mix 7: 1,5%   Generation 3
  - Mix 8: 2%   Generation 3

The concrete was in durability class M60 and strength class B35 according to NS-EN 206-1, a standard given by the Norwegian standards organization Standard Norge. It was named M60 B35 SCC fiber as before in FA 2.2. The particle packing program "EMMA" was applied to reach the desired flowable and stable SCC.

First, the materials used and the tests performed in these experiments will be listed. The specific dates of the various tests will also be shown. Also, the mixing process along with the handling concrete process will be described. Finally, the fresh and hardened concrete properties that were achieved in these experiments will be shown and discussed.

3.3.1 Materials used

The materials that were used in these experiments were basically the same as those used in the master thesis early 2013. The only difference was one additional aggregate type (A-4045) and fiber type (basalt fibers) used in current experiments. For product data sheet for the different materials, see appendix.

Fibers

Totally four different fiber types were used in the experiments:

- Dramix 65/60 RC BN. The commercially correct name is Dramix RC - 65/60 - BN. It is a cold drawn steel wire fiber with hooked ends, identified as Group I in NS-EN 14889-1 and as type I in ASTM A820.

- Dramic 65/35 3D BG. The commercially correct name is Dramix 3D – 65/35 – BG.

- Straight 13 mm long high carbon steel fibres with 0.16 mm diameter, l/d = 81,25., commercially known as Bekaert OL13/.16. Purchased from Bekaert Norge AS.

- Basalt minibars generation 3, produced by Norwegian company ReforceTech. They are 42 mm in length, have cross-section area of 0,35 mm^2 and equivalent diameter of 0,67 mm.

Concerning the Dramix fibers, both are made of low-carbon steel with bright steel surface and eventually the fibers are glued together. Table 2-17 shows the comparison of both fiber types (data from product data sheet):

	Performance class	Fiber length, l [mm]	Fiber diameter, d [mm]	Aspect ratio, l/d	Tensile strength [MPa]	E-modulus [MPa]
Dramix 65/60	65	60	0,9	66,7	1160	210000
Dramix 65/35	65	35	0,55	63,6	1345	210000

Table 2-17 Fiber characteristics from product data sheets

In a pull-out test conducted by Sandbakk (5), he found that Dramix 65/35 might have improved the residual tensile strength at small deformations. After more testing, it was clear that the shorter Dramix fibers had contributed to an increase in the capacity at small deformations, but the capacity at larger deformations were reduced compared to tests done with Dramix 65/60. At the same time, the ductility is reduced compared to the ductility of concrete with the longer Dramix fibers.

Cement

The cement type used in all mixes was of type Norcem Standard FA; CEM II /A-V 42,5 R. It contains 20% siliceous fly ash. The strength class of the cement is 42,5. The letter "R" is related to high early age strength development. This cement is best suited for SCC in durability classes M90 and M60, and strength classes B35 and lower. It gives a higher resistance to flow than the pure Norcem Standard cement, providing somewhat better stability (73).

This cement was also used previously in FA 2.2 and the master thesis conducted in early 2013.

Silica fume

The type of silica fume used in these experiments was Elkem Microsilica Powder 920 D. The letter "D" stands for densified.

Sika demper

An admixture used to decrease the air content in the mixture.

Superplasticizer

A high range water reducing admixture was used; Dynamon SX-N. This is produced by a company called Mapei in Norway and based on Mapei's DPP-technology (Design Performance Polymers).

Filler

The filler used in the experiment was a limestone powder, purchased from Franzefoss Miljøkalk in Norway. The product type used is called "NSCC Coarse VK".

Fly ash

Additional fly ash was inserted in the mixes.

Aggregate

All of the aggregates were produced by Norstone in Norway. Totally three types of aggregates were used:

- Årdal 0-2 mm (A-4065)
- Årdal 0-8 mm (A-3899)
- Årdal 0-8 mm (A-4045)

A-4065 was used for all the mixes. A-3899 was used for Mix 1-3. A-4045 was used for Mix 4-8.

3.3.2   Mixing and handling processes

The mixer was a 10-litre flat-bottomed mixer with a counter current paddle. The following mixing process was applied once the materials were ready:

1. Dry mixing 1 minute. All the constituents of the mix recipe (except the water, superplasticizer and sika demper) were mixed together in the mixing machine.
2. Wet mixing 2 minutes. The water and sika demper were added first. Then the addition of superplasticizer written in the recipe took place.
3. Standstill 2 minutes. The mixing machine was turned off.
4. Wet mixing, adjustment of workability. Additional amount of necessary superplasticizer was added in order to reach the desired slump-flow value.
5. Addition of fibers.

Figure 2-15 Mixing process

To check if the fresh concrete had obtained the desired workability, the slump-flow test was performed. If the slump-flow value was below 710-720 mm, the test-concrete was put back into the mixer and step 4 was repeated. Once the desired slump-flow value (710/720 mm or more) was reached, the test-concrete was put back into the mixer and step 5 was initiated. This is the reason why the amount of superplasticizer used is slightly different in each mix.

The standard casting technique for the beam molds was applied for each mix. This casting method is defined in NS-EN 14651 (118) and in section 1.9.6.2 of this thesis. Due to the results from the casting technique investigations in the thesis in early 2013 (section 2.2.2.1), it was decided to apply the standard technique. The figures below show this casting technique.
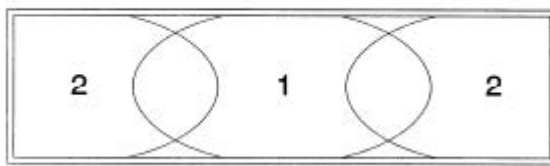
Figure 2-16 The standard casting technique

The new method of filling the bucket/pitcher with concrete was applied. This decision was also a result of the investigations in the previous thesis in 2013. This method was described in section 2.2.2.1. It should be noted that this method was only applied after the desired slump-flow value of 710+ mm was reached. This means that before fiber addition, the old method of filling the bucket/pitcher (by inserting the bucket directly into the mixer) was used in order to measure the slump-flow value and simultaneously save time. This was done to make sure the fresh concrete retained its flowability properties. The figure below shows this filling method.

Figure 2-17 The new method for filling the bucket

3.3.3   Tests performed

The tests were performed at SINTEF/NTNU laboratory. All the tests were applied after fiber addition. In addition, the value from the slump-flow test done before fiber addition (to reach the minimum value) was written down. The various fresh and hardened concrete tests are listed below.

- Fresh concrete: Slump-flow and T_{500}
                         Density
                         Air content
                         LCPC-Box

- Hardened concrete: Compression test
                         Three-point bending test
                         Fiber counting

Slump-flow and T_{500} were conducted according to NS-EN 12350-8 (83). The time of the tests conducted after the start of mixing was also written down. The density was measured according to NS-EN 12350-6 (139) and the air-void content according to NS-EN 12350-7 (140). The LCPC-Box test was performed after Roussel's paper (86). These tests are also described in section 1.8.7. The picture below shows the pressure-type air meter with a container-volume of 1000 cm^3 that was used to measure the density and air-void content of fresh mortar.

Figure 2-18 Pressure-type air meter

For the hardened concrete properties, the compressive strength was measured according to NS-EN 12390-3 (116) and the flexural strength according to NS-EN 14651 (118). These tests are also described in section 1.9.6. Concerning the compression test, three φ100x200 mm cylinders from each mix were tested. Concerning the bending test, three 150x150x550 mm beams with a 25 mm notch from each mix were tested.

The hardened concrete tests were conducted after over 40 days, due to the laboratory being closed one week in the month of August. The fresh and hardened concrete tests were performed on the following dates for the mixes:

	Mix no.	Casting date/fresh concrete test date	Hardened concrete test date	Days between casting and hardened test
Steel FRC	Mix 1	2 July 2013	14 August 2013	43
	Mix 2	2 July 2013	14 August 2013	43
	Mix 3	4 July 2013	14 & 15 August 2013	41-42
	Mix 4	4 July 2013	14 & 15 August 2013	41-42
Basalt FRC	Mix 5	10 July 2013	21 August 2013	42
	Mix 6	10 July 2013	21 August 2013	42
	Mix 7	12 July 2013	21 August 2013	40
	Mix 8	12 July 2013	21 August 2013	40

Table 2-18 Testing dates of the mixes

3.3.4   Steel fibers – Mix 1: 1% Dramix 65/60

This mix was the first of totally three mixes from Roca's thesis (137) that were remade in order to reevaluate the properties. It corresponds to Mix 2 in his thesis and the mixing and handling (new method of bucket-filling and standard casting technique) processes that were used are exactly the same. Also, the materials and the initial amounts of the various constituents that were mixed in the mixing machine are exactly the same. The reason for remaking the original mix was that Mix 2 was tested for hardened concretes properties after 14 days, which deviates from normal practice.

Fresh properties

The values from the slump-flow, density and air content tests are shown in Table 2-19 below.

Mix 1	Time of test (min)	Slump-flow (mm)	T_{500} (s)	Density (kg/m^3)	Air content (%)
Before fibers	16	740	5,5	2270	3,2
After fibers	40	480	-	2300	3,5

Table 2-19 Fresh properties of Mix 1

The initial slum-flow was 700 mm. After adding more superplasticizer, the values above were obtained. A visual observation showed that this concrete had good stability in the fresh state; no evidence of segregation or bleeding was observed. This same behavior was also observed after fiber addition, even though the concrete spread did not make the 500 mm mark on the base plate. The density increased after fiber addition, which means that there was a good compaction process in the mix after adding fibers. Due to human error, the picture of the slump flow was not taken.

The values from LCPC-Box test is shown below in Table 2-20.

Mix 1	After adding fibers
Density (kg/m^3)	2300
Volume (m^3)	0,0056
h_0 (m)	0,075
Laverage (m)	0,335
u_0 (-)	0,750
τ_0 (Pa)	**73,31**

Table 2-20 Values from LCPC-Box test for Mix 1

The obtained yield stress value of 73,31 Pa is very close to the recommended values (0-60 Pa, section 1.8.6) of regular SCC's, thus the result was satisfactory. There was also no difference worth of mentioning in the fresh behavior between the slump-flow test and the LCPC-Box test. The picture below shows the concrete in the box.

Figure 2-19 LCPC-Box of Mix 1

Hardened properties

The following table shows the compression values obtained from the test.

Mix 1	Cylinder 1	Cylinder 2	Cylinder3	Average
f_{cm} (MPa)	53,63	58,97	59,19	**57,26**
Density (t/m^3)	2,42	2,42	2,42	**2,42**

Table 2-21 Compressive strength for Mix 1

The results from the bending tests are shown in Figure 2-20 as flexural tensile stress vs. CMOD. The black curve shows the average value.
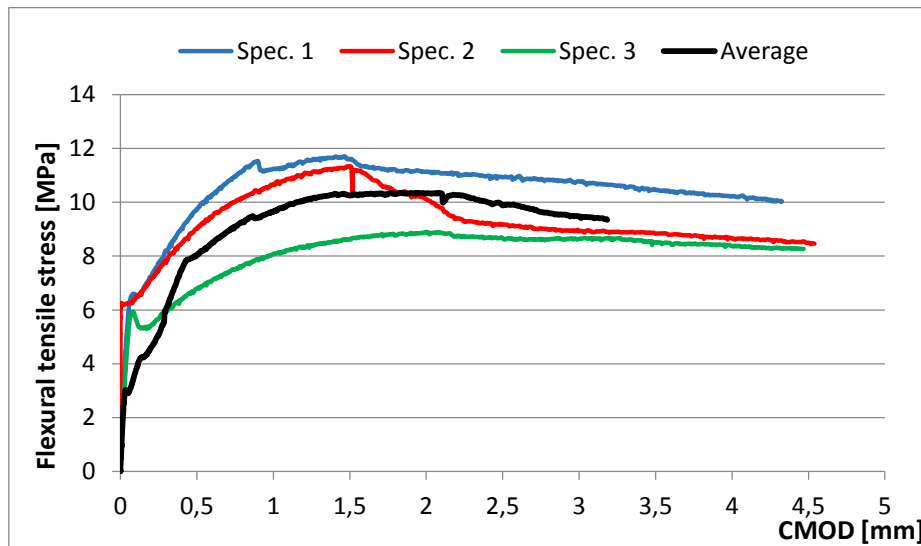
Figure 2-20 Stress vs. CMOD curves for Mix 1

All the beam specimens show deflection hardening and ductile behavior. However, we can see that specimen 3 shows lower flexural stress than the other specimens throughout the figure. The reason for this must be that this specimen had some damage on the surface which was visible. This was noted down on papers during the flexural testing. This beam shows a more significant drop in the stress reaching LOP than the other beams. Also, it should be mentioned that the metalplate (which is

in contact with the specimen's bottom surface at the notch) was not entirely in contact with the surface for specimen 1 due to uneven bottom. This was also noted down. But as we can see from Figure 2-20, this beam actually showed the best results in terms of max flexural stress.

Figure 2-21 shows the number of fibers in the different beam specimens. The corresponding orientation factor is shown in Table 2-22. According to the orientation factor, specimen 3 is supposed to have the highest flexural strength, while specimen 2 the second largest. This finding does not correlate with the stress vs. CMOD curves. Again, the reason for specimen 3 showing worst performance must be the damage it received. For specimen 1 and 2, the table below correlates with the curves.
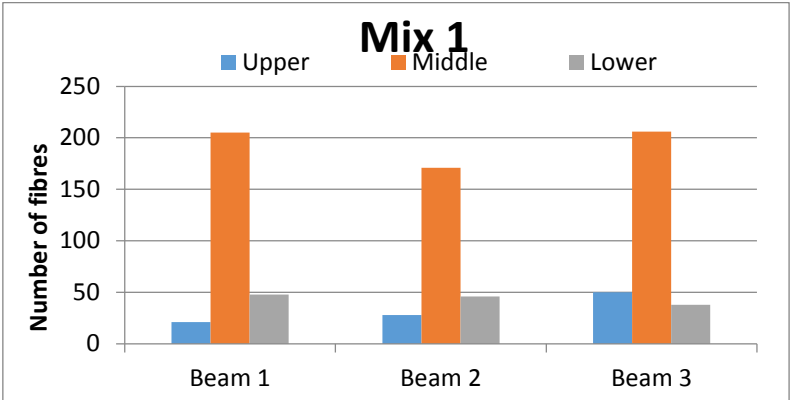
Figure 2-21 Fiber counting of Mix 1

	Number of Fibres		
	Beam 1	Beam 2	Beam 3
Upper	21	28	50
Middle	205	171	206
Lower	48	46	38
Total	274	245	294
Orientation factor	0,77	0,69	0,83

Table 2-22 Fiber counting and orientation factor for Mix 1

Comparing with previous work

Mix 1 with 1% Dramix 65/60 was also tested before; Mix 2 in Roca's work (137). The results from that test can be seen in section 2.2.2.1 in this thesis. Below, the fresh and hardened concrete properties of these two mixes will be compared.

Fresh properties

By comparing Table 2-19 and Table 2-7, it can be seen that the slump-flow values before fiber addition are similar. But after fiber addition, the values are quite different. Mix 1 seems to behave stiffer than did Mix 2, both before and after fiber addition. This is supported by T_{500} values; Mix 2 quickly reaching the 500 mm mark. Density and air content seems to be a bit higher for Mix 2.

The reason for the different behavior in flowability is unknown. Even though the materials used and the mixing process were exactly the same, Mix 1 showed worse performance. The reason could be that something went wrong during testing, and we did not notice due to lack of experience (this was our first mix).

The LCPC-Box was not applied for Mix 2. Hence, it is not possible to compare the yield stress directly. Comparing with the yield stress from rheometer; Mix 1 obtained a value of 73 Pa, while Mix 2 obtained 19 Pa. This is a huge difference, and it supports the fact that Mix 1 was stiffer in terms of flowability.

Hardened properties

It is important to note that the hardened properties tests were conducted after only 14 days for Mix 2, while for Mix 1 they were conducted after 43 days. This is the reason why Mix 1 shows better performance in compression; 57 MPa versus 41 MPa for Mix 2. Also, the flexural behavior is better for Mix 1; the average flexural stress is 10,6 MPa versus 8,9 for Mix 2. It should be noted that beam 3 (the damaged one) in Mix 1 showed 8,9 MPa, which is the same as the average value for Mix 2.

The ductile behavior seems to be more or less the same for the two mixes.

The fibers counted seem to be a bit higher for Mix 1 in general. The same is observed for the orientation factor. Both both parameters are not higher by much.

3.3.5   Steel fibers – Mix 2: 1,5% Dramix 65/60
Fresh properties

The table below shows the fresh properties for Mix 2.

Mix 2	Time of test (min)	Slump-flow (mm)	T_{500} (s)	Density (kg/m^3)	Air content (%)
Before fibers	20	730	2,9	2310	3,5
After fibers	41	465	7,4	2320	4,6

Table 2-23 Fresh properties of Mix 2

The first slum-flow measured was 715 mm. The values above were obtained after adding more superplasticizer. Again, the slump-flow mark of 500 mm was not reached. The pictures below show the concrete spread in the slump-flow test. Before fiber addition, the concrete showed no trends of segregation or bleeding; the concrete spread was homogeneous. After adding fibers, the concrete seemed to have good flow properties in the mixer. After the slump-flow test, it was obvious that the mix was stiffer. The picture to the right shows a slight accumulation of fibers on the left side due to the cone being lifted in a asymmetrical manner. However, the fibers would be accumulated in the middle if the cone was lifted the way it was supposed to anyway. Overall, the mixture showed a quite good behavior.
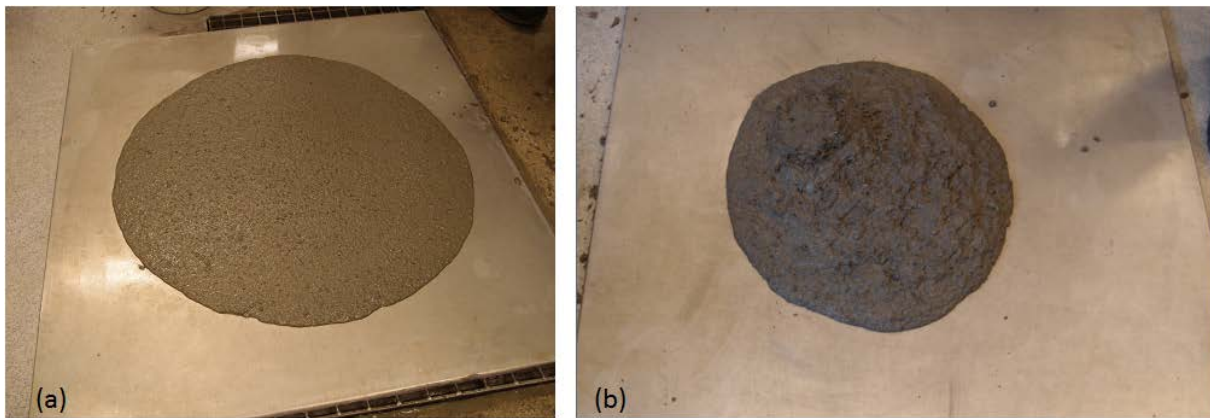
Figure 2-22 Mix 2 (a) before fiber addition (b) after fiber addition

For LCPC-Box results, see Table 2-24 below.

Mix 2	After adding fibers
Density (kg/m^3)	2320
Volume (m^3)	0,0052
h_0 (m)	0,075
Laverage (m)	0,325
u_0 (-)	0,75
τ_0 (Pa)	**79,65**

Table 2-24 Values from LCPC-Box test for Mix 2

The obtained yield stress value of 79,65 Pa was satisfactory; it was close to the recommended values of 0-60 Pa. When comparing the flow behavior of this test and the SF test, there was not much difference. The picture below shows this mix in the LCPC-Box. Also here, a slight accumulation of fibers can be seen at the top.

Figure 2-23 LCPC-Box of Mix 2

Hardened properties

Table 2-25 below shows the results from the compression test, while Figure 2-24 shows the results from the bending test. This time around, we made sure that the metalplate was in contact with the bottom surface of the beam in its entity.

Mix 2	Cylinder 1	Cylinder 2	Cylinder3	Average
f_{cm} (MPa)	54,15	57,57	42,45	**51,39**
Density (t/m^3)	2,42	2,42	2,42	**2,42**

Table 2-25 Compressive strength for Mix 2
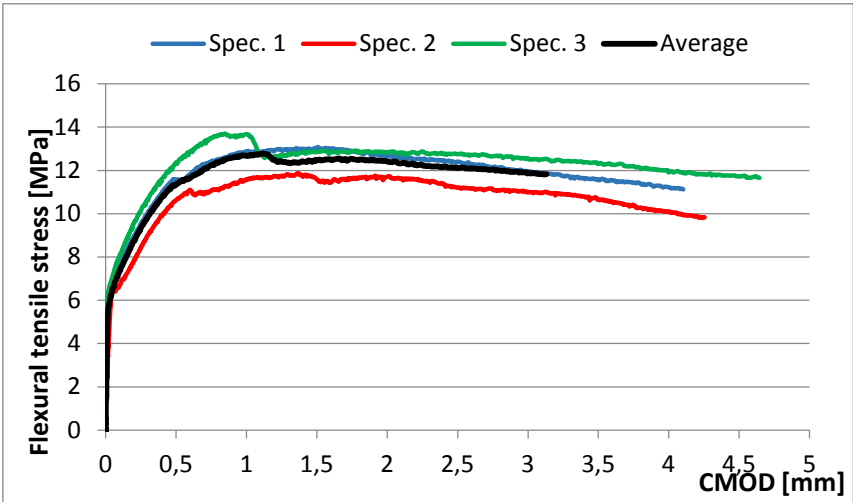
Figure 2-24 Stress vs. CMOD curves for Mix 2

The beam specimens show a very similar behavior; there is not much scattering. The average value of the max flexural tensile stress is 12,9 MPa, which is quite good and very close to the desired value of 15 MPa. The concrete also shows a hardening and ductile behavior as expected, reaching around 12 MPa at 2,5 mm of crack width.

Figure 2-25 and Table 2-26 show the fiber counting and orientation factors for Mix 2. Judging by the orientation factor, beam 3 should show the best performance in flexural strength and beam 2 should show the worst. These assumptions seem to correlate with the stress vs. CMOD curves. Also, we see how close the strengths are for beam 1 and beam 3.
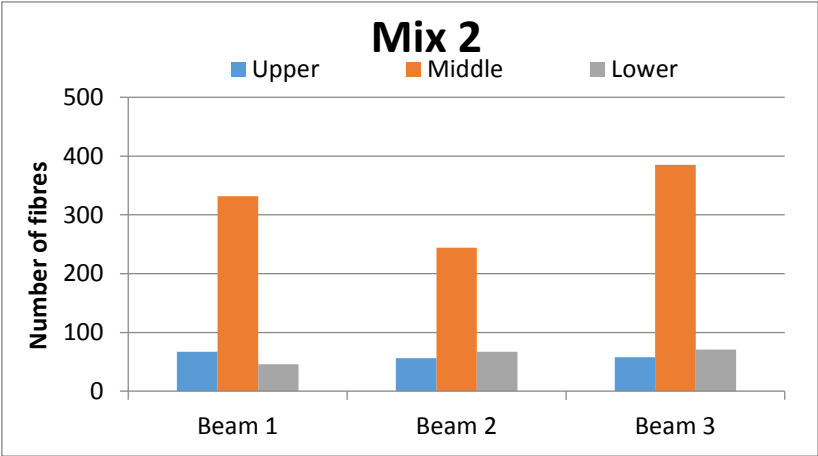
Figure 2-25 Fiber counting of Mix 2

	Number of Fibres		
	Beam 1	Beam 2	Beam 3
Upper	67	56	58
Middle	332	244	385
Lower	46	67	71
Total	445	367	514
Orientation factor	0,84	0,69	0,97

Table 2-26 Fiber counting and orientation factor for Mix 2

Comparing with Mix 1

Fresh properties

The SF-values of Mix 2 were a bit less than the values of Mix 1, which is expected due to the fact that Mix 2 contains higher content of fibers. However, it is interesting that T_{500} value for Mix 2 is less than for Mix 1 even though the total amount of superplasticizer used in Mix 1 was higher. Also, the concrete spread of Mix 1 was more stable and homogeneous than that of Mix 2. The density and air content was higher for Mix 2, especially after fiber addition; showing 4,6% versus 3,5% for Mix 1. This should lead to less compressive strength for Mix 2.

When comparing the yield stress values from LCPC-Box test, Mix 2 obtained a higher value. This is expected since Mix 2 contains a higher content of fibers. However, the rest of the parameters

(volume, laverage etc.) have very similar values. Judging from the pictures, it seems that Mix 1 is (slightly) more homogeneous than Mix 2 due to the accumulation of fibers at the top in Mix 2.

Hardened properties

In section 1.9.1, it was discussed whether or not the addition of fibers increased the compressive strength. Most researchers conclude with a negative; no major increase is observed. The same if observed for mixes when the fiber content is increased, see Figure 1-59 a. The average compressive strength of Mix 2 is actually lower than that of Mix 1. This must be due to the air content of Mix 2 being higher. The density is the same for both mixes.

Judging from the stress vs. CMOD curves for both mixes, they both show a very similar ductile behavior. For example for the black curve of Mix 1, the value is decreased with 1,1 MPa going from $CMOD_2$ to $CMOD_4$. For the same interval for Mix 2, the value is decreased with 1,0 MPa. However, the flexural strength of Mix 2 is higher. This emphasizes the findings of a lot of researchers. For example, it was stated in section 1.9.3 that Pajak and Ponikiewski (102) found increasing flexural strength with increasing fibers volume. Also, Wang (103) found that the curves give a smoother transition from first crack for increasing fiber content (Figure 1-68). This is also found for Mix 2 compared with Mix 1. The toughness (area under the curves) is also greater for Mix 2.

It is difficult to conclude whether or not the orientation factor is affected by the volume% of fibers. Overlooking beams 3 due to damage in Mix 1, we see that this factor remains the same for beams 2, while increasing for beams 1 with increasing volume% of fibers.

3.3.6   Steel fibers – Mix 3: 1% Dramix 65/60 + 0,5% Dramix 65/35

This mix was the second of totally three mixes from Roca's thesis (137) that were remade in order to reevaluate the properties. It corresponds to Mix 6 in his thesis.

Fresh properties

The table below shows the fresh properties of Mix 3. Due to a human error, the density and the air content before fiber addition were not measured. Also, a video was taped during the slump-flow test. This video can be watched from the CD delivered with this thesis.

Mix 3	Time of test (min)	Slump-flow (mm)	T_{500} (s)	Density (kg/m^3)	Air content (%)
Before fibers	15	740	2,1	-	-
After fibers	35	515	3,65	2226,7	3,5

Table 2-27 Fresh properties of Mix 3

The first slum-flow measured was 705 mm after 9 minutes. Adding more superplasticizer gave higher slump-flow value. Compared with the previous mixes, the SF-values are similar before fiber addition, while Mix 3 shows better spread after fiber addition. No segregation or bleeding was observed. By watching the video, it can be seen that the concrete spread passed the 500 mm mark very fast compared to Mix 1; 2,1 seconds versus 5,5 seconds for Mix 1. The flow behavior was quite fluid. After fiber addition, it can be seen from Figure 2-26 that the concrete showed a homogeneous spread with a very slight fiber accumulation in the middle. However, this accumulation was less than that of Mix 2, even though both mixes contained the same volume% of fibers. The reason for this could be that the aspect ratio is lower for Mix 3.

Figure 2-26 Mix 3 after fiber addition

The table below shows the results from the LCPC-Box test.

Mix 3	After adding fibers
Density (kg/m^3)	2227
Volume (m^3)	0,0047
h_0 (m)	0,07
Laverage (m)	0,3075
u_0 (-)	0,7
τ_0 (Pa)	**74,51**

Table 2-28 Values from LCPC-Box test for Mix 3

Also here, the yield stress value of 74,51 Pa lies in a close range to the recommended values for SCC. This value is close to the value for Mix 1. Comparing with Mix 2, we see that this value is lower for Mix 3. The corresponding T_{500} values emphasize this finding, being 7,4 seconds for Mix 2 and 2,1 seconds for Mix 3. The picture below shows the concrete in LCPC-Box test.

Figure 2-27 Mix 3 in LCPC-Box

Hardened properties

Table 2-29 below shows the results from the compression test, while Figure 2-28 shows the results from the bending test.

Mix 3	Cylinder 1	Cylinder 2	Cylinder3	Average
f_{cm} (MPa)	49,97	52,61	52,25	**51,61**
Density (t/m^3)	2,43	2,45	2,44	**2,44**

Table 2-29 Compressive strength for Mix 3

The average compressive strength is very similar to the strength of Mix 2, while it is lower than the compressive strength of Mix 1. The air content of Mix 1 and Mix 3 are similar; 3,5% for both. These findings again support the statement that increased fiber content does not increase the compressive strength (Figure 1-59 a).
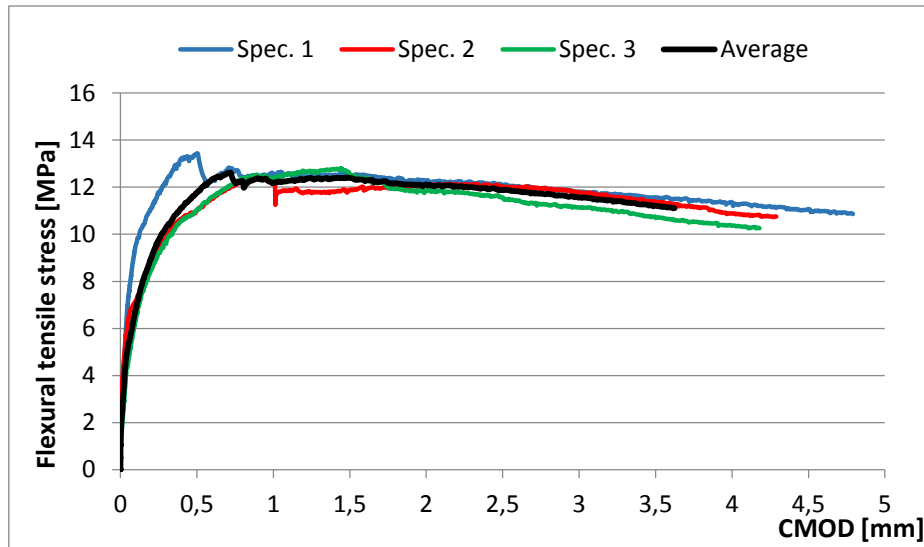
Figure 2-28 Stress vs. CMOD curves for Mix 3

Comparing stress vs. CMOD curves for Mix 1, Mix 2 and Mix 3, we can find the least scattering in the results of Mix 3. However, the max flexural stress for the average curve is the same as for Mix 2; 12,9 MPa. The load F_L is also very similar; 36,8 kN versus 36,3 kN for Mix 2.

This is the mix where the effective orientation factor equation was applied. Judging by the orientation factors for the beam specimens in Table 2-30, the beams should show similar behavior in flexural strengths. As already seen above in the stress vs. CMOD curves, this holds true.
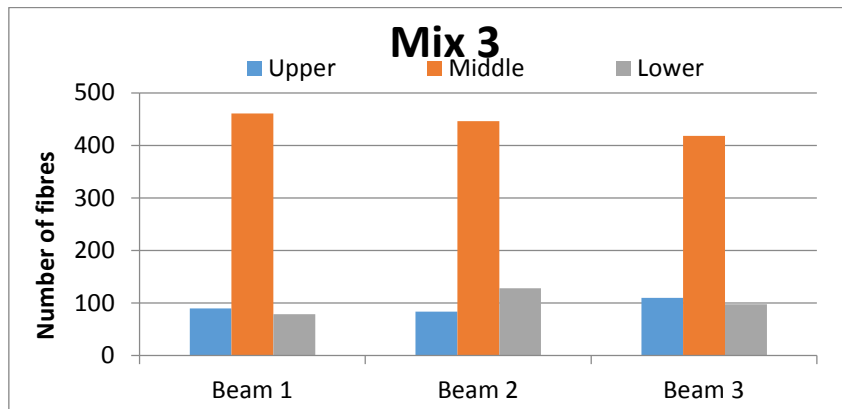
Figure 2-29 Fiber counting of Mix 3

	Number of Fibres		
	Beam 1	Beam 2	Beam 3
Upper	90	84	110
Middle	461	446	418
Lower	79	128	98
Total	630	658	626
Orientation factor	0,93	0,98	0,93

Table 2-30 Fiber counting and orientation factor for Mix 3

Comparing with previous work

The fresh and hardened concrete properties will be compared between Mix 3 of this thesis and Mix 6 of Roca's thesis (137), see section 2.2.2.2 for a summary of tests conducted on Mix 6.

Fresh properties

By comparing Table 2-27 and Table 2-13, it can be seen that the slump-flow value of Mix 3 before fiber addition is 50 mm lower, while after fiber addition it is 50 mm higher. This means that Mix 3 showed a more fluid behavior after fiber addition than did Mix 6. Even the total amount of superplasticizer used in Mix 6 was higher; 470 ml (by this authors calculation) versus 460 ml for Mix 3. The reason for this behavior could be that the time at which the slump-flow tests were taken are different (It is widely known that the time affects the workability of concrete). Nevertheless, if we compare the values of T_{500} for both mixes, we can see that the values are very similar both before and after fiber addition. The density, however, is lower for Mix 3.

Comparing the LCPC-Box test, we can see that all parameters of Mix 6 have higher values than those of Mix 3. The yield stress value is 82 Pa for Mix 6 and 74,5 Pa for Mix 3. This supports the fact that SF-value of Mix 6 was lower than that of Mix 3.

By comparing the pictures of both mixes (Figure 2-13 and Figure 2-26), we can see that they look very much alike; a very slightly accumulation of fibers in the middle.

An overall conclusion of the behavior in the fresh state is that both mixes showed similar workability characteristics. There was not much differences.

Hardened properties

The average compression value of Mix 3 is a bit higher than that of Mix 6, but not much; 51,61 MPa versus 49,26 MPa for Mix 6. Also the density was similar. Therefore it can be concluded that both mixes showed similar performance in compression.

The stress vs. CMOD curves show a slightly more scattering for Mix 6. Mix 3 obtained a bit higher max flexural tensile stress; 12,9 MPa versus 11,8 MPa for Mix 6. The load F_L was also higher; 36,8 kN versus 32,6 kN for Mix 6. Both mixes show more or less similar ductile behavior.

It should be noted that the days between the casting and the hardened concrete testing was different for these mixes. Mix 6 was tested after 28 days, while Mix 3 was tested after 41 days. This could explain the slightly higher strengths obtained in Mix 3.

Mix 3 has higher orientation factor value than does Mix 6. This is due to the number of fibers being a lot higher in Mix 3; numbers in the range of 620-650 versus 420-510 for Mix 6. It should be mentioned that, as the fiber counting graphs correlated with the stress vs. CMOD curves in Mix 3, so did those for Mix 6.

3.3.7   Steel fibers – Mix 4: 1% Dramix 65/60 + 1% micro 13 mm

This mix was the third of totally three mixes from Roca's thesis (137) that were remade in order to reevaluate the properties. It corresponds to Mix 9 in his thesis.

Fresh properties

Table 2-31 shows the slump-flow, T_{500}, density and air content values for Mix 4. Before fiber addition, no segregation or bleeding was observed. During the addition of short fibers into the mixer, we observed that the fiber balls occurred very easily. This affected also the long fibers, making them take part in the fiber balls. Further, this mix showed a very stiff behavior; there was no point in measuring the SF- and T_{500} values. A picture was not taken, but the concrete spread after fiber addition looked slightly more flowable than that of Mix 9, see Figure 2-13. It should be noted that the initial mix recipes for Mix 9 and Mix 4 were slightly different. Additionally, a different 0-8 mm aggregate type was used. This could be the reason why the diameter of the concrete spread of Mix 4 was a little bit higher. However, the concrete was so stiff that it showed no flow. We had to use tools to drag the concrete out of the mixer. Therefore, it was decided not to test this concrete in the LCPC-Box.

Mix 4	Time of test (min)	Slump-flow (mm)	T_{500} (s)	Density (kg/m^3)	Air content (%)
Before fibers	8	775	3,4	2280	2,4
After fibers	-	-	-	2430	2,4

Table 2-31 Fresh properties of Mix 4

Hardened properties

The table below shows the values obtained in the compression test, while Figure 2-30 shows the stress vs. CMOD curves for Mix 4.

Mix 4	Cylinder 1	Cylinder 2	Cylinder3	Average
f_{cm} (MPa)	56,15	58,01	58,94	**57,82**
Density (t/m^3)	2,46	2,46	2,47	**2,46**

Table 2-32 Compressive strength for Mix 4

Comparing the average value with Mix 1, we can see that they are very much similar. This again emphasizes the statement that increased volume% of fibers does not contribute to increased compressive strength. This time around, the strength was not reduced however.
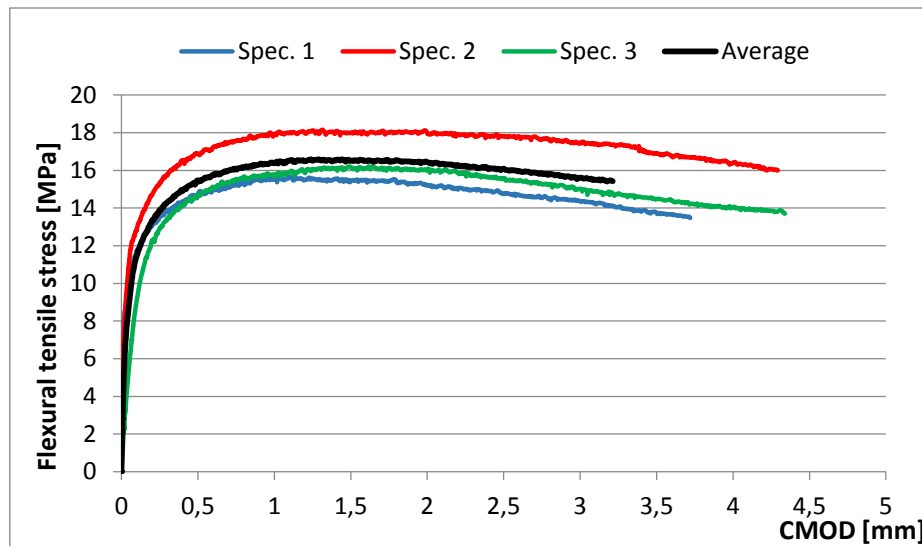
Figure 2-30 Stress vs. CMOD curves for Mix 4

The beams specimens had little scattering in the values, but nevertheless they showed a quite similar behavior, judging by the similar curve directions and overall behavior. Unlike the previous mixes (Mix 1, Mix 2 and Mix 3) in this thesis, the beams in this mix showed no reduction in stress after reaching LOP. In addition, this mix showed the best performance in flexural strength compared to the other mixes. The obtained max flexural tensile stress of the average curve was 16,7 MPa. This supports the findings of Pajak and Ponikiewski (102) and Wang (103); the flexural strength increases with increasing volume% of fibers in a self-compacting concrete. The 16,7 MPa is higher than the desired 15 MPa, which is very positive. Also, the mix showed a ductile behavior.

It should be mentioned that the casting of the beams was not satisfactory because a lot of pores were visible on the surfaces of the beam specimens. Therefore, it is unknown why these beams still showed such a good performance in the bending test.

Figure 2-31 and Table 2-33 show the fiber counting results for Mix 4. Due to the 13 mm fibers being impossible to count, the orientation factor was not calculated for this mix. However, judging by the numbers of long fibers in the different beam specimens, we see that Figure 2-31 correlates very much with Figure 2-30 (stress vs. CMOD curves for Mix 4); beam 2 shows the best flexural performance, while beam 3 shows the second best performance.
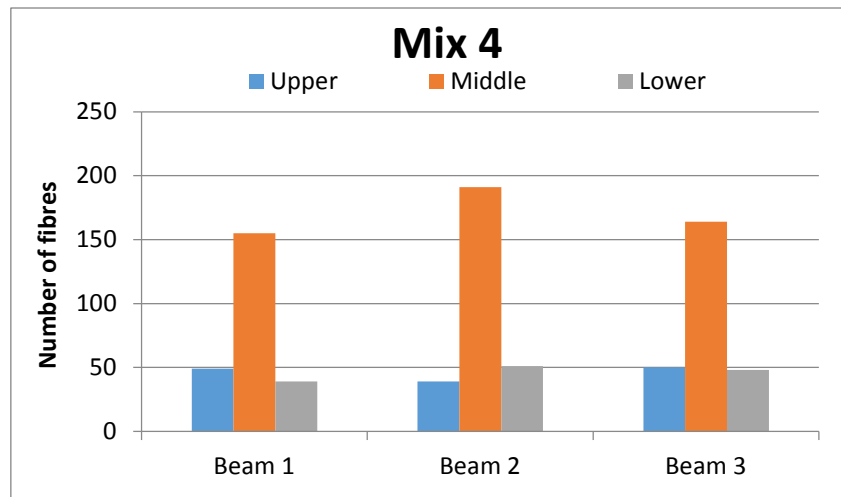
Figure 2-31 Fiber counting of Mix 4

	Number of Fibres		
	Beam 1	**Beam 2**	**Beam 3**
Upper	49	39	50
Middle	155	191	164
Lower	39	51	48
Total	243	281	262

Table 2-33 Fiber counting of Mix 4

Comparing with previous work

Fresh properties

Mix 4 in this thesis and Mix 9 in Roca's thesis show the same behavior in workability characteristics; the concrete is very stiff and shows no flow and tools had to be used in order to get the concrete out of the mixer.

By comparing the fresh properties values, we can see that the slump-flow obtained was higher for Mix 4 (before fiber addition). Also, the corresponding T_{500} value was higher for Mix 4. These findings correlate with the attempted concrete spread after fiber addition; even though both "spreads" were much alike, Mix 4 showed a little bit more fluidity. However, for both mixes, the slump-flow test after fiber addition was a failure; there was no point in measuring the diameter. Also, the LCPC-Box test was not conducted for either mix due to no flow.

The density was higher for Mix 4, while the air content was higher for Mix 9. This should give reduced compressive strength in Mix 9 compared to Mix 4.

Hardened properties

By comparing the compression values of both mixes, the statement about reduced strength in Mix 9 holds true. The difference in values is high; 57,82 MPa versus 43,02 MPa for Mix 9. The reason is obvious; due to a different degree of compaction, the air content in Mix 9 was much higher (6,8% versus 2,4% for Mix 4). Even though the cylinders of Mix 4 were cured 14 days more than the cylinders of Mix 9, the resulting difference in compressive strength could not be that high. Reason: As

already mentioned in the previous section, the difference in the compression strengths for Mix 3 in this thesis and Mix 6 in Roca's thesis due to different testing days was very little.

The performance in flexural stress was similar for both mixes. Mix 9 also obtained a high max flexural tensile stress for the average curve, being 15 MPa. The corresponding value for Mix 4 was 16,7 MPa, thus, a bit higher. Regardless, they both showed a high ductile behavior. But as already pointed out by Roca (137), even though this mix showed a very good flexural performance and obtained higher stress than 15 MPa, the bad performance in the fresh state leads to one conclusion; this concrete cannot be used for the purpose the COIN project is looking for.

The number of counted fibers for Mix 9 is a bit higher than that of Mix 4. But the average max flexural tensile strength is higher for Mix 4. According to the theory (section 1.9.3), higher amount of fibers should give higher flexural strength. This shows us that we cannot always rely completely on fiber counting giving the same results as the bending test.

3.3.8 Steel fibers – Results, discussion and conclusions

Results

All mixes showed satisfying fresh concrete properties before fiber addition. No signs of bleeding or segregation were observed, both in the mixer and on the slump-flow baseplate during testing. The flowability of the mixes was also quite good. The ability to bring coarse aggregate to the rim and the slurry at the periphery confirm these observations.

After fiber addition, the mixes with a maximum of 1,5% fibers by volume still showed good flowability characteristics. Generally, there was not segregation or bleeding, but a very slight accumulation of fibers was observed for the mixes with 1,5% fibers by volume. This slight accumulation was even less for the mix with 35 mm fibers. The mix with 2% fibers by volume was very stiff and showed no flow during SF-test. The yield stress values were satisfying for mixes with a maximum of 1,5% fibers by volume.

The 1% and 2% mixes obtained higher compressive strengths than the mixes with 1,5% of fibers by volume. All beam specimens showed a ductile behavior. The flexural strength and toughness increased with increasing volume% of steel fibers. The average max flexural tensile stress reached 10,6 MPa, 12,9 MPa, 12,9 MPa and 16,7 MPa for Mix 1, Mix 2, Mix 3 and Mix 4, respectively.

An increased orientation factor gave an increased flexural strength. Also, the orientation factor showed a tendency of increasing with increased volume% of fibers in the concrete. The orientation factor for Mix 4 was not possible to calculate due to the inability to count 13 mm fibers.

Discussion and conclusions

The concrete mixes appeared stable and homogeneous in the fresh state before steel fiber addition. These characteristics have also been observed during the previous works in 2011 and 2013. However, after fiber addition, the obtained results in the fresh state in this experiment were similar only to the work in 2013. Roca (137) suggested that a part of the reasons why the fresh behavior was different from the work in 2011 was due to the change in aggregate distribution and the replacement of limestone with fly ash. Also, it is apparent by the results in this thesis, together with the results in 2011 and 2013, that the fresh properties become unsatisfactory when the volume of fibers is equal to or higher than 2%, which is apparently a conclusion.

It can be concluded that the compressive strength is not enhanced with increased volume% of fibers. From the comressive strength results, we see that the effect of increased volume% of fibers on the strengths is modest, if any. The results gives both a very modest increase and a decrease in strength. This was also the case with Roca's results; a modest reduction in compressive strength took place each time the volume% of fibers was increased, see Table 2-16. These finding are in compliance with the statements of a number of researchers; Fanella and Naaman (93), Hsu and Hsu (91) and König and Kützing (92).

It is obvious that the flexural strength and toughness increase with increased volume% of fibers. This emphasizes the findings and conclusions of a lot of researhers, for instance Pajak and Ponikiewski (102), Wang (103) and Namaan and Reinhardt (106). Also, just as in (104), the ultimate flexural load increases as the steel fiber content increases.

The orientation factor seemed to correlate with the stress vs CMOD curves, giving higher strengths for increased factors. Therefore, fiber counting is a good tool to predict the flexural behavior.

3.3.9 Basalt fibers – Mix 5: 0,5% Generation 3

All the materials that were used in basalt test series were the same as those used in steel test series, except the 0-8 mm aggregate type and fiber type. Also, Mix 4 contained the same 0-8 mm aggregate type that was used in basalt test series.

Fresh properties

Table 2-34 shows the values obtained from the slump-flow test for Mix 5. After the added superplasticizer, the flowability was quite good. This is shown by the T_{500} values. Comparing this value before fiber addition with the steel mixes, we can see that they are very similar except for the value in Mix 1. The SF-value of 710 mm is lower than that of steel mixes which seems odd because all the steel mixes contain higher contents of fibers by volume. The reason lies in the time of the SF-test. By comparing the time at which the tests were conducted, we find that this mix has the highest value; 32 minutes.

Mix 5	Time of test (min)	Slump-flow (mm)	T_{500} (s)	Density (kg/m^3)	Air content (%)
Before fibers	32	710	2,29	2225	3,4
After fibers	46	610	4,1	2198	4,2

Table 2-34 Fresh properties of Mix 5

Visual observation showed no signs of segregation and bleeding in the concrete spread both before and after fiber addition. The mix was homogeneous and showed good stability. The ability to bring coarse aggregate to the rim and the slurry at the periphery confirm these observations.

Mix 5	After adding fibers
Density (kg/m^3)	2198
Volume (m^3)	0,0049
h_0 (m)	0,07
Laverage (m)	0,355
u_0 (-)	0,7
τ_0 (Pa)	**71,59**

Table 2-35 Values from LCPC-Box test for Mix 5

The above table shows the fresh properties from the LCPC-Box test. It was noted down that the time of mixing was longer in this mix than the other basaltic mixes. The value of 71,59 Pa obtained lies close to the recommended values for SCC mixes. This value is actually lower than all the steel mixes conducted in this thesis.

Hardened properties

The table and figure below show the compressive and flexural tensile strengths, respectively, for Mix 5. The average compressive strength value is similar to the steel mixes; a bit higher than that of Mix 2 and Mix 3, while close to those of Mix 1 and Mix 4. However, the density was lower for Mix 5 than all the steel mixes.

Mix 5	Cylinder 1	Cylinder 2	Cylinder3	Average
f_{cm} (MPa)	59,42	59,25	56,52	**58,40**
Density (t/m^3)	2,35	2,34	2,34	**2,34**

Table 2-36 Compressive strength for Mix 5
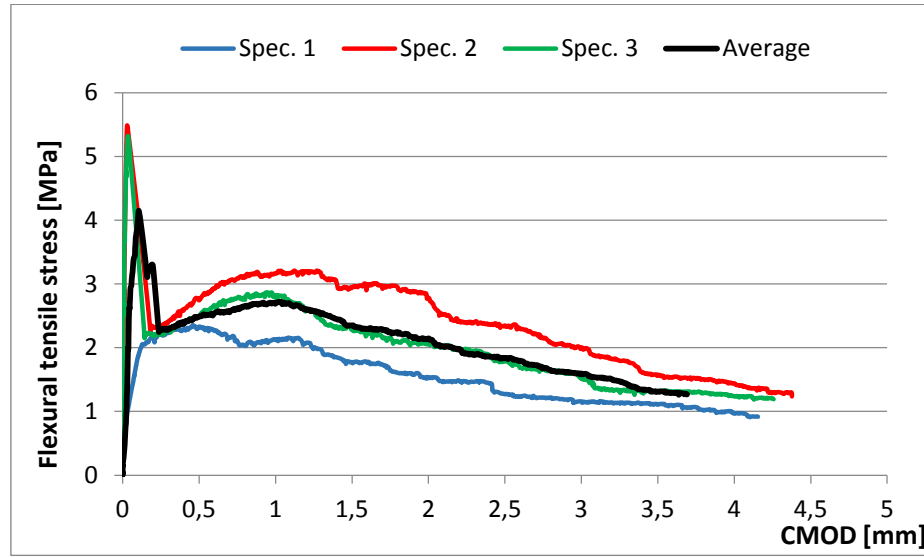
Figure 2-32 Stress vs. CMOD curves for Mix 5

Figure 2-32 shows the flexural performance of this concrete. Before analyzing the results, it should be mentioned that the results for beam specimen 1 and specimen 3 should be overlooked. For specimen 1, a preload was applied before testing which could be the reason why this specimen showed the worst performance. For specimen 3, a software problem occurred. Therefore it was decided to overlook the results from this specimen also. However, we can see from Figure 2-32 that the behavior of specimen 2 and 3 are very similar.

The average max flexural stress value is 4,4 MPa. This is very low and it should be concluded that this mix showed a very bad flexural performance. Also, we can see that the behavior is not ductile; a dramatic and sudden decrease of strength at low CMOD-values. This is similar to a brittle failure. The F_L load obtained was 12,4 kN.

Comparing the flexural performance of this mix with the steel mixes', we see how low both the stress and load are for Mix 5. Whether or not this bad performance is due to problems during testing, remains to be seen.

3.3.10 Basalt fibers – Mix 6: 1% Generation 3

Fresh properties

Table 2-37 and Table 2-38 show the fresh properties of this mix.

Mix 6	Time of test (min)	Slump-flow (mm)	T_{500} (s)	Density (kg/m^3)	Air content (%)
Before fibers	10	770	2,7	2279	2,5
After fibers	-	465	3,9	2325	3,2

Table 2-37 Fresh properties of Mix 6

The slump-flow value was very high; 770 mm before fiber addition. This time around, the 500 mm mark was not reached after fiber addition. The picture below shows the concrete spread before fiber addition. It showed no signs of segregation or bleeding; the mix was homogeneous. Also, the flowability was high; T_{500} value of 2,7 seconds.

After the fiber addition, the concrete spread still showed no signs of fibre segregation. The performance in the slump-flow test was considered satisfactory.

Figure 2-33 Slump-flow of Mix 6 before fiber additon

The Obtained value of 65,27 Pa in the LCPC-Box test is very close to the recommended values of SCC mixes. The pictures in Figure 2-34 show the same behavior as described in the slump-flow test; a high flowability with no trends of segregation of any material constituents.

Mix 6	After adding fibers
Density (kg/m^3)	2325
Volume (m^3)	0,005
h_0 (m)	0,070
Laverage (m)	0,445
u_0 (-)	0,700
τ_0 (Pa)	**65,267**

Table 2-38 Values from LCPC-Box test for Mix 6

Figure 2-34 Mix 6 in LCPC-Box

Hardened properties

Table 2-39 shows the obtained compressive strengths for the cylinders, while Figure 2-35 shows the stress vs. CMOD curves for Mix 6.

Mix 6	Cylinder 1	Cylinder 2	Cylinder3	Average
f_{cm} (MPa)	57,19	57,00	57,1	**57,1**
Density (t/m^3)	2,35	2,35	2,35	**2,35**

Table 2-39 Compressive strength for Mix 6
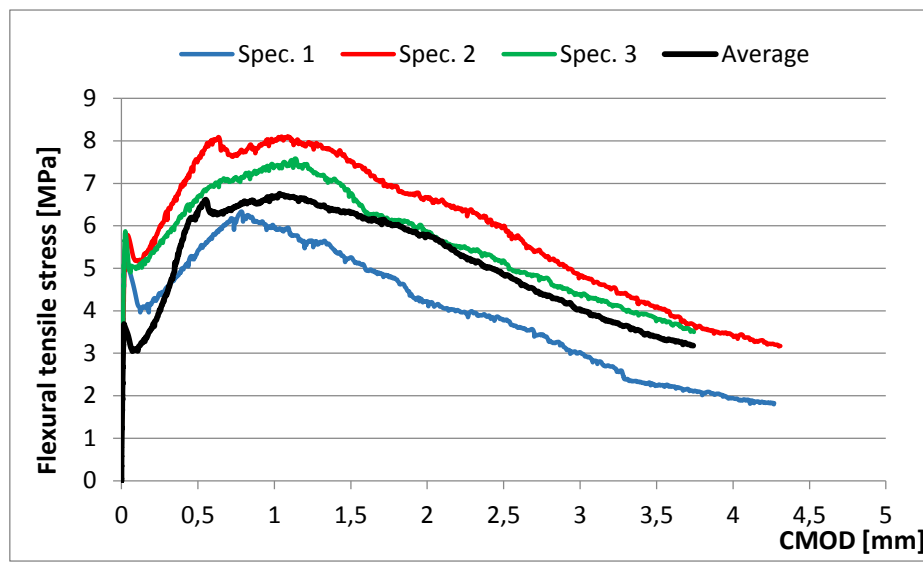
Figure 2-35 Stress vs. CMOD curves for Mix 6

By analyzing Figure 2-35, we see that all the specimens show a sudden decrease in stress after reaching LOP. But this decrease is quickly changed to increase and the concrete starts to show deflection hardening behavior. The post-cracking ductility is somewhat good for the specimens. The average max flexural stress obtained was 7,3 MPa and the F_L was 20,9 kN.

Comparing with Mix 5

Fresh properties

The slump-flow value before fiber addition is a lot higher than that of the previous mix. The main reason lies in the time of this test; 10 min versus 32 min for Mix 5. The total amount of superplasticizer added in Mix 6 was slightly higher; 451,4 ml versus 449,5 for Mix 5, indicating that it was not high enough to contribute to higher slump-flow value. Therefore it can be concluded that the time of the test is the reason for the higher SF-value.

Comparing with Mix 5, the SF-value after fiber addition is lower than that of Mix 5, which is understandable due to higher volume% of fibers in Mix 6. However, even though the volume% of fibers is higher, the air content of Mix 6 is surprisingly lower. If we compare this finding with the comparison between Mix 1 and Mix 2, we see that the air content was increased with higher volume% of fibers for those mixes. The reason for this could lie in a more compacted concrete for Mix 6. This statement is supported by the higher density in Mix 6.

The yield stress value for Mix 6 is lower. Due to higher volume% of fibers, this value should be higher than that of Mix 5. But since the time of mixing was longer for Mix 5, it behaved stiffer. Therefore it is reasonable to believe that this caused the value to be higher than that of Mix 6.

Hardened properties

The compression strength seems to be similar. It is not affected by the increasing volume% of fibers.

The average flexural strenght of Mix 6 is higher. For different CMOD-values, the stress is more than doubled. For example, the stress at $CMOD_1$ is 2,6 for Mix 5 and 6,8 for Mix 6. Similarly, at $CMOD_2$ the value is 2,3 and 6,4 for Mix 5 and Mix 6 respectively. Mix 6 shows a better overall flexural performance considering the strength, toughness and ductility.

3.3.11 Basalt fibers – Mix 7: 1,5% Generation 3

Fresh properties

Table 2-40 and Table 2-41 show the fresh properties obtained in the slump-flow test and the LCPC-Box test, respectively. Figure 2-36 shows the concrete spread in the slump-flow test.

Mix 7	Time of test (min)	Slump-flow (mm)	T_{500} (s)	Density (kg/m^3)	Air content (%)
Before fibers	12	770	2,09	2317	2,7
After fibers	31	480	5,46	2328	3,4

Table 2-40 Fresh properties of Mix 7

As the picture to the left in Figure 2-36 shows, the concrete spread was homogeneous with no signs of instability before fiber addition. The obtained SF-value was also high and the T_{500} value shows a quite fluid concrete. Naturally, the concrete behaved stiffer after fiber addition, as seen in the picture to the right. It showed a very little fiber accumulation in the middle, but it was so little that we concluded this concrete to show an overall good stability.
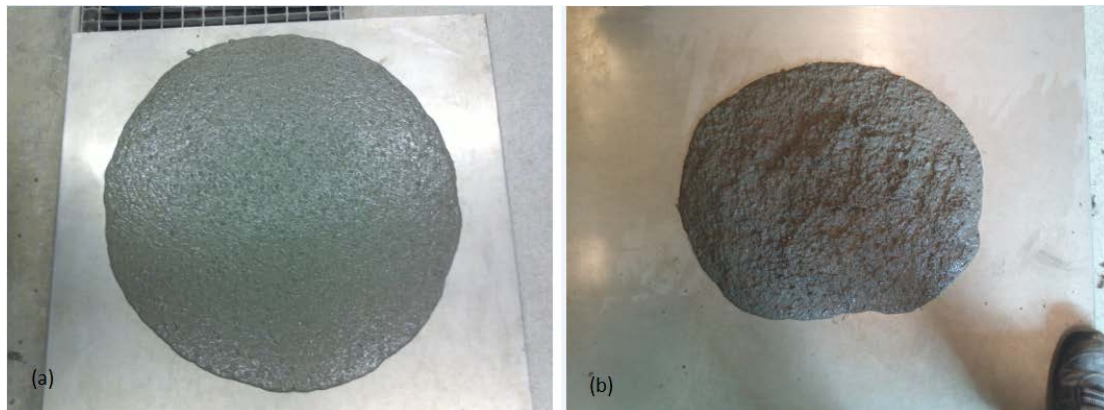
Figure 2-36 Mix 7 (a) before fiber addition (b) after fiber addition

The concrete showed good workability characteristics in the LCPC-Box test. The yield stress value from Table 2-41 shows a value that is a bit far from 60 Pa (Figure 1-43). But we have to remember that those recommended values concern regular SCC (without fibers). Therefore we can conclude that the yield stress value obtained is satisfying. Pictures were not taken.

Mix 7	After adding fibers
Density (kg/m^3)	2328
Volume (m^3)	0,005
h_0 (m)	0,075
Laverage (m)	0,353
u_0 (-)	0,750
τ_0 (Pa)	**86,408**

Table 2-41 Values from LCPC-Box test for Mix 7

Hardened properties

Table 2-42 shows the values obtained in the compression test, while Figure 2-37 shows the flexural tensile stresses obtained in the three-point bending test.

Mix 7	Cylinder 1	Cylinder 2	Cylinder3	Average
f_{cm} (MPa)	53,84	53,85	54,01	**53,90**
Density (t/m^3)	2,35	2,35	2,34	**2,35**

Table 2-42 Compressive strength for Mix 7
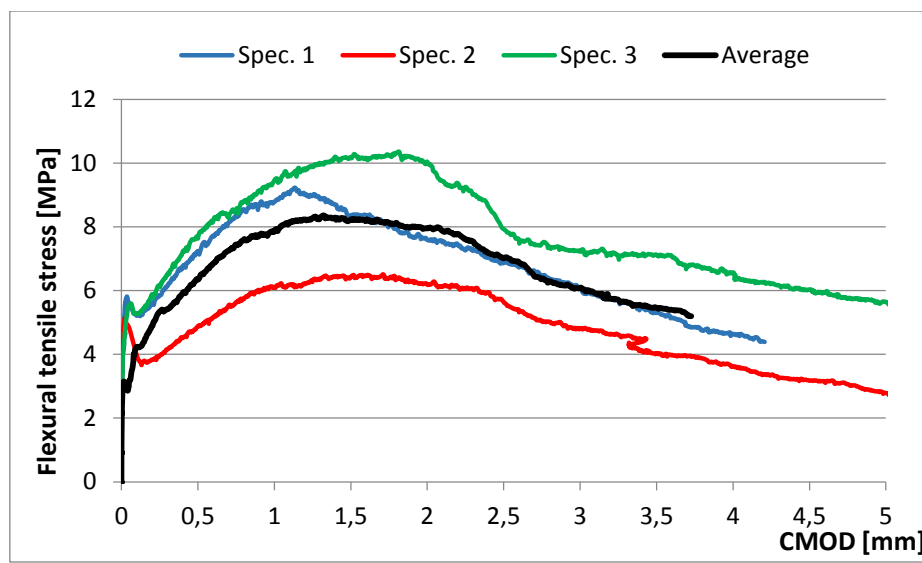
Figure 2-37 Stress vs. CMOD curves for Mix 7

All the beam specimens show a ductile behavior. They also show a tendency of scattering, especially due to beam specimen 2. The average max flexural tensile stress obtained was 8,7 MPa and the F_L load was 25 kN.

Comparing with previous basalt mixes

Fresh properties

Even though Mix 7 showed a very little fiber accumulation at the top, the fresh behavior of all mixes was satisfying; showing no signs of segregation or bleeding. The concretes were quite fluid and the yield stress values were also satisfying.

The SF-value for Mix 7 is similar to that of Mix 6 and higher to that of Mix 5 before fiber addition. For comparison; the total amount of superplasticizer used was lower than the amount used in Mix 5 and Mix 6. Therefore we can conclude that the SF-value was affected considerably by the time of testing.

The SF-value after fiber addition is a bit higher in Mix 7 than in Mix 6, but not by much. The air content of these two mixes is very similar, both before and after fiber addition. Mix 5 contains higher air content than these two mixes, for which the reason could lie in more compacted concrete for Mix 6 and Mix 7. This is also supported by the higher densities in these mixes.

Hardened properties

Mix 7 obtained a bit lower compressive strength compared to the other mixes. Again, the statement concerning fiber volume and compressive strength holds true; higher volume% of fibers does not increase the compressive strength of the concrete (see Figure 1-59 a).

The flexural strength increased considerably for Mix 7 compared with Mix 5. Also, the toughness increased and the ductile behavior was better.

3.3.12 Basalt fibers – Mix 8: 2% Generation 3

Fresh properties

Table 2-43 and Table 2-44 show the fresh properties obtained in the slump-flow test and the LCPC-Box test, respectively. Figure 2-38 shows the concrete spread in the slump-flow test.

Mix 8	Time of test (min)	Slump-flow (mm)	T_{500} (s)	Density (kg/m³)	Air content (%)
Before fibers	17	760	3,1	2282	3
After fibers	43	450	2,72	2251	3,5

Table 2-43 Fresh properties of Mix 8

The total amount of superplasticizer used was 450,8 ml and the corresponding slump-flow was 760 mm before fiber addition. The concrete showed, as the previous mixes, no signs of segregation of any material constituents. However, this time around, the addition of fibers led to a significant fiber segregation. This is shown in Figure 2-38 b. The fibers tend to cluster together in the middle and having virtually no bond with the matrix. This leads to the matrix flowing under and separately from the fiber cluster, which probably is a result of a rather low viscosity. This is the reason why the T_{500} value is very low (even though the 500 mm mark was not reached).
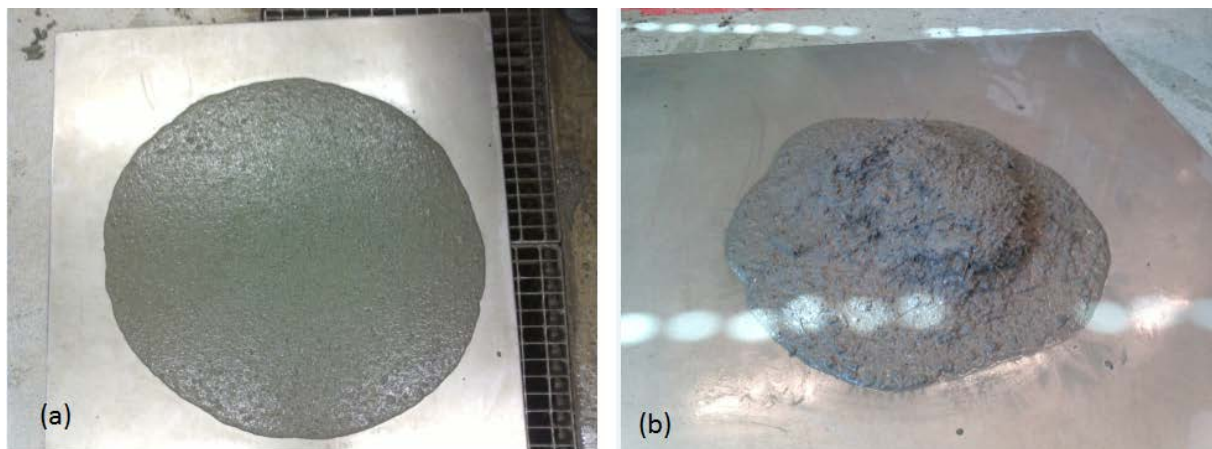
Figure 2-38 Mix 8 (a) before fiber addition (b) after fiber addition

Table 2-44 and Figure 2-39 show the values and behavior of of Mix 8 in the LCPC-Box test.

Mix 8	After adding fibers
Density (kg/m³)	2251
Volume (m³)	0,005
h_0 (m)	0,075
Laverage (m)	0,370
u_0 (-)	0,750
τ_0 (Pa)	**80,011**

Table 2-44 Values from LCPC-Box test for Mix 8

Mix 8 showed a better performance in the LCPC-Box test than it did in the slump-flow test. This is shown in the picture below. The concrete looked more homogeneous and more stable. But still, a slight fiber accumulation could be seen at the top of the concrete.

Figure 2-39 Mix 8 in LCPC-Box

Hardened properties

Table 2-45 shows the values obtained in the compression test, while Figure 2-40 shows the flexural tensile stresses obtained in the three-point bending test.

Mix 8	Cylinder 1	Cylinder 2	Cylinder3	Average
f_{cm} (MPa)	53,27	53,27	54,01	**53,52**
Density (t/m^3)	2,33	2,34	2,34	**2,34**

Table 2-45 Compressive strength for Mix 8
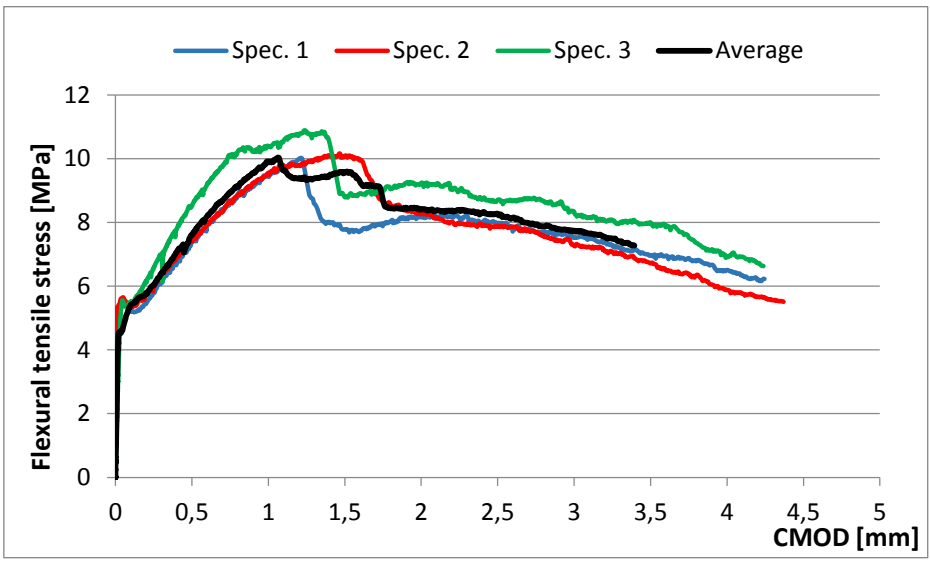
Figure 2-40 Stress vs. CMOD curves for Mix 8

The stress vs. CMOD curves show a deflection hardening behavior. The beam specimens show similar values values and behavior. The average max flexural tensile stress obtained was 10,4 MPa and the F_L load was 29,5 kN. The flexural performance was satisfying.

Comparing with previous basalt mixes

Fresh properties

Mix 8 obtained the lowest slump-flow value after fiber addition. The air content was a bit higher than those of Mix 6 and Mix 7. While the density after fiber addition increased for Mix 6 and Mix 7, it decreased for Mix 8.

Mix 8 showed the worst behavior of all mixes in the fresh state, obtaining fiber accumulation. This mix was stiffer and less fluid than the others due to the higher volume% of fibers. This is apparent by the yield stress values; even though Mix 8 obtained a similar value to Mix 7, the difference was higher compared to Mix 5 and Mix 6.

Hardened properties

The obtained compressive strength in Mix 8 was lower than Mix 5 and Mix 6, while it was similar to that of Mix 7. The corresponding densities were similar for all mixes.

By comparing the flexural strength values of the various mixes, we can see that the flexural strength obtained in Mix 8 is the highest with its 10,4 MPa value. Also, the F_L load is the highest; 29,5 kN. Moreover, Mix 8 shows a higher toughness and better ductile behavior than the other mixes.

When comparing Mix 8 with the 2% basalt mix (Mix 1.3) in FA 2.2 (134), we see that the hardened properties are higher for Mix 1.3 Also, the curve in stress vs. CMOD figure is smoother, indicating a better ductile performance.

3.3.13 Basalt fibers - Results, discussion and conclusions

Results

All mixes showed good stability and homogeneous flow before fiber addition. Generally, the slump-flow values were high, indicating a quite good flowability. After the addition of fibers, the mixes with a maximum of 1,5% fibers by volume still showed good stability and flowability characteristics. For 2% mix, a significant fiber segregation was observed.

The LCPC-Box test was conducted very late for Mix 1 compared with the other basaltic mixes. Therefore it had a bit higher value than Mix 2. Otherwise, the obtained yield stress values showed trends of increasing with increased volume% of fibers. And the values were satisfying, giving generally good flow.

The compressive strengths decreased (with low values) with increasing volume% of fibers. The density remained generally the same for each mix. The flexural strength, on the other hand, seemed to increase with increasing volume% of basalt fibers. The average max flexural tensile stress reached 4,4 MPa, 7,3 MPa, 8,7 MPa and 10,4 MPa for Mix 5, Mix 6, Mix 7 and Mix 8, respectively.

Discussion and conclusions

The properties of the basalt mixes in the fresh state indicate that the material composition is optimal for the mixes with a maximum of 1,5% fibers by volume. For higher volume% of basalt fibers, the concrete shows clear signs of fiber segregation and bleeding, due to too low viscosity. This has also been experienced in the previous work in 2011 (134); 2% and 3% basalt mixes showing satisfying behavior before fiber addition, but after fiber addition the concrete spread showed clear fiber segregation. A different material composition with the focus on increasing the viscosity for mixes containing equal to or higher than 2% fibers by volume may give better stability and thus satisfactory fresh state behavior. For now though, we can conclude that the fresh state behavior of mixes with equal to or higher than 2% basalt fibers by volume becomes unsatisfactory.

The fact that the compressive strength was slightly reduced each time the fiber content was increased leads to one conclusion: the compressive strength is not affected by increased volume% of basalt fibers any significantly. This conclusion is in compliance with the experimental studies on compressive strengths of fiber-reinforced composites by a number of researchers, see (91-93) or section 1.9.1.

The flexural strength and toughness increases with the basalt fiber content. This is supported by studies of several researchers (101-103), finding that the flexural strength increases with the addition of fibers. However, we have to take into account the findings in the previous work in 2011 (134); no significant increase in the hardened properties of basalt concrete going from 2% to 3% of fibers by volume. Therefore, we can conclude that the flexural strength and toughness increase with the increasing basalt fiber contents up to 2% by volume.

3.3.14 Discussion – Steel vs. basalt composites

A part of this thesis consisted of replacing the steel fibers with the basaltic fibers and compare the performance of the two fiber types. Here, a comparison of the two will take place and a conclusion of which fiber type gives the best overall performance will be taken.

Comparison steel vs. basalt

The slump-flow values obtained for both fiber concrete types before fiber addition were more or less the same; the concretes' material composition for basalt led to slightly higher values regardless of the subsequent volume% of fibers. The corresponding densities were similar for concretes with the same subsequent volume% of fibers. The air content both before and after fiber addition was slightly less in basalt concretes for the same volume% of fibers, except for the 2% mix.

The fresh behavior of both concrete types before fiber addition was similar; no segregation or bleeding was observed. The fluids were homogeneous and stable. After fiber addition, the mixes with a maximum of 1,5% volume of fibers still showed satisfactory fresh behavior. For the 2% mixes, the fresh behavior was unsatisfactory; a clear fiber segregation was observed for both concretes.

The compressive strengths of both concrete types were not affected by the increased volume% of fibers to any significant degree. The flexural strength and toughness increased with increasing contents of fibers by volume.

Discussion and conclusions

Both concrete types seem to behave in the similar way in the fresh state both before fiber addition and after fiber addition. Concerning the fresh properties, the concretes with a maximum of 1,5% of fibers by volume give satisfying results, while the concretes with 2% of fibers by volume give unsatisfying results. This similar behavior of the same volume% of fibers of the two concrete types does not get us any closer to conclude which fiber type gives the best results. Therefore, we have to also look at the performance in the hardened state.

There was not much difference in the obtained compressive strengths for both concrete types. They obtained more or less the same values in the range of 51-57 MPa. One interesting observation is seen: the strength values for the cylinders of the same mix show less scattering for basalt mixes than steel mixes.

The steel fiber-reinforced concretes showed a significantly better flexural performance in the hardened state than did the basalt fiber-reinforced concretes. The obtained strengths were higher and the toughness and ductility was also significantly better. The deflection hardening bahavior was more apparent in the steel mixes. Also, the scattering between the beam specimens of each mix was less for steel mixes.

Based on the better flexural performance of steel fiber-reinforced concretes, it can be concluded that the steel fibers gave the better overall performance in the experiments.

3.3.15 Final discussion and conclusions

The experiments conducted in this thesis was a part of the ongoing project within COIN to develop a pure fiber-reinforced concrete (without conventional steel reinforcement) with residual flexural tensile strength in the range of 10-15 MPa that can be applied in load carrying structures. Here, it will be discussed and finally concluded whether or not the studied steel- and basalt fiber-reinforced concretes can be applied for that purpose.

The mixes containing 2% of fibers by volume showed very good compressive and flexural strengths, the flexural being 16,7 MPa (Mix 4) for steel FRC and 10,4 MPa (Mix 8) for basalt FRC. Thereby, they meet the desired flexural tensile strength of 10-15 MPa. However, their behavior in the fresh state was not satisfactory. Mix 4 behaved very stiff, while Mix 8 showed clear signs of fiber segregation. Therefore, it can be concluded that these mixes cannot be used for the purpose the COIN project is aiming for.

The rest of the mixes showed good and satisfying behavior in the fresh state. Concerning the hardened state, all of the remaining steel mixes showed very good flexural performance. The obtained average flexural tensile strength values for Mix 1, Mix 2 and Mix 3 ranged from 10,6 MPa to 12,9 MPa, thus meeting the desired strength of 10-15 MPa. Regarding the remaining basalt mixes, Mix 6 and Mix 7 showed acceptable/passable flexural strengths of 7,3 MPa and 8,7 MPa, respectively, while Mix 5 obtained too low flexural strength of 4,4 MPa. By these findings, it can be concluded that all of the remaining steel mixes can be used for the purpose the COIN project is aiming for. Of the remaining basalt mixes that show passable flexural strengths, we can include Mix 7 for that very purpose because two of the beam specimens showed high max strength values of 9,2 MPa and 10,4 MPa in the bending test, while the last specimen showed bad performance and thereby dragged the average stress downwards. This statement could also be made for Mix 6, where two of the beams showed max strengths of 8,1 MPa and 7,6 MPa, but the post-cracking ductility was not good enough. Therefore, it can be concluded that Mix 5 and Mix 6 do not meet the desired requirements of the COIN project.

The table below summarizes the conclusions:

Mix	Fulfills the requirements of FA 2.2?
Mix 1: 1% Dramix 65/60	Yes
Mix 2: 1,5% Dramix 65/60	Yes
Mix 3: 1% Dramix 65/60 + 0,5% Dramix 65/35	Yes
Mix 4: 1% Dramix 65/60 + 1% micro 13 mm	No
Mix 5: 0,5% Generation 3	No
Mix 6: 1% Generation 3	No
Mix 7: 1,5% Generation 3	Yes
Mix 8: 2% Generation 3	No

Table 2-46 Final conclusions

3.4 Future studies

Steel fiber-reinforced concretes clearly show a better performance in the hardened state than basalt fiber-reinforced concretes. Therefore, the future studies should definitely focus on steel fibers.

By studying the previous work in FA 2.2 and Roca's thesis, and the current work in this thesis, it can be seen that the concretes can handle a maximum 2% of steel fibers by volume, excluding the micro steel fibers (13 mm). However, these fibers should not be overlooked; the content may be decreased in a future work to for instance 0,5% or 0,25% and the effect of this together with the longer fibers could be further studied. For example, a mix with Dramix 65/35 and micro fibers should be carried out and evaluated:

- 1% 65/60 + 0,25% 13
- 1% 65/60 + 0,50% 13 (studied in Roca's thesis)
- 1% 65/35 + 0,25% 13
- 1% 65/35 + 0,5% 13
- 1% 65/35 + 1% 13

There is not much literature and studies on basalt fiber-reinforced concretes. From the experience in this thesis, it is easy to exclude these fibers in a future study. However, it should be remembered that the basalt mixes in this thesis were carried out with almost identical material composition as the steel mixes. Therefore, if more study is done with basalt fibers with different material composition, it could lead to a potentially strong fiber-reinforced composite. For instance, the aggregate size distribution could be more varied; the admixtures could be replaced by better ones, etc. The future study on basalt fibers should be done in such a quantity that a conclusion can be taken, of whether or not it is worth the time to study more on this fiber type. Below is a suggestion of future studies on basalt mixes:

- 1% basalt (again)
- 1,25% basalt
- 1,5% basalt (again)

References

1.   Delatte NJ. Lessons from Roman cement and concrete. Journal of Professional Issues in Engineering Education and Practice. 2001;127(3):109-15.
2.   Blezard RG. 1 - The History of Calcareous Cements. Lea's Chemistry of Cement and Concrete (Fourth Edition). Oxford: Butterworth-Heinemann; 2003. p. 1-23.
3.   Löfgren I. Fibre-reinforced Concrete for Industrial Construction-a fracture mechanics approach to material testing and structural analysis. Gothenburg, Sweden: CHALMERS UNIVERSITY OF TECHNOLOGY; 2005.
4.   Kanstad T, Juvik DA, Vatnar A, Mathisen AE, Sandbakk S, Vikan H, et al. Forslag til retningslinjer for dimensjonering, utførelse og kontroll av fiberarmerte betongkonstruksjoner: FA 2 competitive constructions : SP 2.2 high tensile strength all round concrete. Oslo: SINTEF Building and Infrastructure; 2011. 51 s. : ill. ; 30 cm p.
5.   Sandbakk S. Fibre reinforced concrete: evaluation of test methods and material development. Trondheim: Norges teknisk-naturvitenskapelige universitet; 2011. 1 b. (flere pag.) : ill. p.
6.   Bentur A, Mindess S. Fibre reinforced cementitious composites. London: Taylor & Francis; 2007. XX, 601 s. : ill. p.
7.   Brandt AM. Fibre reinforced cement-based (FRC) composites after over 40 years of development in building and civil engineering. Composite Structures. 2008;86(1–3):3-9.
8.   Naaman AE, Willie K. The Path to Ultra-High Performance Fiber Reinforced Concrete (UHP-FRC): Five Decades of Progress. Third International Symposium on UHPC; Kassel, Germany2012.
9.   Vikan H. Concrete workability and fibre content: state of the art. Trondheim: SINTEF; 2007. 38 bl. : ill. p.
10.   Naaman AE. Engineered Steel Fibers with Optimal Properties for Reinforcement of Cement Composites. Journal of Advanced Concrete Technology. 2003;1(3):241-52.
11.   Krenchel H. FIBRE SPACING AND SPECIFIC FIBRE SURFACE. SAE Preprints. 1975:69-79.
12.   Li VC, Stang H. Meso: Averaging, In Mechanics of Fibre Reinforced Cement Based Composites. International Graduate Research School in Applied Mechanics, course material, Lyngby, Denmark. 2001.
13.   Kooiman AG. Modelling steel fibre reinforced concrete for structural design: The University of Delft; 2000.
14.   Shah SP, Rangan VB. Fiber reinforced concrete properties. J American Concrete Institute. 1971;61:126-35.
15.   A820 AS. Standard Specification for Steel Fibers for Fiber-Reinforced Concrete. West Conshohocken: ASTM International; 2011.
16.   Hoy CW, Bartos PJM. Interaction and packing of fibres: Effects of the mixing process. RILEM proceedings PRO. 1999;6:181-91.
17.   Majumdar AJ. Glass fibre reinforced cement and gypsum products. Philos Trans R Soc London. 1970;A 319:69-78.
18.   Majumdar AJ, Ryder JF. Glass fibre reinforcement for cement products. Glass Technol. 1968;9:78-84.
19.   Majumdar AJ, Singh B. The effect of fibre length and content on the durability of glass reinforced cement-ten year result. Journal of Materials Science Letters. 1985;4:961-71.
20.   Majumdar AJ, Singh B, Langley AA, Ali MA. The durability of glass fibre cement-the effect of fibre length and content. Journal of Materials Science. 1980;15:1085-96.
21.   Anon. A study of the properties of Cem-FIL/OPC composites. Building Research Establishment Current Paper CP. 1976;38/76.
22.   Selikoff IJ. Perspectives in the investigation of health hazards in the chemical industry. Ecotoxicology and Environmental Safety. 1977;1(3):387-97.
23.   White asbestos to be banned in all EU countries. Sealing Technology. 1999;1999(69):1.

24.   Williden JE. A guide to the Art of Asbestos Cement. London: J.E. Williden; 1986.
25.   Studinka JB. Asbestos substitution in the fibre cement industry. International Journal of Cement Composites and Lightweight Concrete. 1989;11(2):73-8.
26.   Allen HG. Tensile properties of seven asbestos cements. Composites. 1971;2(2):98-103.
27.   Akers SAS, Garrett GG. The influence of processing parameters on the strength and toughness of asbestos cement composites. International Journal of Cement Composites and Lightweight Concrete. 1986;8(2):93-100.
28.   Militký J, Kovačič Vr, Rubnerová J. Influence of thermal treatment on tensile failure of basalt fibers. Engineering Fracture Mechanics. 2002;69(9):1025-33.
29.   Wei B, Cao H, Song S. Degradation of basalt fibre and glass fibre/epoxy resin composites in seawater. Corrosion Science. 2011;53(1):426-31.
30.   Ritchie AGB, Mackintosh DM. Selection and rheological characteristics of polyproplylene fibers. Concrete (London). 1979;13:36-9.
31.   Vondran G. Making more durable concrete with polymeric fibers. Proceedings of the Catharine and Bryant Mather International Symposium. 1987;ACI Special Publication(SP (100-23)):337-96.
32.   544, ACI. State of the Art Report on Synthetic Fibre-Reinforced Concrete. Draft Document. 2005.
33.   Krenchel H, Jensen HW. ORGANIC REINFORCING FIBRES FOR CEMENT AND CONCRETE. Serie R - Danmarks Tekniske Hojskole, Afdelingen for Baerende Konstruktioner. 1982(151).
34.   Trottier J-F, Mahoney M. Innovative synthetic fibers. Concrete Institute. 2001;23(6):23-8.
35.   Kraii PP. A proposed test to determine the cracking potential due to drying shrinkage of concrete. Concrete Construction. 1985;30:775-8.
36.   Soroushian P, Mirza F, Alhozaimy A. Plastic shrinkage cracking of PP fiber reinforced concrete. ACI Mater. 1995;92:553-60.
37.   Berke NS, Dallaire MP. The effect of low addition rates of polypropylene fibers on plastic shrinkage cracking and mechanical properties of concrete. Fiber Reinforced Concrete: Developments and Innovations. 1994;SP142(American Concrete Institute):19-42.
38.   Kovler K, Sikuler J, Bentur A. Restrained shrinkage tests of fibre reinforced concrete ring specimens: effect of core thermal expansion. Mater Struct (RILEM). 1992;26:231-7.
39.   Krenchel H, Shah SP. Restrained shrinkage tests with polypropylene fiber reinforced concrete. Fibre Reinforced Concrete Properties and Applications. 1987;SP-105(American Concrete Institute):141-58.
40.   Zollo RF. Collated fibrillated polypropylene fibers in FRC. Fiber Reinforced Concrete. 1984;SP-81(American Concrete Institute):397-409.
41.   Badr A, Hassan KE, Richardson IG, Cabrerea JG, editors. Third International Conference on Advanced Compostie Materials in Bridges and Structures; 2000; Montreal.
42.   Mindess S, Vondran G. Properties of concrete reinforced with fibrillated polypropylene fibers under impact loading. Cen Concr Res. 1988;8:109-15.
43.   Hasaba S, Kawamura M, Koizumi T, Takemoto K. Resistibility agairts impact load and deformation characteristics under bending load in polymer and hubrid (polymer and steel) fiber reinforced concrete. Fiber Reinforced Concrete. 1984;ACI SP-81(American Concrete Institute):187-96.
44.   Wang Y, Backer S, Li VC. An experimental study of the synthetic fibre reinforced cementitious composites. Journal of Materials Science. 1987;22:4281-91.
45.   Gale DM. Cement reinforcement with man made fibres. International Man-Made Congress; Dornbirn, Austria.1986.
46.   Laning A. Synthetic fibers 1992. Available from: http://www.concreteconstruction.net/images/Synthetic%20Fibers_tcm45-342406.pdf.
47.   Hughes DC, Hannant DJ. Brittle matrices reinforced with polyalkaline films of varying elastic moduli. Journal of Materials Science. 1982;17:508-16.
48.   Kobayashi K, Cho R. Flexural behaviour of polyethylene fibre reinforced concrete. International Journal of Cement Composites and Lightweight Concrete. 1981;3(1):19-25.

49.	Nishioka K, Yamakawa S, Shirakawa K. Properties and applications of carbon fibre reinforced cement composites. Developments in Fibre Reinforced Cement and Concrete. 1986;2.2.

50.	Li VC, Obla K. Effect of fiber length cariation on tensile properties of carbon-fiber cement composites. Composite Eng. 1994;4:947-64.

51.	Li VC, Mishra DK. Micromechanics of fiber effect on the uniaxial compressive strength o cementitious composites. Fiber Reinforced Cement and Concrete. 1992;17:400-14.

52.	Akihama S, Suenaga T, Banno T. Mechanical properties of carbon fibre reinforced cement composites. International Journal of Cement Composites and Lightweight Concrete. 1986;8(1):21-38.

53.	Briggs A. CARBON FIBRE-REINFORCED CEMENT. Journal of Materials Science. 1977;12(2):384-403.

54.	Ohama Y, Amano M, Endo M. Properties of carbon fiber reinforced cement with silica fume. Concr Int Design and Construction. 1985;7(3):58-62.

55.	Briggs A, Bowen DH, Kollek J. MECHANICAL PROPERTIES AND DURABILITY OF CARBON-FIBRE-REINFORCED CEMENT COMPOSITES. 1974.

56.	Akihama S, Suenaga T, Nakagawa H. CARBON FIBER REINFORCED CONCRETE. Concrete International. 1988;10(1):40-7.

57.	Walton PL, Mujamdar AJ. Properties of cement composites reinforced with Kevlar fibres. Journal of Materials Science. 1978;13:1075-83.

58.	Ohgishi S, Ono H, Tanahashi I. Mechanical properties of cement mortar pastes reinforced with polyamide fibres. Trans Japan Concrete Institute. 1984;6:309-15.

59.	Naaman AE, Reinhardt HW. High performance fiber reinforced cement composites HPFRCC-4: International workshop Ann Arbor, Michigan, June 16–18, 2003. Cement and Concrete Composites. 2004;26(6):757-9.

60.	Lankard DR, editor SLURRY INFILTRATED FIBER CONCRETE (SIFCON): PROPERTIES AND APPLICATIONS. Very High Strength Cement-Based Materials; 1985; Boston, MA, USA: Material Research Soc.

61.	Lankard DR, editor PREPARATION, PROPERTIES AND APPLICATIONS OF CEMENT-BASED COMPOSITES CONTAINING 5 TO 20 PERCENT STEEL FIBER. Steel Fiber Concrete, US-Sweden Joint Seminar (NSF-STU); 1985; Stockholm, Swed: Swedish Cement & Concrete Research Inst.

62.	Lankard DR, Newell JK, editors. PREPARATION OF HIGHLY REINFORCED STEEL FIBER REINFORCED CONCRETE COMPOSITES. Fiber Reinforced Concrete: International Symposium Based on papers presented at the ACI Fall Convention; 1984; Detroit, MI, Engl: American Concrete Inst.

63.	Homrich JR, Naaman AE. Stress-strain properties of SIFCON i compression. American Concrete Institute. 1987;ACI SP-105:283-394.

64.	Naaman AE, Homrich JR. Tensile stress-strain properties of SIFCON. ACI Materials Journal. 1989;86(3):244-51.

65.	Hackmann LE, Farell MB, Dunham OO. Slurry infiltrated mat concrete (SIMCON). Concrete Int. 1992:53-6.

66.	Bentur A, Cree R. Cement reinforced with steel wool. International Journal of Cement Composites and Lightweight Concrete. 1987;9(4):217-23.

67.	Bentur A. Unpublished work.

68.	Krstuloic-Opara N, Malak S. Tensile behavior of slurry infiltrated mat concrete (SIMCON). ACI Materials Journal. 1997;94:39-46.

69.	Krstuloic-Opara N, Malak S. Micromechanical tensile behavior of slurry infiltrated mat concrete (SIMCON). ACI Materials Journal. 1997;94:373-84.

70.	Richard P, Cheyrezy M. Composition of reactive powder concretes. Cement and Concrete Research. 1995;25(7):1501-11.

71.	Technology C. compact reinforced composite Denmark: CRC Technology. Available from: http://www.crc-tech.com/Files/Billeder/crc-tech_uk/docs/crc_presentation.pdf.

72.	Smeplass S, Maage M. TKT 4215 Concrete Technology 1. NTNU2004.

73.	Gjerp P, Opsahl M, Smeplass S. Grunnleggende betongteknologi2004.

74.   Holton I, Day R, Domone P, Bartos PJM. Self-compacting Concrete - A review. Concrete Society. 2005;62.

75.   Geiker MR, Brandl M, Thrane LN, Bager DH, Wallevik O. The effect of measuring procedure on the apparent rheological properties of self-compacting concrete. Cement and Concrete Research. 2002;32(11):1791-5.

76.   Wallevik JE. Rheology of particle suspensions; fresh concrete, mortar and cement paste with various types of lignosulphonates [PhD]. Norway: Norwegian University of Science and Technology; 2003.

77.   Wallevik O. Practical description of rheology of SCC. SF Day of the Our World of Concrete; Singapore2002.

78.   Nielsson I, Wallevik O. Rheological evaluation of some empirical test methods, preliminary results. RILEM publications PRO. 2003;33:59-68.

79.   Krieger IM, Dougherty TJ. A mechanism for non-Newtonian flow of suspensions of rigid spheres. Transactions of the Society of Rheology. 1959;3:137-52.

80.   Ildefonse B, Allain C, Coussot C. Des grands écoulements naturels à la dynamique du tas de sable: introduction aux suspensions en géologie et en physique. Editions Cemagref. 1997.

81.   Flatt RJ. Towards a prediction of superplasticized concrete rheology. Materials and Structures/Materiaux et Constructions. 2004;37(269):289-300.

82.   ASTM. ASTM C1611-Standard Test Method for Slump Flow of Self-Consolidating Concrete. 2010.

83.   Standard N. NS-EN 12350-8: Prøving av fersk betong-Del 8: Selvkomprimerende betong-Synkutbredelsesmetode. 2010.

84.   ASTM. ASTM C1621-Standard Test Method for Passing Ability of Self-Consolidating Concrete by J-Ring. 2009.

85.   Standard N. NS-EN 12350-12: Prøving av fersk betong - Del 12: Selvkomprimerende betong - J-ringmetode. 2010.

86.   Roussel N. The LCPC BOX: a cheap and simple technique for yield stress measurements of SCC. Materials and Structures. 2007;40(9):889-96.

87.   Grünewald S. Performance-based design of self-compacting fibre reinforced concrete. Netherlands: Delft University of Technology; 2004.

88.   Standard N. NS-EN 12350-3: Testing fresh concrete-Part 3: Vebe test. Norsk Standard; 2009.

89.   ASTM. ASTM C995-Standard Test Method for Time of Flow of Fibre-Reinforced Concrete Through Inverted Slump Cone. 1994.

90.   Johnston CD. Measures of the workability of steel fiber reinforced concrete and their precision. Cem Concr Agg. 1984;6:74-83.

91.   Hsu LS, Hsu C-TT. Stress-strain behavior of steel-fiber high-strength concrete under compression. ACI Structural Journal. 1994;91(4):448-57.

92.   König G, Kützing L. Modelling the increase of ductility of HPC under compressive forces - a fracture mechanical approach. High Performance Fiber Reinforced Cement Composites. 1999;3:251-60.

93.   Fanella DA, Naaman AE. STRESS-STRAIN PROPERTIES OF FIBER REINFORCED MORTAR IN COMPRESSION. Journal of the American Concrete Institute. 1985;82(4):475-83.

94.   Karihaloo BL, de Vriese KMB. Short-fibre reinforced reactive powder concrete High Performance Fiber Reinforced Cement Composites. 1999;3:53-63.

95.   Sun W, Liu S, Lai J. Study on the properties and mechanism of ultra-high performance ecological reactive powder concrete. High Performance Fiber Reinforced Cement Composites. 2003;PRO 30:409-17.

96.   Hughes BP. Experimental test results for flexure and direct tension of fibre cement composites. International Journal of Cement Composites and Lightweight Concrete. 1981;3(1):13-8.

97.   Bulletin. Structural Concrete Textbook. Bulletin 51. 2009;1:95-149.

98.   Naaman AE, Visalvanich K. Fracture model for fiber reinforced concrete. ACI Matererial Journal. 1983;86:128-38.

99.   Krstulovic-Opara N. Use of SIMCON in seismic retrofit and new construction. High Performance Fiber Reinforced Cement Composites. 1999;PRO 6:629-49.

100.   Johnston CD, Coleman RA. Strength and deformation of steel fiber reinforced mortar in uniaxial tension. Fiber Reinforced Concrete. 1974;ACI SP-44:177-93.

101.   Altun F, Haktanir T, Ari K. Effects of steel fiber addition on mechanical properties of concrete and RC beams. Construction and Building Materials. 2007;21(3):654-61.

102.   Pająk M, Ponikiewski T. Flexural behavior of self-compacting concrete reinforced with different types of steel fibers. Construction and Building Materials. 2013;47(0):397-408.

103.   Wang Q-s, Li X-b, ZhAo G-y, Shao P, Yao J-r. Experiment on mechanical properties of steel fiber reinforced concrete and application in deep underground engineering. Journal of China University of Mining and Technology. 2008;18(1):64-81.

104.   Padmarajaiah SK, Ramaswamy A. Flexural strength predictions of steel fiber reinforced high-strength concrete in fully/partially prestressed beam specimens. Cement and Concrete Composites. 2004;26(4):275-90.

105.   Johnston CD. Definition and measurement of flexural toughness parameters for fiber reinforced concrete. Cem Concr Agg. 1982;4:53-60.

106.   Naaman AE, Reinhardt HW. Setting the stage: Toward performance based classification of FRC composites. High Performance Fiber Reinforced Cement Composites. 2003;PRO 30:1-4.

107.   Soutsos MN, Le TT, Lampropoulos AP. Flexural performance of fibre reinforced concrete made with steel and synthetic fibres. Construction and Building Materials. 2012;36(0):704-10.

108.   Williamson GR. Steel Fibers as Web Reinforcement in Reinforced Concrete. Proceedings, US Army Servie Conference. 1978;3:363-77.

109.   Valle M, Buyukozturk O. Behavior of fiber reinforced high-strength concrete under direct shear. ACI Materials Journal. 1993;90(2):122-33.

110.   Sun W, Pan G, Yan H, Chen H. Study on the anti-exploding characteristics of fiber reinforced cement composites. High Performance Fiber Reinforced Cement Composites. 1999;PRO 6:565-74.

111.   Barr B. The fracture characteristics of FRC materials in shear. Fiber Reinforced Concrete-Properties and Application. 1987;ACI SP-105:27-54.

112.   Institution BS. BS 1881-116-Method for determination of compressive strength of concrete cubes. 1983.

113.   Zhang L, Mindess S. The compressive toughness of high strength fiber reinforced concrete. Construction Materials. 2005;ConMat 05.

114.   RILEM-TC. RILEM-TC 148-SCC-Test method for the measurement of the strain-softening behavior of concrete under uniaxial compression Mater Struct (RILEM). 2000;33(230):347-51.

115.   Standard N. NS-EN 12390-4: Prøving av herdnet betong - Del 4: Trykkfasthet - Krav til prøvingmaskiner. 2000.

116.   Standard N. NS-EN 12390-3: Prøving av herdnet betong - Del 3: Prøvelegemers trykkfasthet. 2009.

117.   Mindess S, Chen L, Morgan DR. Determination of the first-crack strength and flexural toughness of steel fiber-reinforced concrete. Advanced Cement Based Materials. 1994;1(5):201-8.

118.   Standard N. NS-EN 14651:2005+A1:2007-Prøvingsmetode for betong med metalliske fibere-Måling av bøystrekkfasthet (proporsjonalitetsgrense og restfastheter). Norway: Standard Norge; 2008.

119.   Trottier J-F, Forgeron D, Mahoney M. Influence of construction joints in wet-mix shotcrete panels. Shotcrete. 2002:26-30.

120.   Deeb R, Ghanbari A, Karihaloo BL. Development of self-compacting high and ultra high performance concretes with and without steel fibres. Cement and Concrete Composites. 2012;34(2):185-90.

121.   Hammer TA. State of the art - Ultra High Performance Fibre Reinforced Concrete (UHPFRC). 2012.

122.   Lowke D. Control of Rheology, Strength and Fibre Bond of UHPC with Additions – Effect of Packing Density and Addition Type. Proceedings of Hipermaterials 2012. 2012.

123.	Markovic I, Walraven JC, van Mier JGM, editors. Self-compacting hybrid-fibre concrete - Mix design, workability and mechanical properties. Third International Symposium of Self-Compacting Concrete; 2003; Reykjavik, Iceland.

124.	Ando T, Sakai H, Takahashi K, Hoshjima T, Awara M, Oka S. Fabrication and properties of a new carbon fibre reinforced cement product, Thin-Section Fiber Reinforced Concrete and Ferrocement. American Concrete Institute Special. 1990;SP-124:39-60.

125.	Swamy RN, Mangat PS. Influence of fiber geometry on the properties of steel fiber reinforced concrete. Cement and Concrete Research. 1974;4(3):451-65.

126.	Edgington J, Hannant DJ, Williams RIT. Steel fibre reinforced concrete, Fibre reinforced materials. The Construction Press; Lancaster, England1978. p. 112-28.

127.	Swamy RN. FIBRE REINFORCEMENT OF CEMENT AND CONCRETE. 1975;8(45):235-54.

128.	Johnston CD. Proportioning, mixing and placement of fibre-reinforced cements and concretes, Production Methods and Workability of Concrete. 1996.

129.	Committee A. ACI 544 IR-82: State of the art report on Fibre Reinforced Concrete. 1982. p. 9-30.

130.	Swamy RN, Mangat PS. Influence of fibre-aggregate interaction on some properties of steel fibre reinforced concrete. Materials and Structures. 1974;7:307-14.

131.	Narayanan R, Kareem-Palanjian AS. Factors influencing the workability of steel-fibre reinforced concrete. Concrete. 1982;1,2:45-8, 3-4.

132.	Rossi P, Harrouche N. Mix design and mechanical behaviour of some steel-fibre-reinforced concretes used in reinforced concrete structures. Materials and Structures. 1990;23:256-66.

133.	Hoy CW. Mixing and Mix Proportioning of Fibre Reinforced Concrete [PhD]: University of Paisley; 1998.

134.	Kjellmark G. COIN P2.2 Ductile Fibre Reinforced Concrete 2011-2012. 2012.

135.	Elkem AS-EMMA. Available from: http://www.elkem.com/en/Silicon-materials/Support/Software-EMMA/.

136.	Hammer TA, Kjellmark G, Kanstad T. On mix design of structural fiber reinforced self-compactinig concrete with high fiber content. 2012.

137.	Roca MB. Fibre Reinforced Concrete: Optimization of fibre content and shear capacity of dapped-end beams [Master]. Norway: NTNU, Universidad Politecnica de Valencia; 2013.

138.	Grünewald S, Walraven JC. Sensitivity of the Bending Behaviour of Self-Compacting Fibre Reinforced Concrete to the Method of Casting. Netherlands: Delft University of Technology; 2004.

139.	Standard N. NS-EN 12350-6: Prøving av fersk betong - Del 6: Densitet. 2009.

140.	Standard N. NS-EN 12350-7: Prøving av fersk betong - Del 7: Luftinnhold - Trykkmetoder. 2009.

Appendix

\-

Materials used

Dramix®

DATA SHEET

R **C** **65** **60** **B** **N**
65 80
45 / l/d
Bright
Low Carbon

RC-65/60-BN

What is Dramix®?

Dramix® steel fibres, from industry specialist Bekaert, have set a new standard for concrete reinforcement with their unique combination of flexibility and cost-efficiency.

Dramix® is a cold drawn steel wire fibre with hooked ends for optimum anchorage.
What you get from Dramix® reinforced concrete is ductility and high load bearing capacity. On top of that, you'll find a quick and easy way to an efficient and cost effective solution.

RC-65/60-BN offers you:

☑ **Dramix® Easy Mix**
Dramix® Easy Mix fibres are engineered in such a way to offer fast and perfect mixing, improved pumpability and optimized fibre distribution. Even complex forms and structures are possible.

☑ **Dramix® Hi Perform**
Dramix® Hi Perform fibres provide high performance and crack resistance. These are products of choice to create optimal ductility. Dramix® Hi Perform is used for structural, designed applications, in situ, precast or sprayed.

GEOMETRY AND PERFORMANCE

length (l)
60 mm

diameter (d)
0,90 mm

80
65
45
Performance class: 65
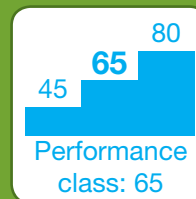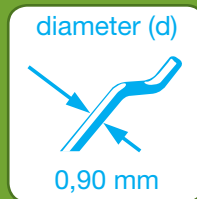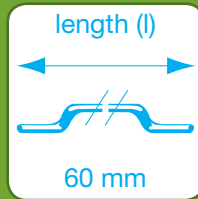
3.200 Fibres/kg

Minimum dosage: 15 kg per m³ (according to **CE**)
Minimum fibre network: 2,9 km per m³ (for 15 kg/m³)

MATERIAL PROPERTIES

Tensile strength: Rm nom**:** 1.160 N/mm²
Tolerances: ± 7,5% Avg
Young's Modulus (Emod): ± 210.000 N/mm²

PACKAGING

60 Bags (20kg)
1200 kg

BIG BAG
1100 kg

STORAGE
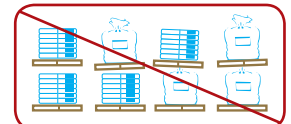
KEEP DRY   **NO STACKING**

PRODUCT APPROVALS

CE
0749-CPD
EN 14889-1
06
CE

Conforms to
ASTM A820
ASTM A820

• **CE LABEL:** Dramix® is certified for CE mark system 1: steel fibres for structural use.
For detailed info: CE info sheet available on request.

SYSTEM APPROVALS

ISO 9001
BUREAU VERITAS
Certification
ISO 9001

ISO 14001
BUREAU VERITAS
Certification
ISO 14001

• **ISO 9001:** All Dramix® plants are ISO 9001 certified. The same quality standards are applied.

• **ISO 14001:** Some plants are already ISO 14001 certified. All plants will be ISO 14001 certified before end 2011.

Bekaert will advise on the most suitable fibre for your application.
- For our recommendations on handling, dosing and mixing.
- For composition and safe application and in the frame of Reach art.33.
Please go to: www.bekaert.com/dosingdramix
infobuilding@bekaert.com

Dramix®

BEKAERT

better together

Data Sheet

Aspect ratio   Length   Bright   Glued

3D Dramix® 65/35BG

CE
0749-CPD
EN 14889-1

Conforms to
ASTM A820

DRAMIX® 3D

Dramix® 3D is the reference in steel fibre reinforcement. Combining high performance, durability and ease-of-use, 3D provides you with a time-saving and cost-efficient solution for most common applications.

> original anchorage
> standard tensile strength

Dramix® 3D is a cost efficient solution for
> flooring
> tunnel applications
> precast
> residential applications

Bekaert supplies all of the support you need for your project. We help you determine the most suitable fibre types, calculate optimal dosages, select the right concrete quality. Contact your local support.

Go to www.bekaert.com/dosingdramix for our recommendations on handling, dosing and mixing.

PERFORMANCE

Material properties

Tensile strength: $R_{m,nom}$: 1.345 N/mm^2
Tolerances: ± 7,5% Avg
Young's Modulus: ± 210.000 N/mm^2

Geometry

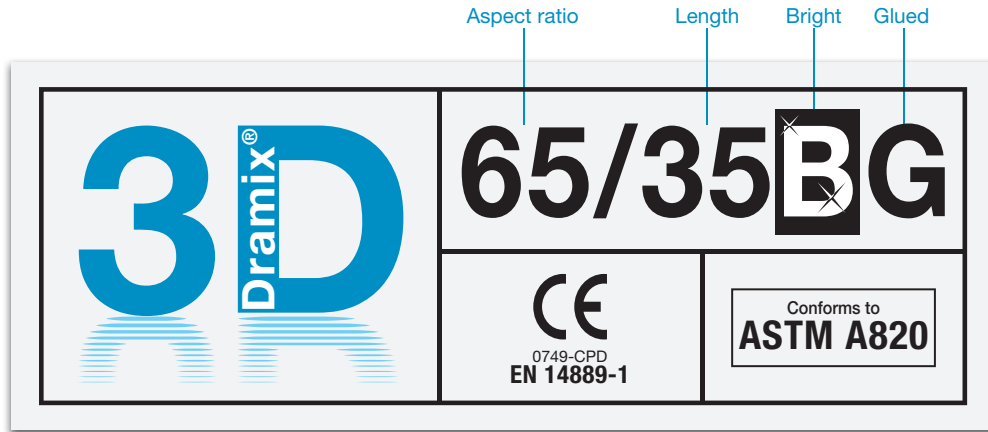|		
Fibre family	3D	
Length (l)	35 mm	
Diameter (d)	0,55 mm	
Aspect ratio (l/d)	65	80 **65** 55 45

Fibre network

8,0 km per m^3 (for 15 kg/m^3)
14.531 fibres/kg

Dramix® range

5D 4D **3D**

	5D	4D	3D
Tensile strength			
Wire ductility			
Anchorage strength			

PRODUCT CERTIFICATES

CE
0749-CPD
EN 14889-1

Conforms to
ASTM A820

Dramix® is certified for structural use according to EN 14889-1 (system '1'). Detailed information is available on request.

SYSTEM CERTIFICATES

ISO 9001
BUREAU VERITAS
Certification
1828

ISO 14001
BUREAU VERITAS
Certification
1828

All Dramix® plants are ISO 9001 and ISO 14001 certified.

PACKAGING

BAGS 20 kg   **BIG BAG** 1100 kg

STORAGE

KEEP DRY   NO STACKING

71.19.05 - 09/2012
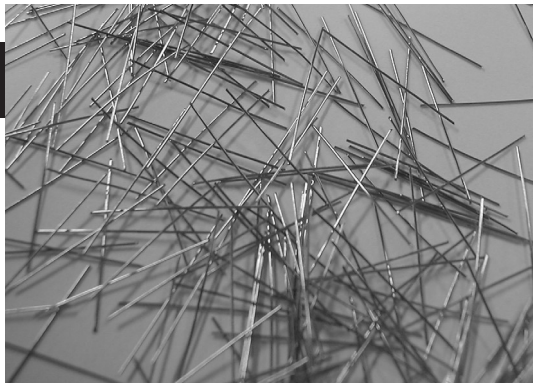
Straight high carbon steel wire fibres

• Description:

Straight high carbon steel wire fibres are filaments of high strength wire, cut to lengths, for the reinforcement of very high strength concrete and mortar (above 100 MPa).

• Applications:

- security business: vaults
- ultra high strength concrete type RPC

• Geometry:

- length: available on request, between 6-15 mm
- diameter: available on request, between 0.15-0.35 mm
- standard types:
  · OL6/.16: length 6 mm; diameter 0.16 mm
  · OL13/.16: length 13 mm; diameter 0.16 mm
  · OL13/.20: length 13 mm; diameter 0.20 mm

• Tensile strength:

- on the wire: minimum 2000 MPa
- high carbon conforms to: EN 10016-2 - C72D

• Coating:

brass coating

• Approvals:

Quality System in Belgian Plants

🔲 BEKAERT
ISO 9001
Dramix
VERITAS - BQ

Recommendations - mixing

✓ Use a central batching plant mixer.

✓ A continuous grading is preferred.

✓ Never add fibres as first component in the mixer.

✓ Fibers can be introduced together with sand, or can be added in freshly mixed concrete or mortar.

Recommendations - storage

Protect the pallets against rain.

Do not stack the pallets on top of each other.

Boxes of 30 kg on pallet 720 kg (24 boxes).

Årdal 0-2 mm A-4065

Type:	Årdal 0-2 mm (A-4065)
Dato:	2013-03-15
FM =	2,47

Åpning	Sikterest (g)		Sikterest	Gjennom-gang
	1	2	(%)	(%)
32	0	0	0,0	100,0
22,4	0	0	0,0	100,0
16	0	0	0,0	100,0
11,2	0	0	0,0	100,0
8	0	0	0,0	100,0
4	46,8	47,2	15,0	85,0
2	92,4	84,5	28,2	71,8
1	137,4	121,6	41,3	58,7
0,5	182,9	163	55,1	44,9
0,25	226	200,8	68,0	32,0
0,125	262,8	233,9	79,2	20,8
0,063	299	266	90,0	10,0
Bunn	332	295		
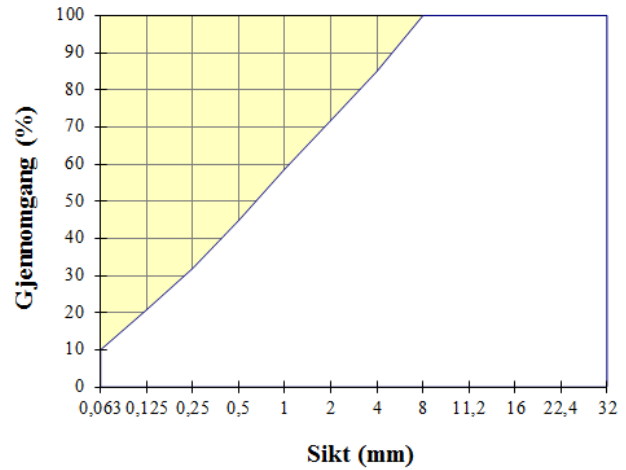
Årdal 0-8 mm A-3899

Type:	Årdal 0-8 mm (A-3899)
Dato:	2012-04
FM =	3,25

Åpning	Sikterest (g)		Sikterest	Gjennom-gang
	1	2	(%)	(%)
32	0	0	0,0	100,0
22,4	0	0	0,0	100,0
16	0	0	0,0	100,0
11,2	0	0	0,0	100,0
8	2,3	0	2,3	97,7
4	19,6	0	19,6	80,4
2	37,1	0	37,1	62,9
1	57,2	0	57,2	42,8
0,5	75,2	0	75,2	24,8
0,25	86,8	0	86,8	13,2
0,125	93,8	0,0	93,8	6,2
0,063	97,8	0,0	97,8	2,2
Bunn	100,0	0,0		
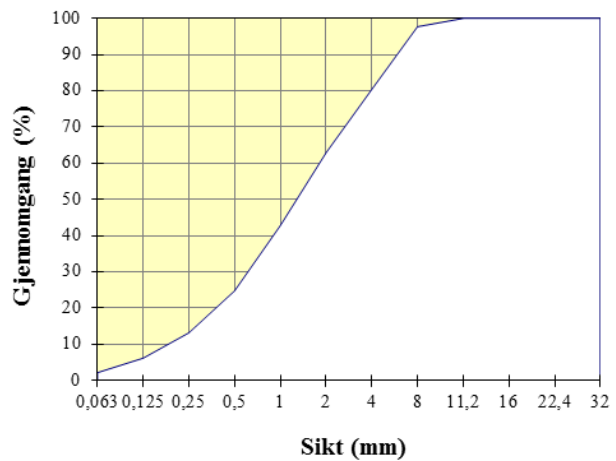
Årdal 0-8 mm A-4045

Type:	Årdal 0-8 mm (A-4045)
Dato:	2012-02
FM =	3,14

Åpning	Sikterest (g)		Sikterest (%)	Gjennom-gang (%)
	1	2		
32	0	0	0,0	100,0
22,4	0	0	0,0	100,0
16	0	0	0,0	100,0
11,2	0	0	0,0	100,0
8	1,5	0	1,5	98,5
4	18	0	18,0	82,0
2	35,6	0	35,6	64,4
1	53,8	0	53,8	46,2
0,5	72,5	0	72,5	27,5
0,25	85,9	0	85,9	14,1
0,125	93,2	0,0	93,2	6,8
0,063	97,0	0,0	97,0	3,0
Bunn	100,0	0,0		

Standard sement FA

NORCEM

Figur 1

Figur 2

Fasthetsutvikling

Fasthetsutvikling er en sentral egenskap for planlegging, styring og utførelse av alle betongarbeider. Fasthetsutviklingen er avhengig av sementtype, tilslag, masseforhold, herdeforhold (temperatur, tid og fuktighet) og eventuell bruk av tilsetningsmateri- aler eller -stoffer. I figur 1 er vist eksempel på trykkfasthetsutviklingen som funksjon av masseforhold og alder ved 20°C vannlagring for betong med Norcem Standardsement FA.

Tidligfasthet

Tidligfastheten i betong er meget avhengig av temperatur og eventuell dosering av tilsetningsstoff med retarderende effekt. I figur 2 er vist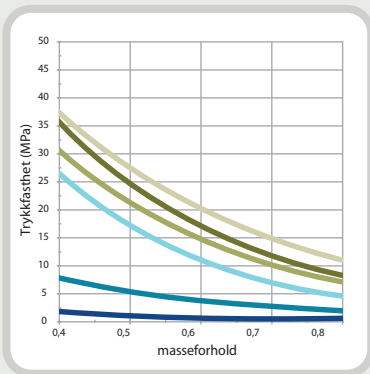 trykkfasthet etter 1 døgn med forskjellige masseforhold med og uten 1% plastiserende tilsetningsstoff (P-stoff) med Standardsement FA. Prøvene er lagret ved 95% luftfuktighet ved varierende temperatur.

Motstand mot alkalireaksjoner

Norsk Betongforenings publikasjon nr. 21 fastsetter retningslinjer for produksjon av bestandig betong med alkalireaktivt tilslag. Publikasjonen fastlegger at for betong med Standardsement FA kan det benyttes alkalireaktivt tilslag dersom betongens totale alkali-innhold ikke overstiger visse verdier.
For betong der Standardsement FA blandes med andre sementtyper, gjelder andre grenser. For grenseverdier - se www.betong.net under Publikasjoner, og Vedlegg C til publikasjon 21.

Fasthetsklasse – masseforhold

Med normalt god styring av betongproduksjonen er det behov for en overhøyde på ca 7 MPa ved de ulike fasthetsklassene for å produsere med tilstrekkelig sikkerhet mot undermålere. Standardsement FA gir følgende retningsgivende verdier for minste og største masseforhold i ulike fasthetsklasser for betong uten luftinnføring.

Fasthetsklasse	B20	B25	B30	B35	B45
Minste - Største masseforhold	0.65 - 0.72	0.57 - 0.65	0.51 - 0.57	0.44 - 0.51	0.35 - 0.44

Tabell 1

Norcem Standardsement FA er tilpasset norske forhold og kan benyttes   til betong i alle eksponerings-, bestandighets- og fasthets- klasser. Standard FA gir bestandig betong også i kombinasjon med alkalireaktivt tilslag. Fasthetsprofilen er tilpasset minimum sement- behov for konstruksjoner utendørs i bestandighetsklasse M60.

Bestandighetsklasse

Figur 3

Bestandighetsklasse

NS-EN 206-1 klassifiserer betongens miljøpåvirkninger i eksponeringsklasser. I nasjonalt tillegg til denne standarden er de ulike eksponeringsklassene gruppert i seks bestandighetsklasser med krav til betongens største masseforhold (se tabell 3). Tabell 2 viser anbefalte kombinasjoner av bestandighets- og fasthetsklasser. Retningsgivende verdier for største masseforhold i de ulike fasthetsklassene er gitt i tabell 1. I figur 3 er vist sammenhengen mellom bestandighetsklasse og fasthetsklasse, i et variasjonsbelte forårsaket av ulike produksjonsforutsetninger. Figuren gjelder for betong uten luftinnføring med Norcem Standardsement FA. I bestandighetsklasse M60 anbefaler vi generelt fasthetsklasse B25.

Anbefalte kombinasjoner

Bestandighetsklasse M90	Fasthetsklasse B20 eller høyere
Bestandighetsklasse M60	Fasthetsklasse B25 eller høyere
Bestandighetsklasse M45	Fasthetsklasse B35 eller høyere
Bestandighetsklasse M40	Fasthetsklasse B45 eller høyere

Tabell 2

Valg av bestandighetsklasse (nasjonale krav)

Eksponeringsklasse	M90	M60	M45	MF45*	M40	MF40*
X0	•	•	•	•	•	•
XCI, XC2, XC3, XC4, XF1		•	•	•	•	•
XD1, XS1, XA1, XA2, XA4			•	•	•	•
XF2, XF3, XF4				•		•
XD2, XD3, XS2, XS3, XA3					•	•
XSA	Betongsammensetning og beskyttelsestiltak fastsettes særskilt. Betongsammensetningen skal minst tilfredsstille kravene til M40.					
Største masseforhold v/(c + kg)	0,90	0,60 ,	0,45	0,45	0,40	0,40

*Minst 4% luft

Tabell 3

Deklarerte verdier

Norcem Standardsement FA tilfredsstiller kravene til Portlandflygeaskesement
EN 197-1 -CEM II/A-V 42,5 R   B = Brevik   K = Kjøpsvik

Kjemiske data

Egenskap	Deklarerte verdier	Krav ifølge NS-EN 197-1
Finhet (Blaine)	450 m²/kg	
Alkali (ekv Na_2O) - Brevik	1,4 %	Deklarert iht NB21
Alkali (ekv Na_2O) - Kjøpsvik	1,5%	Deklarert iht NB21
Flygeaskeinnhold	20,0 %	6-20%
Glødetap	2,0 %	-
Sulfat (SO_3)	3-4 %	≤ 4 %
Klorid	< 0,07%	≤ 0,1%
Vannløselig Cr^{6+}	< 2 ppm	≤ 2 ppm
Spesifikk vekt (kg/dm³)	2,99	

Fysikalske data

Egenskap	Retningsgivende verdier	Krav ifølge NS-EN 197-1
Trykkfasthet 1 døgn	21 MPa	
Trykkfasthet 2 døgn	31 MPa	≥ 20 MPa
Trykkfasthet 7 døgn	40 MPa	
Trykkfasthet 28 døgn	52 MPa	≥ 42,5 MPa ≤ 62,5 MPa
Begynnende bindetid (min)	130 (B) / 120 (K)	≥ 60 min
Ekspansjon	1 mm	≤ 10 mm

*Karakteristiske verdier

Odysse reklamebyrå

Dynamon SX-N

Superplastiserende tilsetningsstoff

BESKRIVELSE

Dynamon SX-N er et svært effektivt superplastiserende tilsetningsstoff basert på modifiserte akrylpolymerer. Produktet tilhører **Dynamon-systemet** basert på den Mapei-utviklede DPP-teknologien (DPP = Designed Performance Polymers), der tilsetningsstoffenes egenskaper skreddersys til ulike betongformål. **Dynamon-systemet** er utviklet på basis av Mapeis egen sammenstilling og produksjon av monomerer.

BRUKSOMRÅDER

Dynamon SX-N er et tilnærmet allround-produkt som er anvendelig i all betong for å øke støpeligheten og/eller redusere tilsatt vannmengde.

Noen spesielle bruksområder er:
- Vanntett betong med krav til høy eller svært høy fasthet og med strenge krav til bestandighet i aggressive miljøer.
- Betong med særlige krav til høy støpelighet; i konsistensklasser S4 og S5 etter NS-EN 206-1.
- Selvkomprimerende betong med ønske om lengre åpentid. Om nødvendig kan SKB stabiliseres med en viskositetsøker - **Viscofluid** eller **Viscostar**.
- Til produksjon av frostbestandig betong - da i kombinasjon med luftinnførende tilsetningsstoffer - **Mapeair**. Valg av type luftinnførende stoff gjøres ut fra egenskapene til de andre delmaterialer som er tilgjengelige.
- Til golvstøp for å oppnå en smidig betong med bedret støpelighet. Store doseringer og lave temperaturer kan retardere betongen noe.

TEKNISKE EGENSKAPER

Dynamon SX-N er en vannløsning av aktive akrylpolymerer som effektivt dispergerer (løser opp) sementklaser.

Denne effekten kan prinsipielt utnyttes på tre måter:
1. For å redusere mengden tilsatt vann, men samtidig beholde betongens støpelighet. Lavere v/c-forhold gir høyere fasthet, tetthet og bestandighet i betongen.
2. For å forbedre støpeligheten sammenlignet med betonger med samme v/c-forhold. Fastheten forblir dermed den samme, men muliggjør forenklet utstøping.
3. For å redusere både vann og sementmengde uten å forandre betongens mekaniske styrke. Gjennom denne metoden kan en blant annet redusere kostnadene (mindre sement), redusere betongens svinnpotensial (mindre vann) og redusere faren for temperaturgradienter på grunn av lavere hydratasjonsvarme.
   Spesielt er denne siste effekten viktig ved betonger med større sementmengder.

Dynamon SX-N

KOMPATIBILITET MED ANDRE PRODUKTER

Dynamon SX-N lar seg kombinere med andre Mapei tilsetningsstoffer, som f.eks størkningsakselererende stoffer som **Mapefast** og størkningsretarderende stoffer som **Mapetard**.
Produktet lar seg også kombinere med luftinnførende tilsetningsstoffer, **Mapeair**, for produksjon av frostbestandig betong.

Valg av type luftinnførende stoff gjøres ut fra egenskapene til de andre delmaterialer som er tilgjengelige.

DOSERING

Dynamon SX-N tilsettes for å oppnå ønsket resultat (styrke, bestandighet, støpelighet, sementreduksjon) ved å variere doseringen mellom 0,4 og 2,0 % av sementmengden. Ved økt dosering økes også betongens åpentid, dvs. tiden betongen lar seg bearbeide. Større doseringsmengder og lave betongtemperaturer gir en retardert betong. Vi anbefaler alltid prøvestøper med aktuelle parametere.
Til forskjell fra konvensjonelle melaminneller naftalenbaserte superplastiserende tilsetningsstoffer, utvikler **Dynamon SX-N** maksimal effekt uavhengig av tilsettingstidspunkt, men tilsetningstidspunktet kan påvirke nødvendig blandetid.
Dersom **Dynamon SX-N** tilsettes etter at minst 80 % av blandevannet er inne vil blandetiden generelt være kortest. Det er likevel viktig med utprøvinger tilpasset eget blandeutstyr.
Dynamon SX-N kan også tilsettes direkte i automikser på bygg- eller anleggsplass. Betongen bør da blandes med maksimal hastighet på trommelen i ett minutt pr. m³ betong i lasset, men minimum 5 minutter.

EMBALLASJE

Dynamon SX-N leveres i 25 liters kanner, 200 liters fat, 1000 liter IBC-tanker og i tank.

LAGRING

Produktet må oppbevares ved temperaturer mellom +8°C og +35°C. I lukket emballasje bevarer produktet sine egenskaper i minst 12 måneder. Forsiktig omrøring før bruk anbefales. Hvis produktet utsettes for direkte sollys, kan det føre til variasjoner i fargetonen uten at dette påvirker egenskapene til produktet.

SIKKERHETSINSTRUKSJONER FOR KLARGJØRING OG BRUK

Dynamon SX-N er ikke merkepliktig etter dagens regelverk når det gjelder tilsetningsstoffer. Det er likevel å anbefale at man benytter hansker, vernebriller og å ta vanlige forholdsregler som gjelder for håndtering av kjemikalier.

For ytterligere og fullstendig informasjon vedrørende sikker håndtering av vårt produkt, vennligst se sikkerhetsdatabladet som du finner på **www.mapei.no**

PRODUKT FOR PROFESJONELL BRUK

MERK

De tekniske anbefalinger og detaljer som fremkommer i denne produktbeskrivelse representerer vår nåværende kunnskap og erfaring om produktene.
All overstående informasjon må likevel betraktes som retningsgivende og gjenstand for vurdering. Enhver som benytter produktet må på forhånd forsikre seg om at produktet er egnet for tilsiktet anvendelse. Brukeren står selv ansvarlig dersom produktet blir benyttet til andre formål enn anbefalt eller ved feilaktig utførelse.

Vennligst referer til siste oppdaterte versjon av teknisk datablad som finnes tilgjengelig på vår webside www.mapei.no

Alle relevante referanser for produktet er tilgjengelige på forespørsel og fra www.mapei.no eller www.mapei.com

Dynamon SX-N

TEKNISKE DATA (typiske verdier)

PRODUKTBESKRIVELSE

Form:	væske
Farge:	gulbrun
Viskositet:	lettflytende; < 30 mPa*S
Tørrstoffinnhold, %:	18,5 ± 1,0
Spesifikk vekt, g/cm³:	1,06 ± 0,02
pH-verdi:	6,5 ± 1
Kloridinnhold, %:	< 0,05
Alkaliinnhold (Na$_2$O-ekvivalenter) %:	< 2,0

BRUKSEGENSKAPER I BETONG

Som vannreduserende stoff (lik konsistens) T 3.1	Referanse	Dynamon SX-N
Sementmengde, kg/m³ (Norcem standard sement):	350	350
Tilsetningsmengde (i % av sementvekt):	0	1,0
Masseforhold (v/c-tall):	0,51	0,41
Vannreduksjon (%):	-	20
Trykkfasthet (i N/mm²):		
- 1 døgn	26	41
- 7 døgn	42	60
- 28 døgn	52	68

Som SP-stoff (slumpforbedrer) T 3.2	Referanse	Dynamon SX-N
Sementmengde, kg/m³ (Norcem standard sement):	350	350
Tilsetningsmengde (i % av sementvekt):	0	1,0
Masseforhold (v/c-tall):	0,48	0,48
Luftinnhold:	2,1	1,8
Konsistens, mm:		
- synkmål, 5 min	30	220
- synkmål, 30 min	20	200
- synkutbredelse, 5 min		420
- synkutbredelse, 30 min		380

27.08.2013 NO

MAPEI®

BUILDING THE FUTURE

Elkem Microsilica®
CONCRETE

Grade 920 for construction

C2-01
Product

General

Elkem Microsilica® Grade 920 is dry silica fume available in two main forms:

- **Undensified** - **920 U**, with a typical bulk density of 200 - 350 kg/m^3
- **Densified** - **920 D**, with a typical bulk density of 500 - 700 kg/m^3

Packaging

The products are supplied in a range of packaging:

- 25 kg paper bags
- Big bags in a variety of designs and sizes depending on product and production plant.
- Bulk in road tanker

Special packaging can be supplied on request.

Quality Control

Elkem Materials is certified according to ISO 9001.

The chemical composition and physical properties are regularly tested in accordance with ASTM standards.

Conformance to Standards

Elkem Microsilica® Grade 920 conforms to the mandatory requirements of ASTM C1240 from **American Society for Testing and Materials**

Mandatory chemical and physical requirements	ASTM C1240	
	Spec.	Frequency
SiO$_2$ (%)	> 85,0	400 MT
Alkalies (as equivalent Na$_2$O, %)	Report	400 MT
Moisture (%)	< 3,0	400 MT
Loss on Ignition, LOI (%)	< 6,0	400 MT
Specific surface (BET - m^2/gram)	> 15	3200 MT/3 months
Bulk density (kg/m^3)	Report	400 MT
Pozz. Activity Index (%) - 7 days accelerated curing	> 105	3200 MT/3 months
Retained on 45 micron sieve (%)	< 10	400 MT
Variation from avg. retained on 45 micron (%-points)	< 5	avg. of last 10 tests
Density (kg/m^3)	Report	400 MT

CONCRETE	PRODUCT	SEPTEMBER 2008	C2-01

Elkem Microsilica® is a registered trademark and belongs to Elkem ASA Materials

Contact/representative:

Elkem Materials

Produktdatablad
NSCC Coarse VK

Franzefoss Miljøkalk AS
Postboks 53
NO-1309 Rud
Telefon :   **+47 05255**   miljokalk@kalk.no
Fax :   **+47 67 15 20 01**   www.kalk.no

Materiale:	Kalk	CaCO3	**Produsent:**	Verdalskalk AS, avd Havna
	NSCC Coarse VK	> 98%	**Råmaterial:**	Kalkstein fra Tromsdalen i Verdal
Reg.nr.:			**Fremstilt:**	Nedmaling av kalkstein
	REACH	-		

Anvendelse: Filler for industriapplikasjoner
Krav:

Parameter		Metode	Enhet	Statistikk		Krav		
				Snitt	**s**	**L**	**H**	**Toleranse +/-**
CaO	Kalsiumoksid	WD-XRF	[%]	55,1	0,14	-	-	
MgO	Magnesiumoksid		[%]	0,3	0,08	-	-	
Ca	Kalsium	Beregnet fra WD-XRF	[%]	39,4	-	-	-	
Mg	Magnesium		[%]	0,2	-	-	-	
Vanninnhold		NS-EN 12048	[%]	<0,2	-	-	-	
Masstetthet		Pyknometer	[kg/dm³]	2,7	-	-	-	
0,001 mm			[%]	4,9	0,8	-	-	
0,002 mm			[%]	12	1,6	-	-	
0,005 mm			[%]	24	2,7	-	-	
0,010 mm			[%]	35	3,3	-	-	
0,020 mm			[%]	50	3,8	-	-	
0,045 mm		Microtrac	[%]	72	4,2	-	-	
0,063 mm			[%]	81	5,1	-	-	
0,075 mm			[%]	86	4,8	-	-	
0,100 mm			[%]	92	3,0	-	-	
0,125 mm			[%]	96	1,7	-	-	
0,209 mm			[%]	99	0,4	-	-	

Kornfordeling
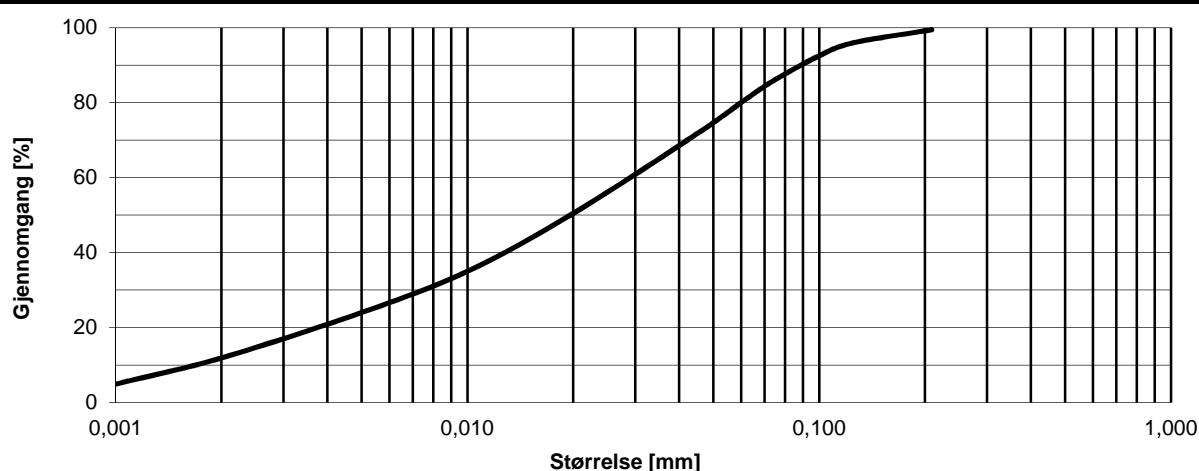
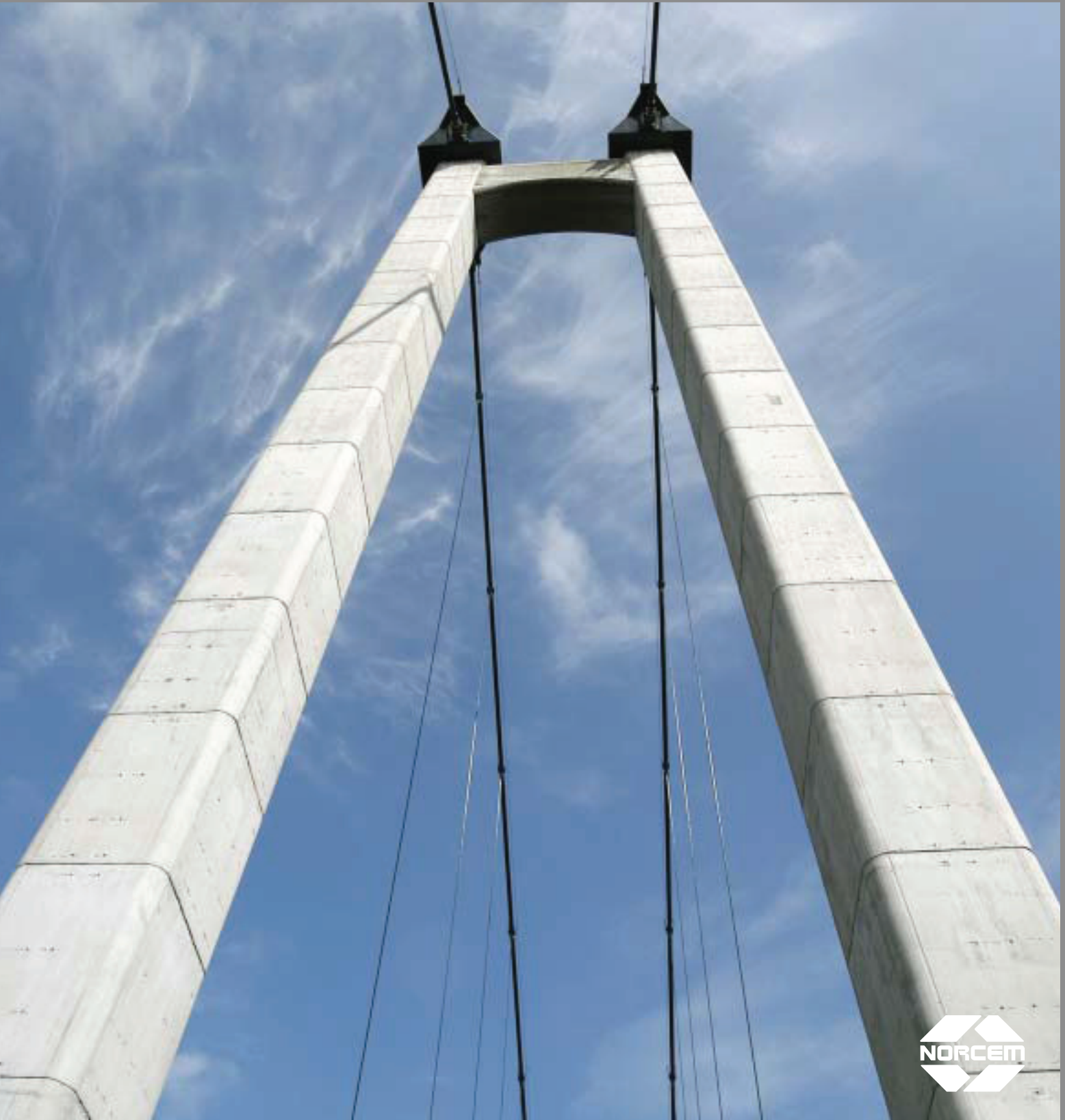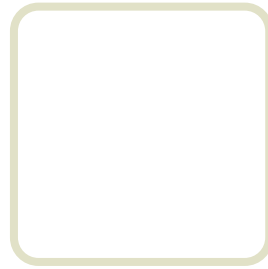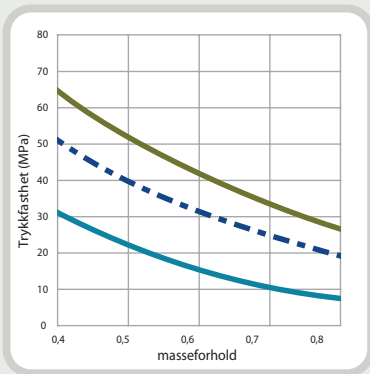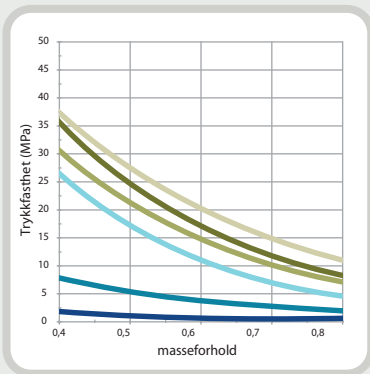| **Råmateriale:**	Råmaterialet er et naturprodukt med variasjoner innenfor visse grenser
Levering:	Bulk
Volumvekt	1,2 [kg/dm³]
Lagring:	Ingen merknad
SDS:	Se produktets sikkerhetsdatablad for informasjon angående helse, miljø og sikkerhet. Les denne informasjonen og iverksett eventuelle sikkerhetstiltak før produktet tas i bruk.

Standard sement FA

NORCEM

Figur 1

Figur 2

Fasthetsutvikling

Fasthetsutvikling er en sentral egenskap for planlegging, styring og utførelse av alle betongarbeider. Fasthetsutviklingen er avhengig av sementtype, tilslag, masseforhold, herdeforhold (temperatur, tid og fuktighet) og eventuell bruk av tilsetningsmateri-aler eller -stoffer. I figur 1 er vist eksempel på trykkfasthetsutviklingen som funksjon av masseforhold og alder ved 20°C vannlagring for betong med Norcem Standardsement FA.

Tidligfasthet

Tidligfastheten i betong er meget avhengig av temperatur og eventuell dosering av tilsetningsstoff med retarderende effekt. I figur 2 er vist trykkfasthet etter 1 døgn med forskjellige masseforhold med og uten 1% plastiserende tilsetningsstoff (P-stoff) med Standardsement FA. Prøvene er lagret ved 95% luftfuktighet ved varierende temperatur.

Motstand mot alkalireaksjoner

Norsk Betongforenings publikasjon nr. 21 fastsetter retningslinjer for produksjon av bestandig betong med alkalireaktivt tilslag. Publikasjonen fastlegger at for betong med Standardsement FA kan det benyttes alkalireaktivt tilslag dersom betongens totale alkali-innhold ikke overstiger visse verdier.
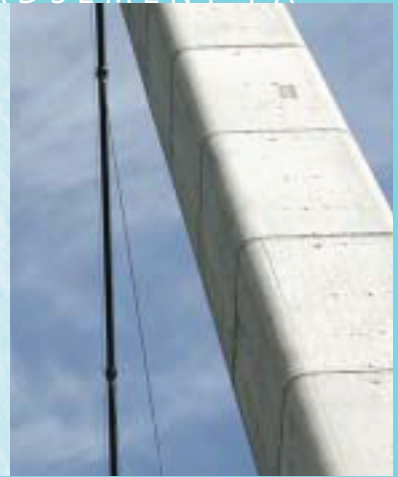For betong der Standardsement FA blandes med andre sementtyper, gjelder andre grenser. For grenseverdier - se www.betong.net under Publikasjoner, og Vedlegg C til publikasjon 21.
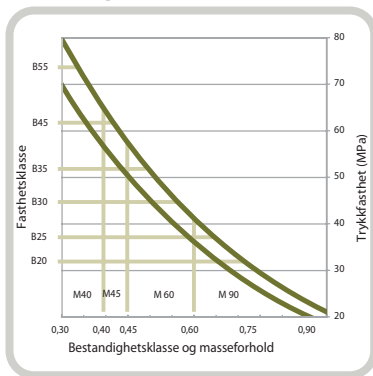
Fasthetsklasse – masseforhold

Med normalt god styring av betongproduksjonen er det behov for en overhøyde på ca 7 MPa ved de ulike fasthetsklassene for å produsere med tilstrekkelig sikkerhet mot undermålere. Standardsement FA gir følgende retningsgivende verdier for minste og største masseforhold i ulike fasthetsklasser for betong uten luftinnføring.

Fasthetsklasse	B20	B25	B30	B35	B45
Minste - Største masseforhold	0.65 - 0.72	0.57 - 0.65	0.51 - 0.57	0.44 - 0.51	0.35 - 0.44

Tabell 1

Norcem Standardsement FA er tilpasset norske forhold og kan benyttes   til betong i alle eksponerings-, bestandighets- og fasthets- klasser. Standard FA gir bestandig betong også i kombinasjon med alkalireaktivt tilslag. Fasthetsprofilen er tilpasset minimum sement- behov for konstruksjoner utendørs i bestandighetsklasse M60.

Bestandighetsklasse

Figur 3

Bestandighetsklasse

NS-EN 206-1 klassifiserer betongens miljøpåvirkninger i eksponeringsklasser. I nasjonalt tillegg til denne standarden er de ulike eksponeringsklassene gruppert i seks bestandighetsklasser med krav til betongens største masseforhold (se tabell 3). Tabell 2 viser anbefalte kombinasjoner av bestandighets- og fasthetsklasser. Retningsgivende verdier for største masseforhold i de ulike fasthetsklassene er gitt i tabell 1. I figur 3 er vist sammenhengen mellom bestandighetsklasse og fasthetsklasse, i et variasjonsbelte forårsaket av ulike produksjonsforutsetninger. Figuren gjelder for betong uten luftinnføring med Norcem Standardsement FA. I bestandighetsklasse M60 anbefaler vi generelt fasthetsklasse B25.

Anbefalte kombinasjoner

Bestandighetsklasse M90	Fasthetsklasse B20 eller høyere
Bestandighetsklasse M60	Fasthetsklasse B25 eller høyere
Bestandighetsklasse M45	Fasthetsklasse B35 eller høyere
Bestandighetsklasse M40	Fasthetsklasse B45 eller høyere

Tabell 2

Valg av bestandighetsklasse (nasjonale krav)

Eksponeringsklasse	M90	M60	M45	MF45*	M40	MF40*
X0	•	•	•	•	•	•
XCl, XC2, XC3, XC4, XF1		•	•	•	•	•
XD1, XS1, XA1, XA2, XA4			•	•	•	•
XF2, XF3, XF4				•		•
XD2, XD3, XS2, XS3, XA3					•	•
XSA	Betongsammensetning og beskyttelsestiltak fastsettes særskilt. Betongsammensetningen skal minst tilfredsstille kravene til M40.					
Største masseforhold v/(c + kg)	0,90	0,60 ,	0,45	0,45	0,40	0,40

*Minst 4% luft

Tabell 3

Deklarerte verdier

Norcem Standardsement FA tilfredsstiller kravene til Portlandflygeaskesement
EN 197-1 -CEM II/A-V 42,5 R   B = Brevik   K = Kjøpsvik

Kjemiske data

Egenskap	Deklarerte verdier	Krav ifølge NS-EN 197-1
Finhet (Blaine)	450 m²/kg	
Alkali (ekv Na_2O) - Brevik	1,4 %	Deklarert iht NB21
Alkali (ekv Na_2O) - Kjøpsvik	1,5%	Deklarert iht NB21
Flygeaskeinnhold	20,0 %	6-20%
Glødetap	2,0 %	-
Sulfat (SO_3)	3-4 %	≤ 4 %
Klorid	< 0,07%	$\leq 0,1$%
Vannløselig Cr^{6+}	< 2 ppm	≤ 2 ppm
Spesifikk vekt (kg/dm³)	2,99	

Fysikalske data

| Egenskap	Retningsgivende verdier	Krav ifølge NS-EN 197-1
Trykkfasthet 1 døgn	21 MPa	
Trykkfasthet 2 døgn	31 MPa	≥ 20 MPa
Trykkfasthet 7 døgn	40 MPa	
Trykkfasthet 28 døgn	52 MPa	$\geq 42,5$ MPa $\leq 62,5$ MPa
Begynnende bindetid (min)	130 (B) / 120 (K)	≥ 60 min
Ekspansjon	1 mm	≤ 10 mm

*Karakteristiske verdier
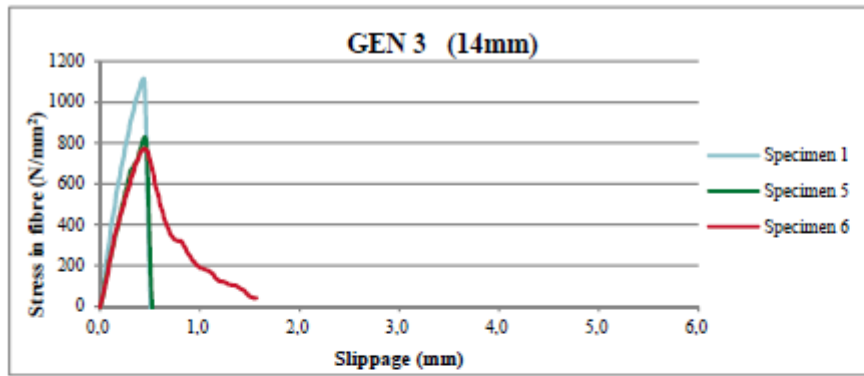
www.norcem.no

Odyssé reklamebyrå

Figure 13 and 14 presents the results achieved with the Generation 3 Minibars. The results for anchorage length 7mm (Figure 13) show maximum stress in the range between 550 and 800N/mm^2 for the four successful tests. All these fibres failed by pullout, and the stresses are somewhat higher than what was achieved for the Generation 2 Minibars.

Figure 14 presents the three tests with anchorage length 14 mm(L/3). In these tests the maximum stress varies between 770 and 1115N/mm^2 which again is a clear improvement compared to the Generation 2 fibres.
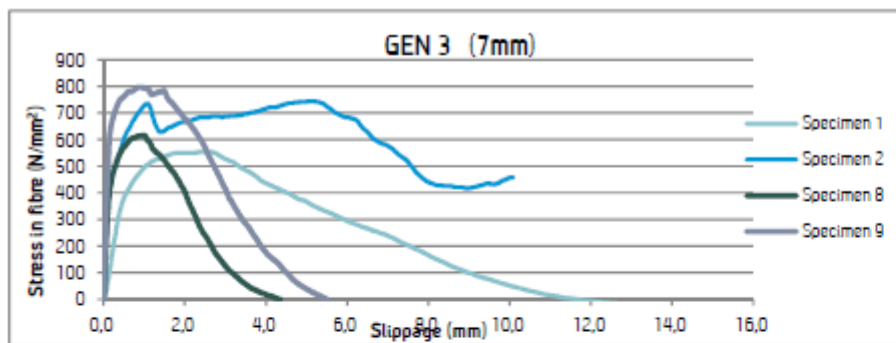
Summary	Gen3.S1	Gen3.S2	Gen3.S8	Gen3.S9
Maximum Load [kN]	0.19	0.26	0.22	0.28
Maxium Stress [N/mm^2]	553.76	743.69	615.55	796.32
Slip$_{max, load}$ [mm]	2.31	0.01	0.98	0.89
Comments all the specimen were protected with aluminium tube glued with epoxy)	Pull-out	Pull-out but after some minutes was sliding	Pull-out	Pull-out

Figure 13. Stress versus slippage for the Generation 3.0 minibar. Embedded length = 7mm.

Gen3	(14mm embedded length) Specimens		
	S1	S5	S6
Max. Load [kN]	0.39	0.29	0.27
Max. Stress in fibre [N/mm²]	1114.29	828.57	771.43
Slip$_{max, load}$ [mm]	0.26	0.44	0.44
Comments all the specimen were protected with aluminium tube glued with epoxy)	Fibre broke at point connection with concrete	Fibre broke at point connection with concrete	Fibre broke at point connection with the clamp

Figure 14. Stress versus slippage for the Generation 3.0 minibar. Embedded length = 14mm.